Experimental Evaluation of Viscous Hydrodynamic Force Models for Autonomous Underwater Vehicles

Brian R. McCarter

Thesis submitted to the Faculty of the
Virginia Polytechnic Institute and State University
in partial fulfillment of the requirements for the degree of

Master of Science in
Electrical Engineering

Daniel J. Stilwell, Chair
William T. Baumann
Craig A. Woolsey

August 15, 2014
Blacksburg, Virginia

Keywords: Dynamical systems, autonomous vehicles

Experimental Evaluation of Viscous Hydrodynamic Force Models for Autonomous Underwater Vehicles

Brian R. McCarter

(ABSTRACT)

A comparison of viscous hydrodynamic force models is presented, with application on an autonomous underwater vehicle (AUV). The models considered here are *quasi-steady*, meaning that force is expressed as a function of instantaneous vehicle state. This is in contrast to physical reality, where the force applied to a rigid body moving through a viscous fluid is history-dependent. As a result, the comparison of models is restricted to how well they are able to recreate a force history, rather than how closely they represent the underlying physics. Of the models under consideration, no single model performs significantly better than the others, but several perform worse.

Each viscous hydrodynamic force model presented here is expressed as a linear combination of basis functions, which are nonlinear functions of body-relative velocity. The greater dynamical model is presented in a rigid-body framework with six degrees of freedom, with terms which account for inviscid fluid flow, restoring forces due to gravity, and control forces due to actuator motion. The models are selected from several that have been proposed in the literature, which include empirically-derived and physics-based models. Some models assume that the relationship between force and velocity is fundamentally linear or quadratic in nature, or make assumptions about coupled motion. The models are compared by their relative complexities, and also by their ability to reproduce data sets generated from field experiments. The complete dynamical equations are presented for each model, including coefficients suitable for use with the Virginia Tech 690 AUV.

Acknowledgments

The author is deeply indebted to Dr. Daniel Stilwell for his continued support and encouragement. He is a colleague as well as a friend, and sets a standard of personal conduct to which we all aspire. The author also wishes to thank Dr. William Baumann, who introduced the author to systems and control, and Dr. Craig Woolsey, who gave the author with his first job in robotics.

Thanks also to Dr. Wayne Neu and his students Ryan Coe and Stephen Portner. They were a pleasure to work with, and provided much of the guidance on hydrodynamics present in this work.

Finally, a special thanks to Deborah Barnes, whose enthusiasm for her craft and creativity in its execution are a source of continuous inspiration to the author. May we all be so fortunate as to find play at work.

Contents

List of Figures

List of Tables

Chapter 1

Introduction

This thesis presents a comparison of several viscous hydrodynamic force models as applied to the Virginia Tech 690 autonomous underwater vehicle (AUV), shown in Figure 1.1. Each model describes the forces and moments experienced by the vehicle as it moves through a viscous fluid. The viscous hydrodynamic force model is one component of a six degree-of-freedom dynamical model which incorporates orthodox representations of rigid-body, added-mass, restoring, and control forces. These components have either analytical solutions based on physics, or can be accurately estimated by low-order representations. The remaning viscous component has no such accepted representation which is generally applicable to complex geometries in six degrees of freedom.

A six-degree-of-freedom dynamical model has been historically determined by building a scale model which represents the vehicle geometry, and measuring the scale model's response to a series of prescribed motions. The measured forces and moments are then fitted to a standard set of equations, such as those proposed by Gertler and Hagen in [1]. This method works well, but requires the expense of building a physical model and access to a suitable test facility. It also relies on selecting an appropriate set of basis functions, which are not usually

Figure 1.1: Virginia Tech 690 AUV

justified in the literature.

The class of model considered herein is *quasi-steady*, in that the generalized forces on the vehicle are represented purely as a function of the instantaneous state. The restriction to quasi-steady effects is necessary to produce a model which is able to accurately model vehicle motion in six degrees of freedom, but which discards the many more degrees of freedom necessary to model the complex fluid flow around the vehicle. No attempt is made to model non-steady fluid motion, such as shed vortices and complex flow interaction [2].

Motivation

This work is motivated by the desire for an accurate 6-DOF model of the VT 690 to be used in model-based control design. The VT 690 is an ocean survey platform, designed for long endurance missions to generate maps of the sea floor. It is equipped with a side-scan sonar payload for acoustic imaging. Navigation capability is provided by a Doppler velocity log (DVL), which generates bottom-relative velocity information. The vehicle is also equipped with an attitude heading reference system (AHRS), which provides vehicle orientation, rotational rates, and translation accelerations. The DVL and AHRS feed information into a navigation filter, which generates an estimate of vehicle pose in inertial coordinates, and

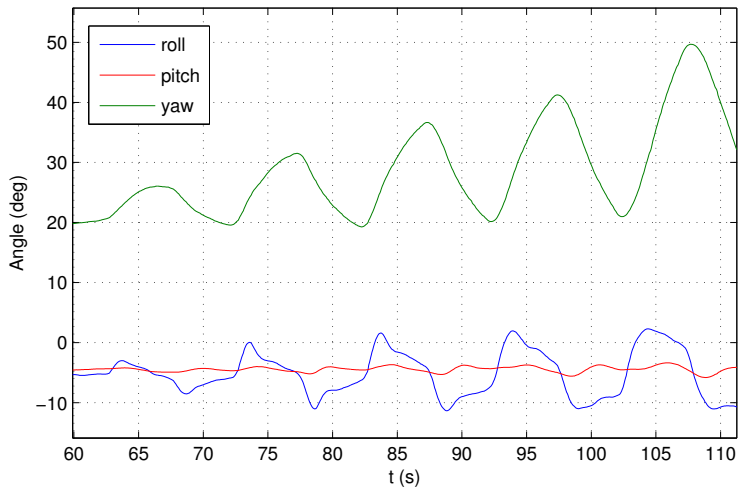

Figure 1.2: Orientation data from VT 690 yaw step maneuvers.

rates in the body frame.

The VT 690 is designed for missions which require steady forward motion while suppressing motion in other dimensions. That is, the sonar requires yaw rate to be minimized during imaging transects. Non-zero yaw rate will corrupt the sonar image by 'smearing' the return signal, or possibly missing objects of interest entirely. Roll and pitch rate are not as critical, but should still be small. The control system which is currently in use on the AUV stabilizes both vehicle yaw and pitch simultaneously. It is an $\mathcal{H}_\infty$ controller, which provides robustness against structured uncertainties [3]. The controller design was initially targeted at the Virginia Tech 475 AUV [4], a small AUV developed for collaborative control experiments. The controller was then redesigned for the 690.

The plant model assumed in the $\mathcal{H}_\infty$ synthesis is coupled in roll, pitch, and yaw, but the coupling signals are treated as exogenous errors to be minimized by the control design. Additionally, the plant model contains only a handful of hydrodynamic parameters.

The data shown in Figure 1.2 demonstrates coupled motion between roll, pitch and yaw. The figure plots vehicle orientation in response to a series of commanded yaw steps with

progressively higher amplitudes. These large yaw steps induce significant vehicle roll and pitch, which may be unacceptable for some mission scenarios. An accurate vehicle model would greatly aid in the design of new controllers for specific applications.

Organization

This completes the Introduction in Chapter 1. A complete dynamical model for an underwater vehicle is presented in Chapter 2, with the viscous hydrodynamic model treated separately in Chapter 3. Synthesis of the viscous hydrodynamic model is further discussed in Chapter 4. The results of applying the model to the VT 690 AUV are presented in Chapter 5. Conclusions are presented in Chapter 6 with further reference in Appendices A - E.

Chapter 2

Dynamical Model of an Underwater Vehicle

2.1 Coordinate systems

Let the vehicle shown in Figure 2.1 be modeled as a rigid body, with the origin of a body-fixed coordinate system centered at the vehicle's center of buoyancy (CB). The location of the vehicle relative to an (Earth-fixed) inertial frame is defined to be the position vector

$$\boldsymbol{r}_0 = [x \; y \; z]^\top , \tag{2.1}$$

where x is the distance in the inertial north direction, y is the distance east, and z is the distance down.

The attitude of the vehicle in the inertial frame is defined by the orientation vector

$$\boldsymbol{\theta} = [\phi \; \theta \; \psi]^\top , \tag{2.2}$$

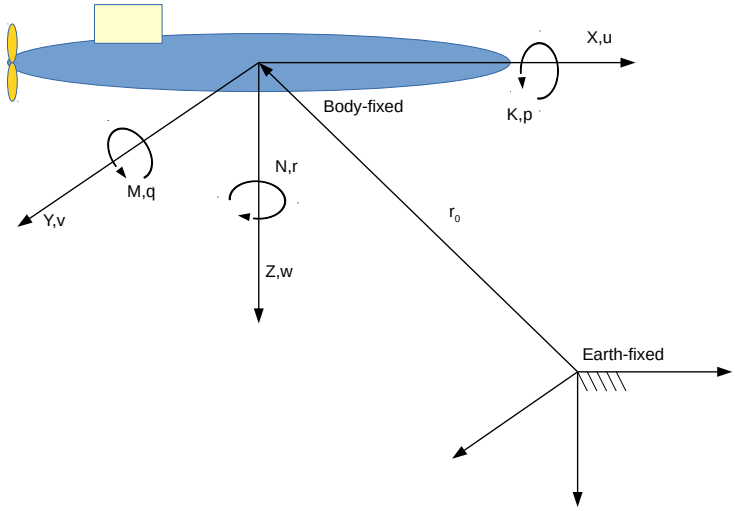

Figure 2.1: Vehicle coordinate system.

where ϕ, θ, and ψ are the Euler angles roll, pitch, and yaw. The vehicle coordinate system is rotated relative to the inertial coordinate system by first aligning the coordinate systems such that the X-axis points north, the Y-axis points east, and the Z-axis point down. The vehicle coordinate system is then rotated by the yaw angle ψ about the vehicle Z-axis, denoted Z_3, then by the pitch angle θ about the resulting Y-axis, denoted Y_2, then finally by the roll angle ϕ about the resulting X axis, denoted X_1. This ZYX series of rotations is the typical way that Euler angles are defined for underwater vehicles [5]. The sequence of rotations is illustrated in Figure 2.2.

Together, the position and orientation make up the pose vector $\boldsymbol{\eta}$, which is defined to be

$$\boldsymbol{\eta} = \left[\boldsymbol{r}_0^\top \ \boldsymbol{\theta}^\top\right]^\top = [x \ y \ z \ \phi \ \theta \ \psi]^\top . \tag{2.3}$$

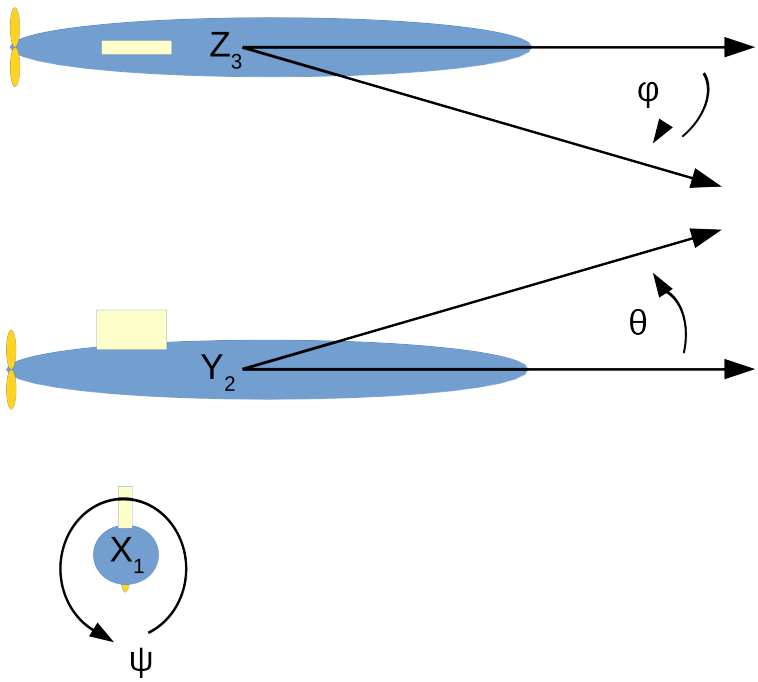

Figure 2.2: Euler angle rotations for underwater vehicles.

2.2 Kinematics

The vehicle's translational velocity vector $\boldsymbol{v} = [u\ v\ w]^\top$ is defined in the body frame as shown in Figure 2.1, where surge velocity u is positive along the vehicle X-axis, sway velocity v is positive along the Y-axis, and heave velocity w is positive along the vehicle Z-axis.

The rotational velocity vector $\boldsymbol{\omega} = [p\ q\ r]^\top$ is also defined in the body frame, where roll rate p is right-hand positive about the vehicle X-axis, pitch rate q is right-hand positive about the Y-axis, and yaw rate r is right-hand positive about the Z-axis.

The velocity vector

$$\boldsymbol{\nu} = \left[\boldsymbol{v}^\top\ \boldsymbol{\omega}^\top\right]^\top = [u\ v\ w\ p\ q\ r]^\top \tag{2.4}$$

is the set of translational and rotational velocities. The translational velocity vector $\boldsymbol{v}$ can

be mapped to the inertial frame by a rotation matrix

$$\boldsymbol{P_v}(\boldsymbol{\theta}) = \begin{bmatrix} c\psi c\theta & -s\psi c\phi + c\psi s\theta s\phi & s\psi s\phi + c\psi c\phi s\theta \\ s\psi c\theta & c\psi c\phi + s\phi s\theta s\psi & -c\psi s\phi + s\theta s\psi c\phi \\ -s\theta & c\theta s\phi & c\theta c\phi \end{bmatrix} \tag{2.5}$$

where $s := \sin$ and $c := \cos$ are used as shorthand, with $t := \tan$ used as well in (2.7). Note that

$$\dot{\boldsymbol{r}}_0 = \boldsymbol{P_v}(\boldsymbol{\theta})\boldsymbol{v}. \tag{2.6}$$

Similarly, the rotational velocity vector $\boldsymbol{\omega}$ can be mapped to the inertial frame by the matrix $\boldsymbol{P_\omega}(\boldsymbol{\theta})$, defined to be

$$\boldsymbol{P_\omega}(\boldsymbol{\theta}) = \begin{bmatrix} 1 & s\phi t\theta & c\phi t\theta \\ 0 & c\phi & -s\phi \\ 0 & s\phi/c\theta & c\phi/c\theta \end{bmatrix} \tag{2.7}$$

where

$$\dot{\boldsymbol{\theta}} = \boldsymbol{P_\omega}(\boldsymbol{\theta})\boldsymbol{\omega}. \tag{2.8}$$

Combining (2.6) with (2.8) gives the relationship

$$\begin{bmatrix} \dot{\boldsymbol{r}}_0 \\ \dot{\boldsymbol{\theta}} \end{bmatrix} = \begin{bmatrix} \boldsymbol{P_v}(\boldsymbol{\theta}) & \mathbf{0}_{3\times3} \\ \mathbf{0}_{3\times3} & \boldsymbol{P_\omega}(\boldsymbol{\theta}) \end{bmatrix} \begin{bmatrix} \boldsymbol{v} \\ \boldsymbol{\omega} \end{bmatrix}. \tag{2.9}$$

Then, by substituting (2.3) and (2.4) into (2.9) and defining

$$\boldsymbol{P}(\boldsymbol{\theta}) = \begin{bmatrix} \boldsymbol{P_v}(\boldsymbol{\theta}) & \mathbf{0}_{3\times3} \\ \mathbf{0}_{3\times3} & \boldsymbol{P_\omega}(\boldsymbol{\theta}) \end{bmatrix}, \tag{2.10}$$

the kinematic relationship may be represented concisely as

$$\dot{\boldsymbol{\eta}} = \boldsymbol{P}(\boldsymbol{\theta})\boldsymbol{\nu}. \tag{2.11}$$

The inverse map $\boldsymbol{P}^{-1}(\boldsymbol{\theta})$ is calculated by first noting that the structure in (2.10) is block diagonal, so

$$\boldsymbol{P}^{-1}(\boldsymbol{\theta}) = \begin{bmatrix} \boldsymbol{P_v}^{-1}(\boldsymbol{\theta}) & \mathbf{0}_{3\times3} \\ \mathbf{0}_{3\times3} & \boldsymbol{P_\omega}^{-1}(\boldsymbol{\theta}) \end{bmatrix}, \tag{2.12}$$

provided $\boldsymbol{P_v}^{-1}(\boldsymbol{\theta})$ and $\boldsymbol{P_\omega}^{-1}(\boldsymbol{\theta})$ exist.

Note that $\boldsymbol{P_v}(\boldsymbol{\theta})$ is a rotation matrix, and so is orthogonal. Therefore,

$$\boldsymbol{P_v}^{-1}(\boldsymbol{\theta}) \equiv \boldsymbol{P_v}^{\top}(\boldsymbol{\theta}) = \begin{bmatrix} c\psi c\theta & s\psi c\theta & -s\theta \\ -s\psi c\phi + c\psi s\theta s\phi & c\psi c\phi + s\phi s\theta s\psi & c\theta s\phi \\ s\psi s\phi + c\psi c\phi s\theta & -c\psi s\phi + s\theta s\psi s\phi & c\theta c\phi \end{bmatrix}. \tag{2.13}$$

The inverse of $\boldsymbol{P_\omega}(\boldsymbol{\theta})$ also has a closed form, where

$$\boldsymbol{P_\omega}^{-1}(\boldsymbol{\theta}) = \begin{bmatrix} 1 & 0 & -s\theta \\ 0 & c\phi & c\theta s\phi \\ 0 & -s\phi & c\theta c\phi \end{bmatrix}. \tag{2.14}$$

Therefore (2.12) exists, and

$$\boldsymbol{\nu} = \boldsymbol{P}^{-1}(\boldsymbol{\theta})\dot{\boldsymbol{\eta}}. \tag{2.15}$$

2.3 Dynamics

2.3.1 Rigid body forces

The forces X, Y, Z acting on a rigid body are defined in the body frame as shown in Figure 2.1, where X is the force acting along the X-axis, Y acts along the Y-axis, and Z acts along the Z-axis. The moments K, M, N acting on the body are defined similarly, where K is the moment acting about the X-axis in a right-hand fashion, M acts about the Y-axis, and N acts about the Z-axis. Together, these make up the rigid-body force vector

$$\boldsymbol{\tau}_{RB} = [X\ Y\ Z\ K\ M\ N]^{\top}. \tag{2.16}$$

The rigid-body equations of motion are

$$\boldsymbol{M}_{RB}\dot{\boldsymbol{\nu}} + \boldsymbol{C}_{RB}(\boldsymbol{\nu})\boldsymbol{\nu} = \boldsymbol{\tau}_{RB} \tag{2.17}$$

where $\boldsymbol{M}_{RB}$ is the rigid-body inertia matrix, and $\boldsymbol{C}_{RB}(\boldsymbol{\nu})\boldsymbol{\nu}$ represents the Coriolis and centripetal forces due to the vehicle's motion in a rotating reference frame.

Let the vehicle's inertia tensor $\boldsymbol{I}_0$ be defined as

$$\boldsymbol{I}_0 = \begin{bmatrix} I_x & -I_{xy} & -I_{xz} \\ -I_{yx} & I_y & -I_{yz} \\ -I_{zx} & -I_{zy} & I_z \end{bmatrix}, \tag{2.18}$$

and the center of gravity $\boldsymbol{r}_G$ be

$$\boldsymbol{r}_G = [x_G \; y_G \; z_G]^\top \tag{2.19}$$

measured relative to the body-fixed origin at the center of buoyancy. Then the rigid-body inertia matrix $\boldsymbol{M}_{RB}$ may be defined by $\boldsymbol{r}_G$, $\boldsymbol{I}_0$, and vehicle mass m as

$$\boldsymbol{M}_{RB} = \begin{bmatrix} m\boldsymbol{I}_{3\times 3} & -m\boldsymbol{S}(\boldsymbol{r}_G) \\ m\boldsymbol{S}(\boldsymbol{r}_G) & \boldsymbol{I}_0 \end{bmatrix} \tag{2.20}$$

$$= \begin{bmatrix} m & 0 & 0 & 0 & mz_G & -my_G \\ 0 & m & 0 & -mz_G & 0 & mx_G \\ 0 & 0 & m & my_G & -mx_G & 0 \\ 0 & -mz_G & my_G & I_x & -I_{xy} & -I_{xz} \\ mz_G & 0 & -mx_G & -I_{yx} & I_y & -I_{yz} \\ -my_G & mx_G & 0 & -I_{zx} & -I_{zy} & I_z \end{bmatrix}. \tag{2.21}$$

The Coriolis and centripetal forces $\boldsymbol{C}_{RB}(\boldsymbol{\nu})\boldsymbol{\nu}$ are uniquely determined by the inertia matrix $\boldsymbol{M}_{RB}$ as a function of velocity $\boldsymbol{\nu}$, but the function $\boldsymbol{C}_{RB}(\boldsymbol{\nu})$ does not have a unique representation.

Let $\boldsymbol{M}$ be an arbitrary inertia matrix, partitioned as

$$\boldsymbol{M} = \begin{bmatrix} \boldsymbol{M}_{11} & \boldsymbol{M}_{12} \\ \boldsymbol{M}_{21} & \boldsymbol{M}_{22} \end{bmatrix}. \tag{2.22}$$

Define the Coriolis and centripetal function $\boldsymbol{C}(\boldsymbol{\nu})$ to be

$$\boldsymbol{C}(\boldsymbol{\nu}) = \begin{bmatrix} 0_{3\times 3} & -\boldsymbol{S}(\boldsymbol{M}_{11}\boldsymbol{v} + \boldsymbol{M}_{12}\boldsymbol{\omega}) \\ -\boldsymbol{S}(\boldsymbol{M}_{11}\boldsymbol{v} + \boldsymbol{M}_{12}\boldsymbol{\omega}) & -\boldsymbol{S}(\boldsymbol{M}_{21}\boldsymbol{v} + \boldsymbol{M}_{22}\boldsymbol{\omega}) \end{bmatrix}, \tag{2.23}$$

which is one form proposed by Fossen in [5]. The matrix-valued function $\boldsymbol{S}(\cdot)$ maps $\mathbb{R}^3$ to the set of skew-symmetric matrices so(3), and is defined in Appendix A.2. Then for the rigid-body inertia matrix $\boldsymbol{M}_{RB}$, the corresponding Coriolis and centripetal function is

$$\boldsymbol{C}_{RB}(\boldsymbol{\nu}) = \boldsymbol{C}(\boldsymbol{\nu})\Big|_{M=\boldsymbol{M}_{RB}} = \begin{bmatrix} 0 & 0 & 0 & m\left(y_G q + z_G r\right) & -m\left(x_G q - w\right) & -m\left(x_G r + v\right) \\ 0 & 0 & 0 & -m\left(y_G p + w\right) & m\left(z_G r + x_G p\right) & -m\left(y_G r - u\right) \\ 0 & 0 & 0 & -m\left(z_G p - v\right) & -m\left(z_G q + u\right) & m\left(x_G p + y_G q\right) \\ -m\left(y_G q + z_G r\right) & m\left(y_G p + w\right) & m\left(z_G p - v\right) & 0 & -I_{yz}q - I_{xz}p + I_z r & I_{yz}r + I_{xy}p - I_y q \\ m\left(x_G q - w\right) & -m\left(z_G r + x_G p\right) & m\left(z_G q + u\right) & I_{yz}q + I_{xz}p - I_z r & 0 & -I_{xz}r - I_{xy}q + I_x p \\ m\left(x_G r + v\right) & m\left(y_G r - u\right) & -m\left(x_G p + y_G q\right) & -I_{yz}r - I_{xy}p + I_y q & I_{xz}r + I_{xy}q - I_x p & 0 \end{bmatrix} \tag{2.24}$$

The equations of motion can then be written in component form by substituting (2.16), (2.21), and (2.24) into (2.17), yielding

$$m\left[\dot{u} - vr + wq - x_G\left(q^2 + r^2\right) + y_G\left(pq - \dot{r}\right) + z_G\left(pr + \dot{q}\right)\right] = X \tag{2.25}$$

$$m\left[\dot{v} - wp + ur - y_G\left(r^2 + p^2\right) + z_G\left(qr - \dot{p}\right) + x_G\left(qp + \dot{r}\right)\right] = Y \tag{2.26}$$

$$m\left[\dot{w} - uq + vp - z_G\left(p^2 + q^2\right) + x_G\left(rp - \dot{q}\right) + y_G\left(rq + \dot{p}\right)\right] = Z \tag{2.27}$$

$$\begin{aligned} I_x\dot{p} + \left(I_z - I_y\right)qr - \left(\dot{r} + pq\right)I_{xz} + \left(r^2 - q^2\right)I_{yz} + \left(pr - \dot{q}\right)I_{xy} \\ + m\left[y_G\left(\dot{w} - uq + vp\right) - z_G\left(\dot{v} - wp + ur\right)\right] = K \end{aligned} \tag{2.28}$$

$$\begin{aligned} I_y\dot{q} + \left(I_x - I_z\right)rp - \left(\dot{p} + qr\right)I_{xy} + \left(p^2 - r^2\right)I_{zx} + \left(qp - \dot{r}\right)I_{yz} \\ + m\left[z_G\left(\dot{u} - vr + wq\right) - x_G\left(\dot{w} - uq + vp\right)\right] = M \end{aligned} \tag{2.29}$$

$$\begin{aligned} I_z\dot{r} + \left(I_y - I_x\right)pq - \left(\dot{q} + rp\right)I_{yz} + \left(q^2 - p^2\right)I_{xy} + \left(rq - \dot{p}\right)I_{zx} \\ + m\left[x_G\left(\dot{v} - wp + ur\right) - y_G\left(\dot{u} - vr + wq\right)\right] = N \end{aligned} \tag{2.30}$$

2.3.2 External forces

The vector of external forces

$$\boldsymbol{\tau}_{RB} = \boldsymbol{\tau}_H + \boldsymbol{\tau}_G + \boldsymbol{\tau}_U \tag{2.31}$$

represents the superposition of hydrodynamic forces $\boldsymbol{\tau}_H$, restoring forces $\boldsymbol{\tau}_G$, and control forces $\boldsymbol{\tau}_U$. Hydrodynamic forces $\boldsymbol{\tau}_H$ are due to pressure exerted on the body by the surrounding fluid as the vehicle moves and accelerates through the fluid in six degrees of freedom. The hydrodynamic force vector can be expressed as a sum of viscous and inviscid effects,

denoted $\boldsymbol{\tau}_\nu$ and $\boldsymbol{\tau}_A$, respectively, so that

$$\boldsymbol{\tau}_H = \boldsymbol{\tau}_\nu + \boldsymbol{\tau}_A. \tag{2.32}$$

An inviscid analysis of the fluid flow around the vehicle generates the $\boldsymbol{\tau}_A$ component, which accounts for the inertia of the surrounding fluid, termed *added mass*. Added mass effects are modeled as a function of both acceleration and velocity. The remaining hydrodynamic effects are entirely velocity dependent. The velocity-dependent viscous hydrodynamic model is denoted $\boldsymbol{\tau}_\nu$, and includes the effect of damping forces due to skin friction and pressure drag, as well as conservative forces such as the "Munk" moment. The viscous hydrodynamic force model $\boldsymbol{\tau}_\nu$ is given special attention in Chapter 3. Inviscid fluid flow, restoring forces, and control forces are discussed in the following sections.

2.3.3 Inviscid flow

The forces $\boldsymbol{\tau}_A$ due to added mass can be modeled as additional inertia on the vehicle. Let $\boldsymbol{M}_A$ be the added-mass inertia matrix, with elements

$$\boldsymbol{M}_A = \begin{bmatrix} X_{\dot{u}} & X_{\dot{v}} & X_{\dot{w}} & X_{\dot{p}} & X_{\dot{q}} & X_{\dot{r}} \\ Y_{\dot{u}} & Y_{\dot{v}} & Y_{\dot{w}} & Y_{\dot{p}} & Y_{\dot{q}} & Y_{\dot{r}} \\ Z_{\dot{u}} & Z_{\dot{v}} & Z_{\dot{w}} & Z_{\dot{p}} & Z_{\dot{q}} & Z_{\dot{r}} \\ K_{\dot{u}} & K_{\dot{v}} & K_{\dot{w}} & K_{\dot{p}} & K_{\dot{q}} & K_{\dot{r}} \\ M_{\dot{u}} & M_{\dot{v}} & M_{\dot{w}} & M_{\dot{p}} & M_{\dot{q}} & M_{\dot{r}} \\ N_{\dot{u}} & N_{\dot{v}} & N_{\dot{w}} & N_{\dot{p}} & N_{\dot{q}} & N_{\dot{r}} \end{bmatrix}. \tag{2.33}$$

The corresponding Coriolis and centripetal forces $\boldsymbol{C}_A(\boldsymbol{\nu})\boldsymbol{\nu}$ due to inviscid effects can be calculated as in (2.23)

$$\boldsymbol{C}_A(\boldsymbol{\nu}) = \boldsymbol{C}(\boldsymbol{\nu})\Big|_{M=\boldsymbol{M}_A}. \tag{2.34}$$

The total force due to added mass $\boldsymbol{\tau}_A$ is of a form similar to the rigid body equations of motion in (2.17):

$$\boldsymbol{\tau}_A = \boldsymbol{M}_A\dot{\boldsymbol{\nu}} + \boldsymbol{C}_A(\boldsymbol{\nu})\boldsymbol{\nu}. \tag{2.35}$$

The matrix $\boldsymbol{M}_A$ is determined by vehicle external geometry. Each term represents the force generated in a given direction by an acceleration in a given direction. For example, the force Z_A along the z-axis due to an acceleration $\dot{u}$ along the x-axis is expressed $Z_A = Z_{\dot{u}}\dot{u}$. The diagonal elements $X_{\dot{u}}, \ldots, N_{\dot{r}}$ are negative. Imlay provides the complete expression for hydrodynamic added mass in [6]. This makes the standard assumption for underwater vehicles that M_A is symmetric, where $X_{\dot{v}} = Y_{\dot{u}}$, $X_{\dot{w}} = Z_{\dot{u}}$, etc. A fully submerged vehicle is assumed to have constant added mass matrix, which is negative definite as defined in (2.60). This fits well with observations made in [7].

Imlay describes an analytic approximation for the added mass of a slender, axisymmetric vehicle by calculating the added mass of a prolate spheroid with equivalent volume. Let

$$e^2 = 1 - \left(\frac{b}{a}\right)^2 \tag{2.36}$$

$$\alpha_0 = \frac{2\left(1-e^2\right)}{e^3}\left(\frac{1}{2}\log\frac{1+e}{1-e} - e\right) \tag{2.37}$$

$$\beta_0 = \frac{1}{e^2} - \frac{1-e^2}{2e^3}\log\frac{1+e}{1-e} \tag{2.38}$$

where a, b are the prolate spheroid semi-axes with $a > b$. Then $\boldsymbol{M}_A$ is defined to be entirely zeros, except for

$$X_{\dot{u}} = -\frac{a_0}{2-a_0}\frac{4}{3}\pi\rho ab^2 \tag{2.39}$$

$$Y_{\dot{v}} = Z_{\dot{w}} = -\frac{\beta_0}{2-\beta_0}\frac{4}{3}\pi\rho ab^2 \tag{2.40}$$

$$N_{\dot{r}} = M_{\dot{q}} = -\frac{1}{5}\frac{\left(b^2-a^2\right)^2\left(\alpha_0-\beta_0\right)}{2\left(b^2-a^2\right)+\left(b^2+a^2\right)\left(\beta_0-\alpha_0\right)}\frac{4}{3}\pi\rho ab^2. \tag{2.41}$$

2.3.4 Restoring forces

Vehicle mass m creates a down force $W = mg$ in the inertial frame, where g is acceleration due to gravity. W is mapped to a force $\boldsymbol{f}_G(\boldsymbol{\nu})$ in the body frame by

$$\boldsymbol{f}_G(\boldsymbol{\eta}) = \boldsymbol{P}_1^{-1}(\boldsymbol{\eta})\begin{bmatrix} 0 \\ 0 \\ W \end{bmatrix}, \tag{2.42}$$

where $\boldsymbol{f}_G(\boldsymbol{\eta})$ acts through the center of gravity $\boldsymbol{r}_G$.

The vehicle displaces a fixed volume of fluid ∇ when fully submerged, with fluid density ρ. The total buoyant force is then $B = \rho g \nabla$, directed up in the inertial frame. B is mapped to a force $\boldsymbol{f}_B(\boldsymbol{\eta})$ in the body frame by

$$\boldsymbol{f}_B(\boldsymbol{\eta}) = \boldsymbol{P}_1^{-1}(\boldsymbol{\eta})\begin{bmatrix} 0 \\ 0 \\ -B \end{bmatrix}, \tag{2.43}$$

where $\boldsymbol{f}_B(\boldsymbol{\eta})$ acts through the center of buoyancy $\boldsymbol{r}_B$.

The net force on the body due to weight and buoyancy is called the restoring force $\boldsymbol{\tau}_G(\boldsymbol{\eta})$.

$$\boldsymbol{\tau}_G(\boldsymbol{\eta}) = \begin{bmatrix} \boldsymbol{f}_G(\boldsymbol{\eta}) + \boldsymbol{f}_B(\boldsymbol{\eta}) \\ \boldsymbol{r}_G \times \boldsymbol{f}_G(\boldsymbol{\eta}) + \boldsymbol{r}_B \times \boldsymbol{f}_B(\boldsymbol{\eta}) \end{bmatrix} \tag{2.44}$$

Small underwater vehicles are typically ballasted to be slightly positively buoyant, meaning the dry mass of the vehicle is slightly less than the mass of the fluid that the vehicle displaces when fully submerged. This produces a negative force in the inertial z direction. Also, the vehicle is typically trimmed such that its center of gravity $\boldsymbol{r}_G$ is beneath the center of buoyancy $\boldsymbol{r}_B$. This provides a static righting moment in roll and pitch. Since the center of buoyancy is purely a function of external geometry and does not change with trim or ballast, $\boldsymbol{r}_B = [0, 0, 0]$ is taken to be the origin of the vehicle's body-fixed coordinate system.

2.3.5 Control forces

External actuators on a small underwater vehicle typically consist of a propeller and a set of control surfaces. The control surfaces are mounted as far aft as possible to produce the maximum moment for a given deflection, while still providing passive stability in yaw and pitch. The propeller is typically located aft of the control surfaces.

Control surfaces

Forces and moments due to control surface deflection can be approximated by a second order polynomial function if the deflection angle is small enough that the flow over the control surface does not stall. A suitable model for generalized forces $\boldsymbol{\tau}_\delta(\boldsymbol{\delta})$ due to control

surface deflection of a four-fin cruciform pattern, such as on the 690 AUV, is

$$\boldsymbol{\tau}_\delta(\boldsymbol{\delta}) = \boldsymbol{K}_\delta \boldsymbol{\delta} + \boldsymbol{K}_{\delta^2} \mathrm{diag}(\boldsymbol{\delta})\boldsymbol{\delta}, \tag{2.45}$$

where control surface deflections $\boldsymbol{\delta} = [\delta_S, \delta_P, \delta_B, \delta_T]$ are the starboard, port, bottom, and top fins, respectively. Model coefficients are

$$\boldsymbol{K}_\delta = \begin{bmatrix} X_{\delta_S} & X_{\delta_P} & X_{\delta_B} & X_{\delta_T} \\ Y_{\delta_S} & Y_{\delta_P} & Y_{\delta_B} & Y_{\delta_T} \\ Z_{\delta_S} & Z_{\delta_P} & Z_{\delta_B} & Z_{\delta_T} \\ K_{\delta_S} & K_{\delta_P} & K_{\delta_B} & K_{\delta_T} \\ M_{\delta_S} & M_{\delta_P} & M_{\delta_B} & M_{\delta_T} \\ N_{\delta_S} & N_{\delta_P} & N_{\delta_B} & N_{\delta_T} \end{bmatrix} \tag{2.46}$$

$$\boldsymbol{K}_{\delta^2} = \begin{bmatrix} X_{\delta_S^2} & X_{\delta_P^2} & X_{\delta_B^2} & X_{\delta_T^2} \\ Y_{\delta_S^2} & Y_{\delta_P^2} & Y_{\delta_B^2} & Y_{\delta_T^2} \\ Z_{\delta_S^2} & Z_{\delta_P^2} & Z_{\delta_B^2} & Z_{\delta_T^2} \\ K_{\delta_S^2} & K_{\delta_P^2} & K_{\delta_B^2} & K_{\delta_T^2} \\ M_{\delta_S^2} & M_{\delta_P^2} & M_{\delta_B^2} & M_{\delta_T^2} \\ N_{\delta_S^2} & N_{\delta_P^2} & N_{\delta_B^2} & N_{\delta_T^2} \end{bmatrix}. \tag{2.47}$$

This model is formulated to account for the forces generated by control surfaces during forward motion with $v = w = 0$. This is a reasonable assumption, especially if the residual control surface forces are accounted for by the viscous hydrodynamic force model $\boldsymbol{\tau}_\nu$.

Coefficients for the VT 690 are presented in Table B.4. The coefficients are presented in nondimensional form $\boldsymbol{K}'_\delta$ and $\boldsymbol{K}'_{\delta^2}$. The relationship between these coefficients and those in

(2.46) and (2.47) are

$$\boldsymbol{K}_{\delta} = \mathrm{diag}([d_2\ d_2\ d_2\ d_3\ d_3\ d_3])\boldsymbol{K}'_{\delta} \tag{2.48}$$

$$\boldsymbol{K}_{\delta^2} = \mathrm{diag}([d_2\ d_2\ d_2\ d_3\ d_3\ d_3])\boldsymbol{K}'_{\delta^2} \tag{2.49}$$

where

$$d_2 = \frac{1}{2}\rho\ell^2 u^2 \tag{2.50}$$

$$d_3 = \frac{1}{2}\rho\ell^3 u^2 \tag{2.51}$$

are dimensionalization constants with fluid density ρ, vehicle forward speed u, and characteristic length ℓ which is usually taken to be the vehicle length along the major axis. These coefficients are listed in Tables B.1 and B.2.

Propeller

The propeller model in [8] defines the thrust T and torque Q generated by the propeller as a function of both the water-relative forward speed of the vehicle u, and of the speed of advance V_A. V_A is calculated from u as

$$V_A = u\,(1 - wf)\,, \tag{2.52}$$

where wake fraction wf is a constant. Thrust and torque are calculated from non-dimensional coefficients $K_T(J)$ and $K_Q(J)$, which in turn are functions of advance ratio J:

$$J = \frac{V_A}{nD} \tag{2.53}$$

$$T = K_T(J)\rho n^2 D^4 \tag{2.54}$$

$$Q = K_Q(J)\rho n^2 D^5 \tag{2.55}$$

$K_T(J)$, $K_Q(J)$, and wf are empirically determined, as in [9]. These are presented for the VT 690 in Table B.5 with coefficients in Tables B.1 and B.2.

The propeller thrust and torque is represented in body coordinates as

$$\boldsymbol{\tau}_P(\boldsymbol{\nu}, n) = \begin{bmatrix} T \\ 0 \\ 0 \\ Q \\ 0 \\ 0 \end{bmatrix}. \tag{2.56}$$

The total generalized control force $\boldsymbol{\tau}_U(\boldsymbol{\nu}, \boldsymbol{u})$ is the superposition of contributions from the control surfaces and propeller:

$$\boldsymbol{\tau}_U(\boldsymbol{\nu}, \boldsymbol{u}) = \boldsymbol{\tau}_\delta(\boldsymbol{\nu}, \delta) + \boldsymbol{\tau}_P(\boldsymbol{\nu}, n), \tag{2.57}$$

where the control vector $\boldsymbol{u}$ is defined to be

$$\boldsymbol{u} = \begin{bmatrix} \delta \\ n \end{bmatrix} = \begin{bmatrix} \delta_s \\ \delta_p \\ \delta_b \\ \delta_t \\ n \end{bmatrix}. \tag{2.58}$$

2.3.6 Viscous hydrodynamics

Force due to viscous hydrodynamics is modeled in this work as a nonlinear function of instantaneous velocity

$$\boldsymbol{\tau}_\nu(\boldsymbol{\nu}) = f(\boldsymbol{\nu}). \tag{2.59}$$

Several viscous hydrodynamic force models are presented in Chapter 3.

2.4 State-space model

The full equations of motion can be represented in matrix form by equating (2.17) with (2.31) and substituting the models in (2.35), (2.59), (2.44), and (2.57) to obtain

$$\boldsymbol{M}_{RB}\dot{\boldsymbol{\nu}} + \boldsymbol{C}_{RB}(\boldsymbol{\nu})\boldsymbol{\nu} = \boldsymbol{M}_A\dot{\boldsymbol{\nu}} + \boldsymbol{C}_A(\boldsymbol{\nu})\boldsymbol{\nu} + \boldsymbol{\tau}_G(\boldsymbol{\eta}) + \boldsymbol{\tau}_U(\boldsymbol{\nu}, \boldsymbol{u}) + \boldsymbol{\tau}_\nu(\boldsymbol{\nu}). \tag{2.60}$$

The form of this equation is similar to that proposed by Caccia in [10], with notation similar to Fossen in [5]. This equation can be reorganized into a form more suitable for simulation

by shifting acceleration terms $\dot{\boldsymbol{\nu}}$ to one side,

$$\boldsymbol{M}_{RB}\dot{\boldsymbol{\nu}} - \boldsymbol{M}_A\dot{\boldsymbol{\nu}} = -\left(\boldsymbol{C}_{RB}(\boldsymbol{\nu})\boldsymbol{\nu} - \boldsymbol{C}_A(\boldsymbol{\nu})\boldsymbol{\nu}\right) + \boldsymbol{\tau}_G(\boldsymbol{\eta}) + \boldsymbol{\tau}_U(\boldsymbol{\nu}, \boldsymbol{u}) + \boldsymbol{\tau}_\nu(\boldsymbol{\nu}), \tag{2.61}$$

and substituting

$$\boldsymbol{M} = \boldsymbol{M}_{RB} - \boldsymbol{M}_A \tag{2.62}$$

$$\boldsymbol{C}(\boldsymbol{\nu}) = \boldsymbol{C}_{RB}(\boldsymbol{\nu}) - \boldsymbol{C}_A(\boldsymbol{\nu}) \tag{2.63}$$

$$\boldsymbol{\tau}(\boldsymbol{\eta}, \boldsymbol{\nu}, \boldsymbol{u}) = -\boldsymbol{C}(\boldsymbol{\nu})\boldsymbol{\nu} + \boldsymbol{\tau}_G(\boldsymbol{\eta}) + \boldsymbol{\tau}_U(\boldsymbol{\nu}, \boldsymbol{u}) + \boldsymbol{\tau}_\nu(\boldsymbol{\nu}), \tag{2.64}$$

to obtain

$$\boldsymbol{M}\dot{\boldsymbol{\nu}} = \boldsymbol{\tau}(\boldsymbol{\eta}, \boldsymbol{\nu}, \boldsymbol{u}). \tag{2.65}$$

Here, $\boldsymbol{M}$ is the total inertia matrix and $\boldsymbol{C}(\boldsymbol{\nu})$ is the total Coriolis and centripetal function. This work adopts the sign convention that the rigid-body inertia matrix $\boldsymbol{M}_{RB} > 0$ is positive definite and that the added-mass inertia matrix $\boldsymbol{M}_A \leq 0$ is negative semi-definite, which holds for fully submerged vehicles [2]. The total inertia matrix $\boldsymbol{M}$ is therefore positive definite, so $\boldsymbol{M}^{-1}$ exists and

$$\dot{\boldsymbol{\nu}} = \boldsymbol{M}^{-1}\boldsymbol{\tau}(\boldsymbol{\eta}, \boldsymbol{\nu}, \boldsymbol{u}). \tag{2.66}$$

The vehicle state $\boldsymbol{x} \in \mathbb{R}^{12}$ is given as

$$\boldsymbol{x} = \begin{bmatrix} \boldsymbol{\eta} \\ \boldsymbol{\nu} \end{bmatrix} \tag{2.67}$$

where $\boldsymbol{\eta}$ is the vehicle pose in the inertial frame, and $\boldsymbol{\nu}$ is the vehicle velocity in the body frame. The derivative of the state is then

$$\dot{\boldsymbol{x}} = \begin{bmatrix} \dot{\boldsymbol{\eta}} \\ \dot{\boldsymbol{\nu}} \end{bmatrix} \tag{2.68}$$

The derivative of the state vector is related to the state through (2.11) and (2.66), which leads to this concise representation

$$\dot{\boldsymbol{x}} = \begin{bmatrix} \dot{\boldsymbol{\eta}} \\ \dot{\boldsymbol{\nu}} \end{bmatrix} = \begin{bmatrix} \boldsymbol{P}(\boldsymbol{\eta}) & 0 \\ 0 & \boldsymbol{M}^{-1} \end{bmatrix} \begin{bmatrix} \boldsymbol{\nu} \\ \boldsymbol{\tau}(\boldsymbol{\eta}, \boldsymbol{\nu}, \boldsymbol{u}) \end{bmatrix}. \tag{2.69}$$

2.5 State estimation

The state vector in (2.67) and derivative of the state vector (2.68) are populated in practice from a set of sensors that generally only measure part of the vehicle state. The rest of the state and derivative of the state must be estimated from known quantities. The 690 AUV is equipped with a Doppler velocity log (DVL), attitude heading reference system (AHRS) and depth sensor, which together provide the raw data which is used to estimate the vehicle state vector. The DVL measures the translational velocity vector $\boldsymbol{v} = [u\ v\ w]$. The AHRS uses a triaxial gyroscope, triaxial accelerometer, and triaxial magnetometer to produce an estimate of vehicle orientation $\boldsymbol{\theta} = [\phi\ \theta\ \psi]$. The gyroscope directly measures the rotational velocity vector $\boldsymbol{\omega} = [p\ q\ r]$. The accelerometer measures the total acceleration vector, which is the sum of vehicle translational acceleration and acceleration due to gravity. The gravity vector in body coordinates is estimated online by the AHRS, and is subtracted from the total acceleration to produce the translational acceleration vector $\dot{\boldsymbol{v}} = [\dot{u}\ \dot{v}\ \dot{w}]$. The depth

sensor measures ambient pressure, and estimates vehicle depth z in the inertial frame.

The sampling time and sampling rate is different for each sensor. Raw data is interpolated and resampled so that all data appears to be sampled at the same time and at the same rate. The data set is also filtered in order to replace inferior data with better estimates. For instance, translational velocity $\boldsymbol{v}$ measured by the DVL is generated at 4Hz, which is much slower than the other sensors. Aggressive maneuvers are not captured by the DVL, and are better represented by estimating velocity from acceleration measured by the AHRS. A rigorous treatment of sensor error is beyond the scope of this work. This section presents an ad-hoc state estimation procedure which fuses the sensor data into a consistent state vector.

The raw data generated by each sensor is used to initially populate the state vector

$$\boldsymbol{x}^0 = [0\ 0\ z\ \phi\ \theta\ \psi\ u\ v\ w\ p\ q\ r]^\top \tag{2.70}$$

and the derivative of the state vector

$$\dot{\boldsymbol{x}}^0 = [0\ 0\ 0\ 0\ 0\ 0\ \dot{u}\ \dot{v}\ \dot{w}\ 0\ 0\ 0]^\top \tag{2.71}$$

where the superscript 0 indicates the step in the data post-processing sequence.

The notation adopted here is that an overbar $\bar{\cdot}$ represents the exact value of a signal, and a tilde $\tilde{\cdot}$ represents the additive measurement error on that signal. For instance, the depth sensor error model is $z(t) = \bar{z}(t) + \tilde{z}$, where the depth sensor error $\tilde{z}$ is a constant bias. Depth z and orientation $\phi\ \theta\ \psi$ are assumed to be exact in (2.70). Therefore depth sensor measurement error $\tilde{z} = 0$, and

$$\bar{z}(t) = z(t). \tag{2.72}$$

Similarly, $\tilde{\phi}, \tilde{\theta}, \tilde{\psi} = 0$, so

$$\bar{\phi}(t) = \phi(t) \tag{2.73}$$

$$\bar{\theta}(t) = \theta(t) \tag{2.74}$$

$$\bar{\psi}(t) = \psi(t). \tag{2.75}$$

Inertial translational rates are estimated from body-frame translational velocities

$$\begin{bmatrix} \dot{x}(t) \\ \dot{y}(t) \\ \dot{z}(t) \end{bmatrix} = \boldsymbol{P_v}(\boldsymbol{\theta}) \begin{bmatrix} u(t) \\ v(t) \\ w(t) \end{bmatrix} \tag{2.76}$$

where the depth rate is replaced by taking the time derivative of depth

$$\bar{\dot{z}}(t) = \frac{d}{dt}\bar{z}(t) \tag{2.77}$$

and mapped back into the body frame

$$\begin{bmatrix} u(t) \\ v(t) \\ \bar{w}(t) \end{bmatrix} = \boldsymbol{P_v}^{-1}(\boldsymbol{\theta}) \begin{bmatrix} \dot{x}(t) \\ \dot{y}(t) \\ \bar{\dot{z}}(t) \end{bmatrix}. \tag{2.78}$$

Similarly, inertial rotational rates are estimated from the time derivative of orientation

$$\dot{\phi}(t) = \frac{d}{dt}\bar{\phi}(t) \tag{2.79}$$

$$\dot{\theta}(t) = \frac{d}{dt}\bar{\theta}(t) \tag{2.80}$$

$$\dot{\psi}(t) = \frac{d}{dt}\bar{\psi}(t). \tag{2.81}$$

The state and state derivative vectors are estimated at step 1 as

$$\boldsymbol{x}^1 = \begin{bmatrix} 0 \; 0 \; \bar{z} \; \bar{\phi} \; \bar{\theta} \; \bar{\psi} \; u \; v \; \bar{w} \; p \; q \; r \end{bmatrix}^\top \tag{2.82}$$

$$\dot{\boldsymbol{x}}^1 = \begin{bmatrix} \dot{x} \; \dot{y} \; \dot{\bar{z}} \; \dot{\phi} \; \dot{\theta} \; \dot{\psi} \; \dot{u} \; \dot{v} \; \dot{w} \; 0 \; 0 \; 0 \end{bmatrix}^\top . \tag{2.83}$$

The gyroscopes and accelerometers are both modeled as having a constant bias offset in their measurements. This is a valid assumption for short data sets, though the gyros in fact drift over time. The accelerometer sensor model is

$$\dot{\boldsymbol{v}}(t) = \bar{\dot{\boldsymbol{v}}}(t) + \tilde{\dot{\boldsymbol{v}}} \tag{2.84}$$

where the 'true' translational acceleration $\bar{\dot{\boldsymbol{v}}}(t)$ is modeled with a constant accelerometer bias $\tilde{\dot{\boldsymbol{v}}}$. The accelerometer bias is calculated to minimize

$$\left\| \boldsymbol{v}(t) - \left(\int_{t_0}^{t} \dot{\boldsymbol{v}}(\tau) d\tau + \boldsymbol{v}(t_0) \right) \right\|_{\mathcal{L}_2} \tag{2.85}$$

where the $\mathcal{L}_2$ norm is defined in [11].

Similarly, the rotational velocity $\boldsymbol{\omega}$ as measured by the AHRS gyroscopes is modeled as

$$\boldsymbol{\omega}(t) = \bar{\boldsymbol{\omega}}(t) + \tilde{\boldsymbol{\omega}} \tag{2.86}$$

where the 'true' rotational velocity $\bar{\boldsymbol{\omega}}(t)$ is modeled with a constant gyro bias $\tilde{\boldsymbol{\omega}}$. The gyro bias is calculated to minimize

$$\left\| \boldsymbol{\theta}(t) - \left(\int_{t_0}^{t} \boldsymbol{P}_{\boldsymbol{\omega}}(\boldsymbol{\theta}(\tau)) \boldsymbol{\omega}(\tau) d\tau + \boldsymbol{\theta}(t_0) \right) \right\|_{\mathcal{L}_2} . \tag{2.87}$$

Translational velocity is then estimated as the integral of translational acceleration

$$\bar{\boldsymbol{v}}(t) = \int_{t_0}^{t} \bar{\dot{\boldsymbol{v}}}(\tau) d\tau + \bar{\boldsymbol{v}}(0) \tag{2.88}$$

which replaces the raw velocity data reported by the DVL. Rotational acceleration is estimated as the derivative of rotational velocity

$$\bar{\dot{\boldsymbol{\omega}}}(t) = \frac{d}{dt}\bar{\boldsymbol{\omega}}(t), \tag{2.89}$$

inertial rotational rates are transformed from body rotational rates

$$\bar{\dot{\boldsymbol{\theta}}}(t) = \boldsymbol{P}_{\boldsymbol{\omega}}(\boldsymbol{\theta})\bar{\boldsymbol{\omega}}(t), \tag{2.90}$$

inertial translational rates are transformed from body translation rates

$$\bar{\dot{\boldsymbol{r}}}_0(t) = \boldsymbol{P}_{\boldsymbol{v}}(\boldsymbol{\theta})\bar{\boldsymbol{v}}(t), \tag{2.91}$$

and inertial position is integrated from inertial translation rates

$$\bar{\boldsymbol{r}}_0(t) = \int \bar{\dot{\boldsymbol{r}}}_0(t) + \boldsymbol{r}_0(0). \tag{2.92}$$

The state vector and derivative of the state vector are updated from (2.88) - (2.92) to become

$$\bar{\boldsymbol{x}} = \left[\bar{x}\ \bar{y}\ \bar{z}\ \bar{\phi}\ \bar{\theta}\ \bar{\psi}\ \bar{u}\ \bar{v}\ \bar{w}\ \bar{p}\ \bar{q}\ \bar{r}\right]^\top \tag{2.93}$$

$$\bar{\dot{\boldsymbol{x}}} = \left[\bar{\dot{x}}\ \bar{\dot{y}}\ \bar{\dot{z}}\ \bar{\dot{\phi}}\ \bar{\dot{\theta}}\ \bar{\dot{\psi}}\ \bar{\dot{u}}\ \bar{\dot{v}}\ \bar{\dot{w}}\ \bar{\dot{p}}\ \bar{\dot{q}}\ \bar{\dot{r}}\right]^\top. \tag{2.94}$$

These are continuous spline representations of the state and rate vectors. Discrete represen-

tations are obtained by sampling $\bar{\boldsymbol{x}}(t)$ and $\bar{\dot{\boldsymbol{x}}}(t)$ at each time in the vector $\boldsymbol{t}(k)$, to obtain $\bar{\boldsymbol{x}}(k)$ and $\bar{\dot{\boldsymbol{x}}}(k)$.

Chapter 3

Viscous hydrodynamics

This chapter defines *viscous hydrodynamics*, and presents several models which describe a rigid body moving through a viscous fluid. Viscous hydrodynamics describes the dissipative forces caused by frictional drag D_F and pressure drag D_P [2], as well as conservative forces such as the "Munk" moment. Frictional drag is influenced by the character of the fluid flow, which can vary between *laminar* and *turbulent* flow. The character of the flow is largely a function of the Reynolds number Re, which is a non-dimensional measure of speed. Flow tends to be laminar at low Reynolds numbers and turbulent at high Reynolds numbers, where the transition typically occurs for Reynolds numbers between 10^5 and 2×10^6. Reynolds number is defined to be

$$Re = \frac{uL}{\nu}, \tag{3.1}$$

where u is forward speed, ν is the fluid kinematic viscosity, and L is a characteristic length, usually the length of the vehicle along the longitudinal axis.

Frictional drag D_F is caused by tangential shear stress, and is defined in terms of a frictional

drag coefficient $C_F(Re)$. The coefficient of friction $C_F(Re)$ varies with Reynolds number, as described in [8] for the example of a series of planks with different surface roughness. Frictional drag is usually expressed

$$D_F = \frac{1}{2} C_F(Re) \rho V^2 A, \tag{3.2}$$

where ρ is the fluid density, V is speed, and A is a characteristic area, usually taken to be the cross-sectional area of the vehicle.

Pressure drag D_P is caused by normal pressure stress, and is defined in terms of a pressure drag coefficient C_P. Unlike the frictional drag coefficient $C_F(Re)$, the pressure drag coefficient C_P for streamlined vehicles is not directly dependent on Reynolds number. Pressure drag is defined to be

$$D_P = \frac{1}{2} C_P \rho V^2 A. \tag{3.3}$$

The total drag $D = D_F + D_P$ is a scalar measure of the hydrodynamic force experienced by an unaccelerated vehicle on a nominal forward trajectory. An underwater vehicle following a trajectory such as that shown in Figure 1.2 is not adequately described by such a model. Instead, viscous viscous hydrodynamic terms should be modeled by estimating the instantaneous contribution $\boldsymbol{\tau}_\nu(\boldsymbol{\nu})$ as a quasi-steady, nonlinear function of body-fixed velocity. There is no analytic form for $\boldsymbol{\tau}_\nu(\boldsymbol{\nu})$ for a particular geometry or configuration, as there is for added-mass and restoring forces.

3.1 Model structure

Let the viscous hydrodynamic force vector $\boldsymbol{\tau}_\nu \in \mathbb{R}^6$ be modeled as a nonlinear function of velocity, $\boldsymbol{\tau}_\nu(\boldsymbol{\nu}) : \mathbb{R}^6 \to \mathbb{R}^6$. This viscous hydrodynamic model is composed of six scalar functions,

$$\boldsymbol{\tau}_\nu(\boldsymbol{\nu}) = \begin{bmatrix} \tau_\nu^X(\boldsymbol{\nu}) \\ \tau_\nu^Y(\boldsymbol{\nu}) \\ \tau_\nu^Z(\boldsymbol{\nu}) \\ \tau_\nu^K(\boldsymbol{\nu}) \\ \tau_\nu^M(\boldsymbol{\nu}) \\ \tau_\nu^N(\boldsymbol{\nu}) \end{bmatrix}, \tag{3.4}$$

where the superscript denotes the axis to which the scalar function applies. For example, $\tau_\nu^X(\boldsymbol{\nu})$ is the viscous hydrodynamic force along the surge axis, and $\tau_\nu^M(\boldsymbol{\nu})$ is the viscous hydrodynamic moment about the pitch axis.

Each scalar function in (3.4) can be expressed as a linear combination of basis functions. For example, the surge force $\tau_\nu^X(\boldsymbol{\nu})$ might be modeled as a function of linear and quadratic surge velocity, u and u^2:

$$\tau_\nu^X(\boldsymbol{\nu}) = X_u u + X_{uu} u^2, \tag{3.5}$$

which can be expressed

$$\tau_\nu^X(\boldsymbol{\nu}) = \begin{bmatrix} X_u & X_{uu} \end{bmatrix} \begin{bmatrix} u \\ u^2 \end{bmatrix}. \tag{3.6}$$

Similarly, the viscous hydrodynamic moment in pitch might be modeled as a function of surge velocity u and heave velocity w:

$$\tau_{\nu}^{M}(\boldsymbol{\nu}) = M_u u + M_{uw} uw, \tag{3.7}$$

which can be expressed

$$\tau_{\nu}^{M}(\boldsymbol{\nu}) = \begin{bmatrix} M_u & M_{uw} \end{bmatrix} \begin{bmatrix} u \\ uw \end{bmatrix}. \tag{3.8}$$

Let $\boldsymbol{\xi}(\boldsymbol{\nu})$ be the vector of basis functions for the model described by (3.5) and (3.8), where

$$\boldsymbol{\xi}(\boldsymbol{\nu}) = \begin{bmatrix} u \\ u^2 \\ uw \end{bmatrix}. \tag{3.9}$$

Then the scalar viscous hydrodynamic functions (3.5) and (3.8) may be rewritten as

$$\tau_{\nu}^{X}(\boldsymbol{\nu}) = \begin{bmatrix} X_u & X_{uu} & 0 \end{bmatrix} \begin{bmatrix} u \\ u^2 \\ uw \end{bmatrix} = \boldsymbol{K}^X \boldsymbol{\xi}(\boldsymbol{\nu}) \tag{3.10}$$

and

$$\tau_{\nu}^{M}(\boldsymbol{\nu}) = \begin{bmatrix} M_u & 0 & M_{uw} \end{bmatrix} \begin{bmatrix} u \\ u^2 \\ uw \end{bmatrix} = \boldsymbol{K}^M \boldsymbol{\xi}(\boldsymbol{\nu}) \tag{3.11}$$

where $\boldsymbol{K}^X = [X_u \; X_{uu} \; 0]$ and $\boldsymbol{K}^M = [M_u \; 0 \; M_{uw}]$ are constant coefficient vectors.

The general viscous hydrodynamic model in 3.4 may be expressed using the notation in (3.10) and (3.11) as

$$\boldsymbol{\tau}_\nu(\boldsymbol{\nu}) = \begin{bmatrix} \boldsymbol{\tau}_\nu^X(\boldsymbol{\nu}) \\ \boldsymbol{\tau}_\nu^Y(\boldsymbol{\nu}) \\ \boldsymbol{\tau}_\nu^Z(\boldsymbol{\nu}) \\ \boldsymbol{\tau}_\nu^K(\boldsymbol{\nu}) \\ \boldsymbol{\tau}_\nu^M(\boldsymbol{\nu}) \\ \boldsymbol{\tau}_\nu^N(\boldsymbol{\nu}) \end{bmatrix} = \begin{bmatrix} \boldsymbol{K}^X\boldsymbol{\xi}(\boldsymbol{\nu}) \\ \boldsymbol{K}^Y\boldsymbol{\xi}(\boldsymbol{\nu}) \\ \boldsymbol{K}^Z\boldsymbol{\xi}(\boldsymbol{\nu}) \\ \boldsymbol{K}^K\boldsymbol{\xi}(\boldsymbol{\nu}) \\ \boldsymbol{K}^M\boldsymbol{\xi}(\boldsymbol{\nu}) \\ \boldsymbol{K}^N\boldsymbol{\xi}(\boldsymbol{\nu}) \end{bmatrix} = \begin{bmatrix} \boldsymbol{K}^X \\ \boldsymbol{K}^Y \\ \boldsymbol{K}^Z \\ \boldsymbol{K}^K \\ \boldsymbol{K}^M \\ \boldsymbol{K}^N \end{bmatrix} \boldsymbol{\xi}(\boldsymbol{\nu}) = \boldsymbol{K}\boldsymbol{\xi}(\boldsymbol{\nu}), \tag{3.12}$$

where $\boldsymbol{\xi}(\boldsymbol{\nu}) \in \mathbb{R}^{n_\xi}$ is the vector of basis functions, and $\boldsymbol{K} \in \mathbb{R}^{6\times n_\xi}$ is the viscous hydrodynamic coefficient matrix.

The following sections will describe several standard viscous hydrodynamic models, and express them in the notation in (3.12). In order to directly compare one model with another, it is necessary to define a unified vector of basis functions which spans all models. This vector $\boldsymbol{\xi}(\boldsymbol{\nu})$ is defined in Appendix C in (C.12).

3.2 Viscous hydrodynamic models

3.2.1 Gertler & Hagen

The prototypical example of a component-form model is that created by Gertler and Hagen in [1]. The hydrodynamic model proposed by Gertler and Hagen is the result of work done by the US Navy between 1956-1967 to produce a 6-DOF model suitable for simulation of a set of submarine maneuvers. These equations form a so called *lumped-parameter* model, because they make no distinction between different physical contributions in the model structure.

Many terms arise in the derivation of added-mass Coriolis and centripetal effects which take the form of coupled velocities (i.e. $u \times r$ or $v \times p$). For that reason, it is not clear which of the terms in the Gertler-Hagen equations are explicitly due to viscous hydrodynamics, or due to Coriolis and centripetal effects, or some combination of the two. Therefore, the terms presented in (3.13) - (3.18) are all those terms from the Gertler-Hagen equations which are not explicitly control or restoring terms. The equations are given as

$$\begin{aligned}\tau_\nu^{\mathrm{X}}(\boldsymbol{\nu}) =& \mathrm{X_{qq}}q^2 + \mathrm{X_{rr}}r^2 + \mathrm{X_{uu}}u^2 + \mathrm{X_{vv}}v^2 + \mathrm{X_{ww}}w^2 + \mathrm{X_{vv\eta}}v^2\left(\eta - 1\right) \\ &+ \mathrm{X_{ww\eta}}w^2\left(\eta - 1\right) + \mathrm{X_{pr}}pr + \mathrm{X_{vr}}vr + \mathrm{X_{wq}}wq\end{aligned} \tag{3.13}$$

$$\begin{aligned}\tau_\nu^{\mathrm{Y}}(\boldsymbol{\nu}) =& \mathrm{Y_{uu}}u^2 + \mathrm{Y_{vV}}v\mathrm{V} + \mathrm{Y_{pq}}pq + \mathrm{Y_{qr}}qr + \mathrm{Y_{up}}up + \mathrm{Y_{ur}}ur + \mathrm{Y_{vq}}vq + \mathrm{Y_{wp}}wp \\ &+ \mathrm{Y_{wr}}wr + \mathrm{Y_{uv}}uv + \mathrm{Y_{vw}}vw + \mathrm{Y_{|r|V_v}}\left|r\right|\mathrm{V_v} + \mathrm{Y_{p|p|}}p\left|p\right| \\ &+ \mathrm{Y_{vV\eta}}v\mathrm{V}\left(\eta - 1\right) + \mathrm{Y_{ur\eta}}ur\left(\eta - 1\right) + \mathrm{Y_{uv\eta}}uv\left(\eta - 1\right)\end{aligned} \tag{3.14}$$

$$\begin{aligned}\tau_\nu^{\mathrm{Z}}(\boldsymbol{\nu}) =& \mathrm{Z_{pp}}p^2 + \mathrm{Z_{rr}}r^2 + \mathrm{Z_{uu}}u^2 + \mathrm{Z_{vv}}v^2 + \mathrm{Z_{u|w|}}u\left|w\right| + \mathrm{Z_{wV}}w\mathrm{V} + \mathrm{Z_{pr}}pr \\ &+ \mathrm{Z_{uq}}uq + \mathrm{Z_{vp}}vp + \mathrm{Z_{vr}}vr + \mathrm{Z_{uw}}uw + \mathrm{Z_{|q|V_w}}\left|q\right|\mathrm{V_w} + \mathrm{Z_{|w|V}}\left|w\right|\mathrm{V} \\ &+ \mathrm{Z_{wV\eta}}w\mathrm{V}\left(\eta - 1\right) + \mathrm{Z_{uq\eta}}uq\left(\eta - 1\right) + \mathrm{Z_{uw\eta}}uw\left(\eta - 1\right)\end{aligned} \tag{3.15}$$

$$\begin{aligned}\tau_\nu^{\mathrm{K}}(\boldsymbol{\nu}) =& \mathrm{K_{uu}}u^2 + \mathrm{K_{uu\eta}}u^2\left(\eta - 1\right) + \mathrm{K_{vV}}v\mathrm{V} + \mathrm{K_{pq}}pq + \mathrm{K_{qr}}qr + \mathrm{K_{up}}up + \mathrm{K_{ur}}ur \\ &+ \mathrm{K_{vq}}vq + \mathrm{K_{wp}}wp + \mathrm{K_{wr}}wr + \mathrm{K_{uv}}uv + \mathrm{K_{vw}}vw + \mathrm{K_{p|p|}}p\left|p\right|\end{aligned} \tag{3.16}$$

$$\begin{aligned}\tau_\nu^{\mathrm{M}}(\boldsymbol{\nu}) =& \mathrm{M_{pp}}p^2 + \mathrm{M_{rr}}r^2 + \mathrm{M_{uu}}u^2 + \mathrm{M_{vv}}v^2 + \mathrm{M_{qV}}q\mathrm{V} + \mathrm{M_{wV}}w\mathrm{V} + \mathrm{M_{pr}}pr + \mathrm{M_{uq}}uq \\ &+ \mathrm{M_{vp}}vp + \mathrm{M_{vr}}vr + \mathrm{M_{uw}}uw + \mathrm{M_{|w|V}}\left|w\right|\mathrm{V} + \mathrm{M_{q|q|}}q\left|q\right| + \mathrm{M_{u|w|}}u\left|w\right| \\ &+ \mathrm{M_{wV\eta}}w\mathrm{V}\left(\eta - 1\right) + \mathrm{M_{uq\eta}}uq\left(\eta - 1\right) + \mathrm{M_{uw\eta}}uw\left(\eta - 1\right)\end{aligned} \tag{3.17}$$

$$\begin{aligned}\tau_\nu^{\mathrm{N}}(\boldsymbol{\nu}) =& \mathrm{N_{uu}}u^2 + \mathrm{N_{rV}}r\mathrm{V} + \mathrm{N_{vV}}v\mathrm{V} + \mathrm{N_{pq}}pq + \mathrm{N_{qr}}qr + \mathrm{N_{up}}up + \mathrm{N_{ur}}ur + \mathrm{N_{vq}}vq \\ &+ \mathrm{N_{wp}}wp + \mathrm{N_{wr}}wr + \mathrm{N_{uv}}uv + \mathrm{N_{vw}}vw + \mathrm{N_{r|r|}}r\left|r\right| + \mathrm{N_{vV\eta}}v\mathrm{V}\left(\eta - 1\right) \\ &+ \mathrm{N_{ur\eta}}ur\left(\eta - 1\right) + \mathrm{N_{uv\eta}}uv\left(\eta - 1\right)\end{aligned} \quad . \tag{3.18}$$

It is instructive to see a component-form model such as (3.13) - (3.18) written out in the form of (3.12). Let $\boldsymbol{\xi}(\boldsymbol{\nu})$ be defined as in (C.12), and let $\boldsymbol{K}$ be defined as the following:

$$\boldsymbol{K} = \left[\begin{matrix} 0 & 0 & 0 & 0 & 0 & 0 & 0 & 0 & 0 & 0 & 0 & 0 & \mathrm{X_{uu}} & 0 & 0 & 0 & 0 & 0 \\ 0 & 0 & 0 & 0 & 0 & 0 & 0 & 0 & 0 & 0 & 0 & 0 & \mathrm{Y_{uu}} & \mathrm{Y_{uv}} & 0 & \mathrm{Y_{up}} & 0 & \mathrm{Y_{ur}} \\ 0 & 0 & 0 & 0 & 0 & 0 & 0 & 0 & 0 & 0 & 0 & 0 & \mathrm{Z_{uu}} & 0 & \mathrm{Z_{uw}} & 0 & \mathrm{Z_{uq}} & 0 \\ 0 & 0 & 0 & 0 & 0 & 0 & 0 & 0 & 0 & 0 & 0 & 0 & \mathrm{K_{uu}} & \mathrm{K_{uv}} & 0 & \mathrm{K_{up}} & 0 & \mathrm{K_{ur}} \\ 0 & 0 & 0 & 0 & 0 & 0 & 0 & 0 & 0 & 0 & 0 & 0 & \mathrm{M_{uu}} & 0 & \mathrm{M_{uw}} & 0 & \mathrm{M_{uq}} & 0 \\ 0 & 0 & 0 & 0 & 0 & 0 & 0 & 0 & 0 & 0 & 0 & 0 & \mathrm{N_{uu}} & \mathrm{N_{uv}} & 0 & \mathrm{N_{up}} & 0 & \mathrm{N_{ur}} \end{matrix} \right. \cdots$$

$$\cdots \begin{matrix} \mathrm{X_{vv}} & 0 & 0 & 0 & \mathrm{X_{vr}} & \mathrm{X_{ww}} & 0 & \mathrm{X_{wq}} & 0 & 0 & 0 & \mathrm{X_{pr}} \\ 0 & \mathrm{Y_{vw}} & 0 & \mathrm{Y_{vq}} & 0 & 0 & \mathrm{Y_{wp}} & 0 & \mathrm{Y_{wr}} & 0 & \mathrm{Y_{pq}} & 0 \\ \mathrm{Z_{vv}} & 0 & \mathrm{Z_{vp}} & 0 & \mathrm{Z_{vr}} & 0 & 0 & 0 & 0 & \mathrm{Z_{pp}} & 0 & \mathrm{Z_{pr}} \\ 0 & \mathrm{K_{vw}} & 0 & \mathrm{K_{vq}} & 0 & 0 & \mathrm{K_{wp}} & 0 & \mathrm{K_{wr}} & 0 & \mathrm{K_{pq}} & 0 \\ \mathrm{M_{vv}} & 0 & \mathrm{M_{vp}} & 0 & \mathrm{M_{vr}} & 0 & 0 & 0 & 0 & \mathrm{M_{pp}} & 0 & \mathrm{M_{pr}} \\ 0 & \mathrm{N_{vw}} & 0 & \mathrm{N_{vq}} & 0 & 0 & \mathrm{N_{wp}} & 0 & \mathrm{N_{wr}} & 0 & \mathrm{N_{pq}} & 0 \end{matrix} \cdots$$

$$\cdots \begin{matrix} \mathrm{X_{qq}} & 0 & \mathrm{X_{rr}} & 0 & 0 & 0 & 0 & 0 & 0 & 0 & 0 & 0 & 0 & 0 & 0 & 0 & 0 & 0 & 0 \\ 0 & \mathrm{Y_{qr}} & 0 & 0 & 0 & 0 & 0 & 0 & 0 & 0 & 0 & 0 & 0 & 0 & 0 & 0 & 0 & 0 & 0 \\ 0 & 0 & \mathrm{Z_{rr}} & 0 & 0 & \mathrm{Z_{u|w|}} & 0 & 0 & 0 & 0 & 0 & 0 & 0 & 0 & 0 & 0 & 0 & 0 & 0 \\ 0 & \mathrm{K_{qr}} & 0 & 0 & 0 & 0 & 0 & 0 & 0 & 0 & 0 & 0 & 0 & 0 & 0 & 0 & 0 & 0 & 0 \\ 0 & 0 & \mathrm{M_{rr}} & 0 & 0 & \mathrm{M_{u|w|}} & 0 & 0 & 0 & 0 & 0 & 0 & 0 & 0 & 0 & 0 & 0 & 0 & 0 \\ 0 & \mathrm{N_{qr}} & 0 & 0 & 0 & 0 & 0 & 0 & 0 & 0 & 0 & 0 & 0 & 0 & 0 & 0 & 0 & 0 & 0 \end{matrix} \cdots$$

$$\cdots \begin{matrix} 0 & 0 & 0 & 0 & 0 & 0 & 0 & 0 & 0 & 0 & 0 & 0 & 0 & 0 & 0 & 0 & 0 & 0 & 0 & 0 \\ 0 & 0 & 0 & 0 & 0 & \mathrm{Y_{p|p|}} & 0 & 0 & 0 & 0 & 0 & 0 & 0 & 0 & 0 & 0 & 0 & 0 & 0 & 0 \\ 0 & 0 & 0 & 0 & 0 & 0 & 0 & 0 & 0 & 0 & 0 & 0 & 0 & 0 & 0 & 0 & 0 & 0 & 0 & 0 \\ 0 & 0 & 0 & 0 & 0 & \mathrm{K_{p|p|}} & 0 & 0 & 0 & 0 & 0 & 0 & 0 & 0 & 0 & 0 & 0 & 0 & 0 & 0 \\ 0 & 0 & 0 & 0 & 0 & 0 & 0 & 0 & 0 & 0 & 0 & 0 & \mathrm{M_{q|q|}} & 0 & 0 & 0 & 0 & 0 & 0 & 0 \\ 0 & 0 & 0 & 0 & 0 & 0 & 0 & 0 & 0 & 0 & 0 & 0 & 0 & 0 & 0 & 0 & 0 & 0 & 0 & \mathrm{N_{r|r|}} \end{matrix} \cdots$$

$$\cdots \begin{matrix} 0 & 0 & 0 & 0 & 0 & 0 & 0 & 0 & 0 & 0 & 0 & 0 & 0 & 0 & 0 & 0 & 0 \\ 0 & \mathrm{Y_{vV}} & 0 & 0 & 0 & 0 & 0 & 0 & 0 & 0 & 0 & 0 & 0 & 0 & 0 & 0 & 0 \\ 0 & 0 & \mathrm{Z_{wV}} & 0 & 0 & 0 & 0 & 0 & \mathrm{Z_{|w|V}} & 0 & 0 & 0 & 0 & 0 & 0 & 0 & 0 \\ 0 & \mathrm{K_{vV}} & 0 & 0 & 0 & 0 & 0 & 0 & 0 & 0 & 0 & 0 & 0 & 0 & 0 & 0 & 0 \\ 0 & 0 & \mathrm{M_{wV}} & 0 & \mathrm{M_{qV}} & 0 & 0 & 0 & \mathrm{M_{|w|V}} & 0 & 0 & 0 & 0 & 0 & 0 & 0 & 0 \\ 0 & \mathrm{N_{vV}} & 0 & 0 & 0 & \mathrm{N_{rV}} & 0 & 0 & 0 & 0 & 0 & 0 & 0 & 0 & 0 & 0 & 0 \end{matrix} \cdots$$

$$
\cdots
\begin{matrix}
0 & 0 & 0 & 0 & 0 & 0 & 0 & 0 & 0 & 0 & 0 & 0 & 0 & 0 & 0 & 0 & 0 & 0 & 0 \\
0 & 0 & 0 & 0 & 0 & 0 & Y_{|r|V_v} & 0 & 0 & 0 & 0 & 0 & 0 & 0 & 0 & 0 & 0 & 0 & 0 \\
0 & 0 & 0 & 0 & 0 & 0 & 0 & 0 & 0 & 0 & 0 & 0 & 0 & 0 & 0 & 0 & 0 & Z_{|q|V_w} & 0 \\
0 & 0 & 0 & 0 & 0 & 0 & 0 & 0 & 0 & 0 & 0 & 0 & 0 & 0 & 0 & 0 & 0 & 0 & 0 \\
0 & 0 & 0 & 0 & 0 & 0 & 0 & 0 & 0 & 0 & 0 & 0 & 0 & 0 & 0 & 0 & 0 & 0 & 0 \\
0 & 0 & 0 & 0 & 0 & 0 & 0 & 0 & 0 & 0 & 0 & 0 & 0 & 0 & 0 & 0 & 0 & 0 & 0
\end{matrix}
\cdots
$$

$$
\cdots
\begin{matrix}
0 & 0 & 0 & 0 & 0 & 0 & X_{vv\eta} & 0 & 0 & 0 & 0 & X_{ww\eta} & 0 & 0 \\
0 & Y_{uv\eta} & 0 & 0 & 0 & Y_{ur\eta} & 0 & 0 & 0 & 0 & 0 & 0 & 0 & 0 \\
0 & 0 & Z_{uw\eta} & 0 & Z_{uq\eta} & 0 & 0 & 0 & 0 & 0 & 0 & 0 & 0 & 0 \\
K_{uu\eta} & 0 & 0 & 0 & 0 & 0 & 0 & 0 & 0 & 0 & 0 & 0 & 0 & 0 \\
0 & 0 & M_{uw\eta} & 0 & M_{uq\eta} & 0 & 0 & 0 & 0 & 0 & 0 & 0 & 0 & 0 \\
0 & N_{uv\eta} & 0 & 0 & 0 & N_{ur\eta} & 0 & 0 & 0 & 0 & 0 & 0 & 0 & 0
\end{matrix}
\cdots
$$

$$
\cdots
\left[
\begin{matrix}
0 & 0 & 0 & 0 & 0 & 0 & 0 & 0 & 0 & 0 & 0 & 0 & 0 \\
0 & 0 & 0 & 0 & 0 & 0 & 0 & 0 & Y_{vV\eta} & 0 & 0 & 0 & 0 \\
0 & 0 & 0 & 0 & 0 & 0 & 0 & 0 & 0 & Z_{wV\eta} & 0 & 0 & 0 \\
0 & 0 & 0 & 0 & 0 & 0 & 0 & 0 & 0 & 0 & 0 & 0 & 0 \\
0 & 0 & 0 & 0 & 0 & 0 & 0 & 0 & 0 & M_{wV\eta} & 0 & 0 & 0 \\
0 & 0 & 0 & 0 & 0 & 0 & 0 & 0 & N_{vV\eta} & 0 & 0 & 0 & 0
\end{matrix}
\right]
\tag{3.19}
$$

There are 88 non-zero terms in $\boldsymbol{K}$ matrix above, out of a total of $6 \times 132 = 792$ possible coefficients.

3.2.2 Prestero

Prestero proposed a model in [12] which is similar to that submitted by Gertler and Hagen, but far less complex. This model attempts to justify the included elements from physics, including axial drag, crossflow drag, and body lift. The Prestero model is defined by the

equations

$$\tau_{\nu}^{\mathrm{X}}(\boldsymbol{\nu}) = \mathrm{X_{qq}}q^2 + \mathrm{X_{wq}}wq + \mathrm{X_{rr}}r^2 + \mathrm{X_{vr}}vr + \mathrm{X_{u|u|}}u\,|u| \tag{3.20}$$

$$\tau_{\nu}^{\mathrm{Y}}(\boldsymbol{\nu}) = \mathrm{Y_{v|v|}}v\,|v| + \mathrm{Y_{pq}}pq + \mathrm{Y_{ur}}ur + \mathrm{Y_{wp}}wp + \mathrm{Y_{uv}}uv + \mathrm{Y_{r|r|}}r\,|r| \tag{3.21}$$

$$\tau_{\nu}^{\mathrm{Z}}(\boldsymbol{\nu}) = \mathrm{Z_{w|w|}}w\,|w| + \mathrm{Z_{pr}}pr + \mathrm{Z_{uq}}uq + \mathrm{Z_{vp}}vp + \mathrm{Z_{uw}}uw + \mathrm{Z_{q|q|}}q\,|q| \tag{3.22}$$

$$\tau_{\nu}^{\mathrm{K}}(\boldsymbol{\nu}) = \mathrm{K_{p|p|}}p\,|p| \tag{3.23}$$

$$\tau_{\nu}^{\mathrm{M}}(\boldsymbol{\nu}) = \mathrm{M_{pr}}pr + \mathrm{M_{uq}}uq + \mathrm{M_{vp}}vp + \mathrm{M_{uw}}uw + \mathrm{M_{q|q|}}q\,|q| + \mathrm{M_{w|w|}}w\,|w| \tag{3.24}$$

$$\tau_{\nu}^{\mathrm{N}}(\boldsymbol{\nu}) = \mathrm{N_{pq}}pq + \mathrm{N_{ur}}ur + \mathrm{N_{wp}}wp + \mathrm{N_{uv}}uv + \mathrm{N_{r|r|}}r\,|r| + \mathrm{N_{v|v|}}v\,|v|. \tag{3.25}$$

There is clear overlap between the Prestero and Gertler-Hagen models, although Prestero omits all terms depending on V and η.

3.2.3 Pitch & Yaw

One may naively construct a 6-DOF dynamical model by superimposing separate models for pitch and yaw. A model of this structure takes the form

$$\begin{aligned}\tau_\nu^{\mathrm{X}}(\boldsymbol{\nu}) =& \mathrm{X_q} q + \mathrm{X_r} r + \mathrm{X_u} u + \mathrm{X_v} v + \mathrm{X_w} w + \mathrm{X_{qq}} q^2 + \mathrm{X_{rr}} r^2 + \mathrm{X_{|q|}} |q| \\ &+ \mathrm{X_{|r|}} |r| + \mathrm{X_{uu}} u^2 + \mathrm{X_{vv}} v^2 + \mathrm{X_{ww}} w^2 + \mathrm{X_{|v|}} |v| + \mathrm{X_{|w|}} |w| + \mathrm{X_{u|r|}} u |r| \\ &+ \mathrm{X_{q|w|}} q |w| + \mathrm{X_{r|v|}} r |v| + \mathrm{X_{v|r|}} v |r| + \mathrm{X_{w|q|}} w |q| + \mathrm{X_{u|v|}} u |v| + \mathrm{X_{u|w|}} u |w| \\ &+ \mathrm{X_{v|v|}} v |v| + \mathrm{X_{w|w|}} w |w| + \mathrm{X_{ur}} ur + \mathrm{X_{vr}} vr + \mathrm{X_{wq}} wq + \mathrm{X_{uv}} uv + \mathrm{X_{uw}} uw + \mathrm{X_{q|q|}} q |q| \\ &+ \mathrm{X_{r|r|}} r |r| + \mathrm{X_{q|u|}} q |u| + \mathrm{X_{u|q|}} u |q|\end{aligned} \tag{3.26}$$

$$\begin{aligned}\tau_\nu^{\mathrm{Y}}(\boldsymbol{\nu}) =& \mathrm{Y_r} r + \mathrm{Y_v} v + \mathrm{Y_{rr}} r^2 + \mathrm{Y_{|r|}} |r| + \mathrm{Y_{uu}} u^2 + \mathrm{Y_{vv}} v^2 + \mathrm{Y_{|u|}} |u| \\ &+ \mathrm{Y_{|v|}} |v| + \mathrm{Y_{u|r|}} u |r| + \mathrm{Y_{r|v|}} r |v| + \mathrm{Y_{v|r|}} v |r| + \mathrm{Y_{u|v|}} u |v| + \mathrm{Y_{v|v|}} v |v| \\ &+ \mathrm{Y_{ur}} ur + \mathrm{Y_{vr}} vr + \mathrm{Y_{uv}} uv + \mathrm{Y_{r|r|}} r |r|\end{aligned} \tag{3.27}$$

$$\begin{aligned}\tau_\nu^{\mathrm{Z}}(\boldsymbol{\nu}) =& \mathrm{Z_q} q + \mathrm{Z_w} w + \mathrm{Z_{qq}} q^2 + \mathrm{Z_{|q|}} |q| + \mathrm{Z_{uu}} u^2 + \mathrm{Z_{|u|}} |u| + \mathrm{Z_{ww}} w^2 \\ &+ \mathrm{Z_{|w|}} |w| + \mathrm{Z_{u|q|}} u |q| + \mathrm{Z_{q|w|}} q |w| + \mathrm{Z_{w|q|}} w |q| + \mathrm{Z_{u|w|}} u |w| + \mathrm{Z_{w|w|}} w |w| \\ &+ \mathrm{Z_{uq}} uq + \mathrm{Z_{wq}} wq + \mathrm{Z_{uw}} uw + \mathrm{Z_{q|q|}} q |q|\end{aligned} \tag{3.28}$$

$$\tau_\nu^{\mathrm{K}}(\boldsymbol{\nu}) = 0 \tag{3.29}$$

$$\begin{aligned}\tau_\nu^{\mathrm{M}}(\boldsymbol{\nu}) =& \mathrm{M_q} q + \mathrm{M_w} w + \mathrm{M_{qq}} q^2 + \mathrm{M_{|q|}} |q| + \mathrm{M_{uu}} u^2 + \mathrm{M_{|u|}} |u| + \mathrm{M_{ww}} w^2 \\ &+ \mathrm{M_{|w|}} |w| + \mathrm{M_{uq}} uq + \mathrm{M_{wq}} wq + \mathrm{M_{uw}} uw + \mathrm{M_{q|q|}} q |q| + \mathrm{M_{u|q|}} u |q| + \mathrm{M_{q|w|}} q |w| \\ &+ \mathrm{M_{w|q|}} w |q| + \mathrm{M_{u|w|}} u |w| + \mathrm{M_{w|w|}} w |w|\end{aligned} \tag{3.30}$$

$$
\begin{aligned}
\tau_{\nu}^{\mathrm{N}}(\boldsymbol{\nu}) =& \mathrm{N_r} r + \mathrm{N_v} v + \mathrm{N_{rr}} r^2 + \mathrm{N_{|r|}} |r| + \mathrm{N_{uu}} u^2 + \mathrm{N_{vv}} v^2 + \mathrm{N_{|u|}} |u| \\
&+ \mathrm{N_{|v|}} |v| + \mathrm{N_{ur}} ur + \mathrm{N_{vr}} vr + \mathrm{N_{uv}} uv + \mathrm{N_{r|r|}} r|r| + \mathrm{N_{u|r|}} u|r| + \mathrm{N_{r|v|}} r|v| \\
&+ \mathrm{N_{v|r|}} v|r| + \mathrm{N_{u|v|}} u|v| + \mathrm{N_{v|v|}} v|v|
\end{aligned} \tag{3.31}
$$

3.2.4 Linear

The linear viscous hydrodynamic model is

$$
\boldsymbol{\tau}_{\nu}(\boldsymbol{\nu}) = \boldsymbol{K}_{\boldsymbol{\nu}} \boldsymbol{\nu}, \tag{3.32}
$$

where the coefficient matrix is

$$
\boldsymbol{K}_{\boldsymbol{\nu}} = \begin{bmatrix} X_u & X_v & X_w & X_p & X_q & X_r \\ Y_u & Y_v & Y_w & Y_p & Y_q & Y_r \\ Z_u & Z_v & Z_w & Z_p & Z_q & Z_r \\ K_u & K_v & K_w & K_p & K_q & K_r \\ M_u & M_v & M_w & M_p & M_q & M_r \\ N_u & N_v & N_w & N_p & N_q & N_r \end{bmatrix}. \tag{3.33}
$$

3.2.5 McFarland & Whitcomb

McFarland and Whitcomb propose in [13] a viscous hydrodynamic model which is fully coupled and assumes a sign-preserved quadratic relationship between velocity and force. The model is of the form

$$
\boldsymbol{\tau}_{\nu}(\boldsymbol{\nu}) = \boldsymbol{K}_{\boldsymbol{\nu}|\boldsymbol{\nu}|} \mathrm{diag}(\boldsymbol{\nu}) |\boldsymbol{\nu}| \tag{3.34}
$$

where the coefficient matrix $\boldsymbol{K}_{\boldsymbol{\nu}|\boldsymbol{\nu}|}$ is defined to be

$$
\boldsymbol{K}_{\boldsymbol{\nu}|\boldsymbol{\nu}|} = \left[\begin{array}{cccccccccccc}
\mathrm{X_{u|u|}} & \mathrm{X_{u|v|}} & \mathrm{X_{u|w|}} & \mathrm{X_{u|p|}} & \mathrm{X_{u|q|}} & \mathrm{X_{u|r|}} & \mathrm{X_{v|u|}} & \mathrm{X_{v|v|}} & \mathrm{X_{v|w|}} & \mathrm{X_{v|p|}} & \mathrm{X_{v|q|}} & \mathrm{X_{v|r|}} \\
\mathrm{Y_{u|u|}} & \mathrm{Y_{u|v|}} & \mathrm{Y_{u|w|}} & \mathrm{Y_{u|p|}} & \mathrm{Y_{u|q|}} & \mathrm{Y_{u|r|}} & \mathrm{Y_{v|u|}} & \mathrm{Y_{v|v|}} & \mathrm{Y_{v|w|}} & \mathrm{Y_{v|p|}} & \mathrm{Y_{v|q|}} & \mathrm{Y_{v|r|}} \\
\mathrm{Z_{u|u|}} & \mathrm{Z_{u|v|}} & \mathrm{Z_{u|w|}} & \mathrm{Z_{u|p|}} & \mathrm{Z_{u|q|}} & \mathrm{Z_{u|r|}} & \mathrm{Z_{v|u|}} & \mathrm{Z_{v|v|}} & \mathrm{Z_{v|w|}} & \mathrm{Z_{v|p|}} & \mathrm{Z_{v|q|}} & \mathrm{Z_{v|r|}} \\
\mathrm{K_{u|u|}} & \mathrm{K_{u|v|}} & \mathrm{K_{u|w|}} & \mathrm{K_{u|p|}} & \mathrm{K_{u|q|}} & \mathrm{K_{u|r|}} & \mathrm{K_{v|u|}} & \mathrm{K_{v|v|}} & \mathrm{K_{v|w|}} & \mathrm{K_{v|p|}} & \mathrm{K_{v|q|}} & \mathrm{K_{v|r|}} \\
\mathrm{M_{u|u|}} & \mathrm{M_{u|v|}} & \mathrm{M_{u|w|}} & \mathrm{M_{u|p|}} & \mathrm{M_{u|q|}} & \mathrm{M_{u|r|}} & \mathrm{M_{v|u|}} & \mathrm{M_{v|v|}} & \mathrm{M_{v|w|}} & \mathrm{M_{v|p|}} & \mathrm{M_{v|q|}} & \mathrm{M_{v|r|}} \\
\mathrm{N_{u|u|}} & \mathrm{N_{u|v|}} & \mathrm{N_{u|w|}} & \mathrm{N_{u|p|}} & \mathrm{N_{u|q|}} & \mathrm{N_{u|r|}} & \mathrm{N_{v|u|}} & \mathrm{N_{v|v|}} & \mathrm{N_{v|w|}} & \mathrm{N_{v|p|}} & \mathrm{N_{v|q|}} & \mathrm{N_{v|r|}}
\end{array}\right. \cdots
$$

$$
\cdots \begin{array}{cccccccccccc}
\mathrm{X_{w|u|}} & \mathrm{X_{w|v|}} & \mathrm{X_{w|w|}} & \mathrm{X_{w|p|}} & \mathrm{X_{w|q|}} & \mathrm{X_{w|r|}} & \mathrm{X_{p|u|}} & \mathrm{X_{p|v|}} & \mathrm{X_{p|w|}} & \mathrm{X_{p|p|}} & \mathrm{X_{p|q|}} & \mathrm{X_{p|r|}} \\
\mathrm{Y_{w|u|}} & \mathrm{Y_{w|v|}} & \mathrm{Y_{w|w|}} & \mathrm{Y_{w|p|}} & \mathrm{Y_{w|q|}} & \mathrm{Y_{w|r|}} & \mathrm{Y_{p|u|}} & \mathrm{Y_{p|v|}} & \mathrm{Y_{p|w|}} & \mathrm{Y_{p|p|}} & \mathrm{Y_{p|q|}} & \mathrm{Y_{p|r|}} \\
\mathrm{Z_{w|u|}} & \mathrm{Z_{w|v|}} & \mathrm{Z_{w|w|}} & \mathrm{Z_{w|p|}} & \mathrm{Z_{w|q|}} & \mathrm{Z_{w|r|}} & \mathrm{Z_{p|u|}} & \mathrm{Z_{p|v|}} & \mathrm{Z_{p|w|}} & \mathrm{Z_{p|p|}} & \mathrm{Z_{p|q|}} & \mathrm{Z_{p|r|}} \\
\mathrm{K_{w|u|}} & \mathrm{K_{w|v|}} & \mathrm{K_{w|w|}} & \mathrm{K_{w|p|}} & \mathrm{K_{w|q|}} & \mathrm{K_{w|r|}} & \mathrm{K_{p|u|}} & \mathrm{K_{p|v|}} & \mathrm{K_{p|w|}} & \mathrm{K_{p|p|}} & \mathrm{K_{p|q|}} & \mathrm{K_{p|r|}} \\
\mathrm{M_{w|u|}} & \mathrm{M_{w|v|}} & \mathrm{M_{w|w|}} & \mathrm{M_{w|p|}} & \mathrm{M_{w|q|}} & \mathrm{M_{w|r|}} & \mathrm{M_{p|u|}} & \mathrm{M_{p|v|}} & \mathrm{M_{p|w|}} & \mathrm{M_{p|p|}} & \mathrm{M_{p|q|}} & \mathrm{M_{p|r|}} \\
\mathrm{N_{w|u|}} & \mathrm{N_{w|v|}} & \mathrm{N_{w|w|}} & \mathrm{N_{w|p|}} & \mathrm{N_{w|q|}} & \mathrm{N_{w|r|}} & \mathrm{N_{p|u|}} & \mathrm{N_{p|v|}} & \mathrm{N_{p|w|}} & \mathrm{N_{p|p|}} & \mathrm{N_{p|q|}} & \mathrm{N_{p|r|}}
\end{array} \cdots
$$

$$
\cdots \left.\begin{array}{cccccccccccc}
\mathrm{X_{q|u|}} & \mathrm{X_{q|v|}} & \mathrm{X_{q|w|}} & \mathrm{X_{q|p|}} & \mathrm{X_{q|q|}} & \mathrm{X_{q|r|}} & \mathrm{X_{r|u|}} & \mathrm{X_{r|v|}} & \mathrm{X_{r|w|}} & \mathrm{X_{r|p|}} & \mathrm{X_{r|q|}} & \mathrm{X_{r|r|}} \\
\mathrm{Y_{q|u|}} & \mathrm{Y_{q|v|}} & \mathrm{Y_{q|w|}} & \mathrm{Y_{q|p|}} & \mathrm{Y_{q|q|}} & \mathrm{Y_{q|r|}} & \mathrm{Y_{r|u|}} & \mathrm{Y_{r|v|}} & \mathrm{Y_{r|w|}} & \mathrm{Y_{r|p|}} & \mathrm{Y_{r|q|}} & \mathrm{Y_{r|r|}} \\
\mathrm{Z_{q|u|}} & \mathrm{Z_{q|v|}} & \mathrm{Z_{q|w|}} & \mathrm{Z_{q|p|}} & \mathrm{Z_{q|q|}} & \mathrm{Z_{q|r|}} & \mathrm{Z_{r|u|}} & \mathrm{Z_{r|v|}} & \mathrm{Z_{r|w|}} & \mathrm{Z_{r|p|}} & \mathrm{Z_{r|q|}} & \mathrm{Z_{r|r|}} \\
\mathrm{K_{q|u|}} & \mathrm{K_{q|v|}} & \mathrm{K_{q|w|}} & \mathrm{K_{q|p|}} & \mathrm{K_{q|q|}} & \mathrm{K_{q|r|}} & \mathrm{K_{r|u|}} & \mathrm{K_{r|v|}} & \mathrm{K_{r|w|}} & \mathrm{K_{r|p|}} & \mathrm{K_{r|q|}} & \mathrm{K_{r|r|}} \\
\mathrm{M_{q|u|}} & \mathrm{M_{q|v|}} & \mathrm{M_{q|w|}} & \mathrm{M_{q|p|}} & \mathrm{M_{q|q|}} & \mathrm{M_{q|r|}} & \mathrm{M_{r|u|}} & \mathrm{M_{r|v|}} & \mathrm{M_{r|w|}} & \mathrm{M_{r|p|}} & \mathrm{M_{r|q|}} & \mathrm{M_{r|r|}} \\
\mathrm{N_{q|u|}} & \mathrm{N_{q|v|}} & \mathrm{N_{q|w|}} & \mathrm{N_{q|p|}} & \mathrm{N_{q|q|}} & \mathrm{N_{q|r|}} & \mathrm{N_{r|u|}} & \mathrm{N_{r|v|}} & \mathrm{N_{r|w|}} & \mathrm{N_{r|p|}} & \mathrm{N_{r|q|}} & \mathrm{N_{r|r|}}
\end{array}\right] .
$$

3.2.6 Uncoupled

The following model assumes that motion in each axis is dependent only on velocity in that dimension.

$$\tau_{\nu}^{\mathrm{X}}(\boldsymbol{\nu}) = \mathrm{X_u} u + \mathrm{X_{uu}} u^2 + \mathrm{X_{|u|}} |u| + \mathrm{X_{u|u|}} u |u| \tag{3.35}$$

$$\tau_{\nu}^{\mathrm{Y}}(\boldsymbol{\nu}) = \mathrm{Y_v} v + \mathrm{Y_{vv}} v^2 + \mathrm{Y_{|v|}} |v| + \mathrm{Y_{v|v|}} v |v| \tag{3.36}$$

$$\tau_{\nu}^{\mathrm{Z}}(\boldsymbol{\nu}) = \mathrm{Z_w} w + \mathrm{Z_{ww}} w^2 + \mathrm{Z_{|w|}} |w| + \mathrm{Z_{w|w|}} w |w| \tag{3.37}$$

$$\tau_{\nu}^{\mathrm{K}}(\boldsymbol{\nu}) = \mathrm{K_p} p + \mathrm{K_{pp}} p^2 + \mathrm{K_{|p|}} |p| + \mathrm{K_{p|p|}} p |p| \tag{3.38}$$

$$\tau_{\nu}^{\mathrm{M}}(\boldsymbol{\nu}) = \mathrm{M_q} q + \mathrm{M_{qq}} q^2 + \mathrm{M_{|q|}} |q| + \mathrm{M_{q|q|}} q |q| \tag{3.39}$$

$$\tau_{\nu}^{\mathrm{N}}(\boldsymbol{\nu}) = \mathrm{N_r} r + \mathrm{N_{rr}} r^2 + \mathrm{N_{|r|}} |r| + \mathrm{N_{r|r|}} r |r| \tag{3.40}$$

3.2.7 Fossen

Fossen presents a viscous hydrodynamic model in [5] which is uncoupled, but contains both linear and quadratic terms. He does this by assuming that 'the vehicle is performing a non-coupled motion, has three planes of symmetry and that terms higher than second order are negligible'. Later authors such as Caccia in [10] and Smallwood and Whitcomb in [14] adopt the same model. It is worth noting that both these references concern rectangular open-frame ROVs, rather than a slender axisymmetric vehicle such as the VT 690.

Fossen proposes a model of the form

$$\begin{aligned}\boldsymbol{\tau}_\nu(\boldsymbol{\nu}) =& \operatorname{diag}([X_u\ Y_v\ Z_w\ K_p\ M_q\ N_r])\boldsymbol{\nu} \\ &+ |\boldsymbol{\nu}|^\top \operatorname{diag}\big(\big[X_{u|u|}\ Y_{v|v|}\ Z_{w|w|}\ K_{p|p|}\ M_{q|q|}\ N_{r|r|}\big]\big)\boldsymbol{\nu}.\end{aligned} \tag{3.41}$$

3.2.8 Coe

Coe presents a novel model in [15] which is based on a Taylor series expansion and assumes port/starboard vehicle symmetry. The model is of the form

$$\boldsymbol{\tau}_\nu(\boldsymbol{\nu}) = C_{\boldsymbol{\nu}\boldsymbol{\nu}^*}\operatorname{diag}(\boldsymbol{\nu})\boldsymbol{\nu} + C_{\boldsymbol{\nu}|\boldsymbol{\nu}|^*}\operatorname{diag}(|\boldsymbol{\nu}|)\boldsymbol{\nu} \tag{3.42}$$

with constant coefficient matrices

$$C_{\boldsymbol{\nu}\boldsymbol{\nu}^*} = \begin{bmatrix} X_{u^2} & X_{v^2} & X_{w^2} & X_{p^2} & X_{q^2} & X_{r^2} \\ 0 & 0 & 0 & 0 & 0 & 0 \\ Z_{u^2} & Z_{v^2} & Z_{w^2} & Z_{p^2} & Z_{q^2} & Z_{r^2} \\ 0 & 0 & 0 & 0 & 0 & 0 \\ M_{u^2} & M_{v^2} & M_{w^2} & M_{p^2} & M_{q^2} & M_{r^2} \\ 0 & 0 & 0 & 0 & 0 & 0 \end{bmatrix} \tag{3.43}$$

$$C_{\boldsymbol{\nu}|\boldsymbol{\nu}|^*} = \begin{bmatrix} X_{u|u|} & 0 & X_{w|w|} & 0 & X_{q|q|} & 0 \\ 0 & Y_{v|v|} & 0 & Y_{p|p|} & 0 & Y_{r|r|} \\ Z_{u|u|} & 0 & Z_{w|w|} & 0 & Z_{q|q|} & 0 \\ 0 & K_{v|v|} & 0 & K_{p|p|} & 0 & K_{r|r|} \\ M_{u|u|} & 0 & M_{w|w|} & 0 & M_{q|q|} & 0 \\ 0 & N_{v|v|} & 0 & N_{p|p|} & 0 & N_{r|r|} \end{bmatrix}. \tag{3.44}$$

Chapter 4

Viscous hydrodynamic model synthesis

4.1 Synthesis model

A model of the form $\boldsymbol{\tau}_\nu(\boldsymbol{\nu}) = \boldsymbol{K}\boldsymbol{\xi}(\boldsymbol{\nu})$ requires coefficient values to be determined by 'training' the model from a sufficiently rich data set, which may be generated from field experiments or from CFD simulation. The equations of motion in (2.60) represent the ideal relationship between rigid-body, viscous and inviscid hydrodynamic, restoring, and control forces. In practice, there will be a force error $\tilde{\boldsymbol{\tau}}$ which is the sum of unmodeled dynamical effects and measurement error.

The force error is treated as an external force, and is incorporated into the equations of motion as

$$\boldsymbol{M}\dot{\boldsymbol{\nu}} = -\boldsymbol{C}(\boldsymbol{\nu})\boldsymbol{\nu} + \boldsymbol{\tau}_G(\boldsymbol{\eta}) + \boldsymbol{\tau}_U(\boldsymbol{\nu}, \boldsymbol{u}) + \boldsymbol{\tau}_\nu, \tag{4.1}$$

where $\boldsymbol{\tau}_\nu$ represents the exact viscous hydrodynamic model, $\boldsymbol{\eta}$, $\boldsymbol{\nu}$, and $\dot{\boldsymbol{\nu}}$ are assumed to be measured exactly, $\boldsymbol{M}$ and the corresponding $\boldsymbol{C}(\boldsymbol{\nu})$ are known, and $\boldsymbol{\tau}_G(\boldsymbol{\eta})$ and $\boldsymbol{\tau}_U(\boldsymbol{\nu}, \boldsymbol{u})$ are assumed to be modeled exactly. Since the viscous hydrodynamic model is assumed to be a function of the instantaneous velocity, which is approximate but not exact for physical systems, the choice of a specific model $\boldsymbol{\tau}_\nu(\boldsymbol{\nu})$ will introduce an error $\tilde{\boldsymbol{\tau}}$ into the equations of motion.

$$\boldsymbol{M}\dot{\boldsymbol{\nu}} = -\boldsymbol{C}(\boldsymbol{\nu})\boldsymbol{\nu} + \boldsymbol{\tau}_G(\boldsymbol{\eta}) + \boldsymbol{\tau}_U(\boldsymbol{\nu}, \boldsymbol{u}) + (\boldsymbol{\tau}_\nu(\boldsymbol{\nu}) - \tilde{\boldsymbol{\tau}}) \tag{4.2}$$

Equation (4.2) can then be reorganized to isolate the unknown quantities, as

$$\boldsymbol{\tau}_\nu(\boldsymbol{\nu}) - \tilde{\boldsymbol{\tau}} = \boldsymbol{M}\dot{\boldsymbol{\nu}} + \boldsymbol{C}(\boldsymbol{\nu})\boldsymbol{\nu} - \boldsymbol{\tau}_G(\boldsymbol{\eta}) - \boldsymbol{\tau}_U(\boldsymbol{\nu}, \boldsymbol{u}). \tag{4.3}$$

The task of model synthesis is to select $\boldsymbol{\tau}_\nu(\boldsymbol{\nu})$ such that $\tilde{\boldsymbol{\tau}}$ is minimized.

Let $\boldsymbol{\eta}(k)$, $\boldsymbol{\nu}(k)$, $\dot{\boldsymbol{\nu}}(k)$, $\boldsymbol{u}(k) \in \mathbb{R}^6$ be the time series data used to train the viscous hydrodynamic model, where k is the sample index. The right hand side of (4.3) is then calculated exactly as the time series

$$\bar{\boldsymbol{\tau}}(k) = \boldsymbol{M}\dot{\boldsymbol{\nu}}(k) + \boldsymbol{C}(\boldsymbol{\nu}(k))\boldsymbol{\nu}(k) - \boldsymbol{\tau}_G(\boldsymbol{\eta}(k)) - \boldsymbol{\tau}_U(\boldsymbol{\nu}(k), \boldsymbol{u}(k)), \tag{4.4}$$

where $\bar{\boldsymbol{\tau}}(k)$ is the residual force time series which is unaccounted for by rigid-body, added-mass, restoring, and control model components.

The residual force time series is related to the viscous hydrodynamic model by

$$\bar{\boldsymbol{\tau}}(k) = \boldsymbol{\tau}_\nu(\boldsymbol{\nu}(k)) - \tilde{\boldsymbol{\tau}}(k). \tag{4.5}$$

If the viscous hydrodynamic model takes the form as in (3.12), then (4.5) may be expressed

$$\boldsymbol{K}\boldsymbol{\xi}(\boldsymbol{\nu}(k)) - \tilde{\boldsymbol{\tau}}(k) = \bar{\boldsymbol{\tau}}(k), \tag{4.6}$$

where $\boldsymbol{K}$ can be determined by least-squares such that $\tilde{\boldsymbol{\tau}}(k)$ is minimized.

Equation (4.6) is of a form suitable for optimizing $\boldsymbol{K}$ for a single instant k, but it is instead desireable to optimize $\boldsymbol{K}$ for an entire time series at once. To that end, let

$$\boldsymbol{\nu}_* = [\boldsymbol{\nu}(0),\ \boldsymbol{\nu}(1),\ \cdots,\ \boldsymbol{\nu}(n_k)] \in \mathbb{R}^{6\times n_k} \tag{4.7}$$

$$\bar{\boldsymbol{\tau}}_* = [\bar{\boldsymbol{\tau}}(0),\ \bar{\boldsymbol{\tau}}(1),\ \cdots,\ \bar{\boldsymbol{\tau}}(n_k)] \in \mathbb{R}^{6\times n_k} \tag{4.8}$$

$$\tilde{\boldsymbol{\tau}}_* = [\tilde{\boldsymbol{\tau}}(0),\ \tilde{\boldsymbol{\tau}}(1),\ \cdots,\ \tilde{\boldsymbol{\tau}}(n_k)] \in \mathbb{R}^{6\times n_k} \tag{4.9}$$

$$\boldsymbol{\xi}_* = [\boldsymbol{\xi}(\boldsymbol{\nu}(0)),\ \boldsymbol{\xi}(\boldsymbol{\nu}(1)),\ \cdots,\ \boldsymbol{\xi}(\boldsymbol{\nu}(n_k))] \in \mathbb{R}^{n_\xi\times n_k} \tag{4.10}$$

be matrix representations of time series, where n_k is the number of samples collected. By substituting the matrix time series (4.7) - (4.10), equation (4.6) can be expressed

$$\tilde{\boldsymbol{\tau}}(k) = \boldsymbol{K}\boldsymbol{\xi}(\boldsymbol{\nu}(k)) - \bar{\boldsymbol{\tau}}(k) \tag{4.11}$$

$$\tilde{\boldsymbol{\tau}}^\top(k) = \boldsymbol{\xi}^\top(\boldsymbol{\nu}(k))\boldsymbol{K}^\top - \bar{\boldsymbol{\tau}}^\top(k) \tag{4.12}$$

$$\tilde{\boldsymbol{\tau}}_*^\top = \boldsymbol{\xi}_*^\top\boldsymbol{K}^\top - \bar{\boldsymbol{\tau}}_*^\top. \tag{4.13}$$

Using the notation in Appendix A.1, apply the vec() operator to equation (4.13)

$$\begin{aligned}\mathrm{vec}\big(\tilde{\boldsymbol{\tau}}_*^\top\big) &= \mathrm{vec}\big(\boldsymbol{\xi}_*^\top\boldsymbol{K}^\top - \bar{\boldsymbol{\tau}}_*^\top\big)\\ &= \mathrm{vec}\big(\boldsymbol{\xi}_*^\top\boldsymbol{K}^\top\big) - \mathrm{vec}\big(\bar{\boldsymbol{\tau}}_*^\top\big)\\ &= \big(\mathbb{I}_6 \otimes \boldsymbol{\xi}_*^\top\big)\,\mathrm{vec}\big(\boldsymbol{K}^\top\big) - \mathrm{vec}\big(\bar{\boldsymbol{\tau}}_*^\top\big),\end{aligned} \tag{4.14}$$

with $\mathrm{vec}\big(\tilde{\boldsymbol{\tau}}_*^\top\big) \in \mathbb{R}^{6n_k}$, $\mathrm{vec}\big(\bar{\boldsymbol{\tau}}_*^\top\big) \in \mathbb{R}^{6n_k}$, $\mathrm{vec}\big(\boldsymbol{K}^\top\big) \in \mathbb{R}^{6n_{\boldsymbol{\xi}}}$, and $\big(\mathbb{I}_6 \otimes \boldsymbol{\xi}_*^\top\big) \in \mathbb{R}^{6n_k \times 6n_{\boldsymbol{\xi}}}$.

It is necessary to further manipulate (4.14) in order to restrict the optimization to a subset of the coefficients in $\boldsymbol{K}$, which is necessary to implement the models described in Section 3.2. It is possible to directly manipulate the dimension of the space of basis functions by applying a masking matrix $\boldsymbol{M} \in \mathbb{B}^{\bar{n} \times 6n_\xi}$, where $\mathbb{B}$ denotes the space of booleans, i.e. $\mathbb{B} = \{0, 1\}$. Each row of $\boldsymbol{M}$ has exactly one non-zero element, which is equal to one. A value of one in a column j of $\boldsymbol{M}$ selects the corresponding basis function $\xi_j(\boldsymbol{\nu})$ from $\boldsymbol{\xi}(\boldsymbol{\nu})$.

The equation which represents the masked model is expressed

$$\mathrm{vec}\big(\tilde{\boldsymbol{\tau}}_*^\top\big) = \big(\mathbb{I}_6 \otimes \boldsymbol{\xi}_*^\top(\boldsymbol{\nu})\big)\, \boldsymbol{M}^\top \boldsymbol{M} \mathrm{vec}\big(\boldsymbol{K}^\top\big) - \mathrm{vec}\big(\bar{\boldsymbol{\tau}}_*^\top\big). \tag{4.15}$$

Choose a mask matrix $\boldsymbol{M}$ for a given model, and let

$$\tilde{\boldsymbol{\sigma}} = \mathrm{vec}\big(\tilde{\boldsymbol{\tau}}_*^\top\big) \in \mathbb{R}^{6n_k} \tag{4.16}$$

$$\bar{\boldsymbol{\sigma}} = \mathrm{vec}\big(\bar{\boldsymbol{\tau}}_*^\top\big) \in \mathbb{R}^{6n_k} \tag{4.17}$$

$$\boldsymbol{\Xi} = \big(\mathbb{I}_6 \otimes \boldsymbol{\xi}_*^\top\big)\, \boldsymbol{M}^\top \in \mathbb{R}^{6n_k \times \bar{n}} \tag{4.18}$$

$$\boldsymbol{\kappa} = \boldsymbol{M} \mathrm{vec}\big(\boldsymbol{K}^\top\big) \in \mathbb{R}^{\bar{n}} \tag{4.19}$$

be a change of variables, where $\boldsymbol{\Xi} \in \mathbb{R}^{6n_k \times \bar{n}}$ is a basis matrix, $\boldsymbol{\kappa} \in \bar{n}$ is a coefficient vector, and $\bar{n}$ is the *model complexity*, or the number of coefficients for a given model. Then (4.15) can be expressed as

$$\tilde{\boldsymbol{\sigma}} = \boldsymbol{\Xi}\boldsymbol{\kappa} - \bar{\boldsymbol{\sigma}}. \tag{4.20}$$

Equation (4.20) is called the *synthesis model*.

The original coefficient matrix $\boldsymbol{K}$ is recoverable from $\boldsymbol{\kappa}$ by

$$\boldsymbol{K} = \mathrm{vec}^{-1}\big(\boldsymbol{M}^\top \boldsymbol{\kappa}\big)^\top, \tag{4.21}$$

where $\mathrm{vec}^{-1}()$ is defined in Appendix A.1.

4.2 Optimization

The synthesis model in (4.20) is directly solvable for $\boldsymbol{\kappa}$ by least-squares, such that the sum of the square of the elements in $\tilde{\boldsymbol{\sigma}}$ is minimized. This is equivalent to minimizing the Frobenius norm of $\tilde{\boldsymbol{\tau}}_*$ in (4.15). The error function implicitly minimized by least-squares is expressed as a function of $\boldsymbol{\kappa}$ as

$$J(\boldsymbol{\kappa}) = \sum_{i=1}^{6n_k} \tilde{\boldsymbol{\sigma}}_i^2. \tag{4.22}$$

One may instead choose an arbitrary error function $J(\boldsymbol{\kappa})$, and implement a search algorithm to select $\boldsymbol{\kappa}$ such that $J(\boldsymbol{\kappa})$ is minimized. One suitable algorithm is the Nelder-Mead simplex algorithm described in [16] and [17]. This is suitable for unconstrained nonlinear optimization, and requires only a starting coefficient vector $\boldsymbol{\kappa}_0$ and scalar cost function as input, and produces a locally optimal coefficient vector as output.

Mean absolute error

Smallwood, McFarland, and Whitcomb introduce mean absolute error (MAE) in [14] and [13] as the metric by which model performance is evaluated. Note that the models proposed therein compare model performance on the basis of output error residual, e.g. yaw error,

where the error function (4.11) measures force residual error. The error function which returns the MAE of the residual $\tilde{\boldsymbol{\tau}}$ is

$$J(\boldsymbol{\kappa}) = \frac{1}{6n_k} \sum_{i=1}^{6n_k} |\tilde{\boldsymbol{\sigma}}_i| \,. \tag{4.23}$$

Mean square error

Let the cost function which minimizes the mean square error (MSE) be defined as

$$J(\boldsymbol{\kappa}) = \frac{1}{6n_k} \sum_{i=1}^{6n_k} \tilde{\boldsymbol{\sigma}}_i^2. \tag{4.24}$$

A similar measure of error is root mean square (RMS) error, defined as

$$J(\boldsymbol{\kappa}) = \sqrt{\frac{1}{6n_k} \sum_{i=1}^{6n_k} \tilde{\boldsymbol{\sigma}}_i^2}. \tag{4.25}$$

These error functions are useful when comparing the relative error of model performance using data sets of different sizes, i.e. where n_k is different.

Median absolute deviation

Another possible error function is a variation on the median absolution deviation, or MAD. Let $\tilde{\boldsymbol{\tau}}(k)$ be recovered from $\tilde{\boldsymbol{\sigma}}(k)$ by (4.16), as

$$\tilde{\boldsymbol{\tau}}(k) = \mathrm{vec}^{-1}(\tilde{\boldsymbol{\sigma}}(k))^\top, \tag{4.26}$$

and define the error function to be

$$J(\boldsymbol{\kappa}) = \sum_{i=1}^{6} \text{median}\, |\tilde{\boldsymbol{\tau}}_{i\cdot}|, \tag{4.27}$$

where $\tilde{\boldsymbol{\tau}}_{i\cdot}$ is the ith row of $\tilde{\boldsymbol{\tau}}$. Note that MAD is generally defined on vectors, and the extension to matrices is done by summing the MAD for each row of $\tilde{\boldsymbol{\tau}}$. This function is robust against outliers in the time series data, but is nonlinear in its output. This means that for a small change in $\tilde{\boldsymbol{\tau}}$, there may be zero change in $J(\boldsymbol{\kappa})$. MAD is not suitable for the Nelder-Mead simplex search algorithm for this reason, but it can be used to compare models after optimization.

Chapter 5

Results

5.1 Data collection

The data presented in this section was collected using the Virginia Tech 690 AUV during field experiments at Claytor Lake in Pulaski County, Virginia. A sample data set representing the state vector $\boldsymbol{x}(k)$ is shown in Figures 5.1 and 5.2. The corresponding state derivative vector $\dot{\boldsymbol{x}}(k)$ is shown in Figures 5.3 and 5.4.

The raw data set was processed using the state estimation procedure described in Section 2.5. In each plot, the raw data is presented in blue with the label 'online', and the processed data is presented in green with the label 'opt'. Of special note are the relatively large biases in $\dot{u}(k)$ and $\dot{v}(k)$ shown in Figure 5.4. These bias errors, and a smaller bias error in $r(k)$ shown in Figure 5.2, are characteristic of the class of sensors used by the AHRS. Another point of note is the large discrepancy in sway velocity $v(k)$ in Figure 5.2. The sway velocity as reported by the DVL is quite dissimilar to the sway velocity estimated by integrating the bias-corrected sway acceleration. This is thought to be due to an incorrect

coordinate transformation when mapping the velocity reported by the DVL into the body frame. Because the DVL measures velocity relative to the sea floor, rotational velocities will couple into the translational velocities measured by the DVL. These effects are not accounted for in the data sets presented here. For this reason, velocity measured by the DVL is used only to estimate the bias on the accelerometer, and is otherwise discarded. Translational velocity is instead estimated by integrating translational acceleration.

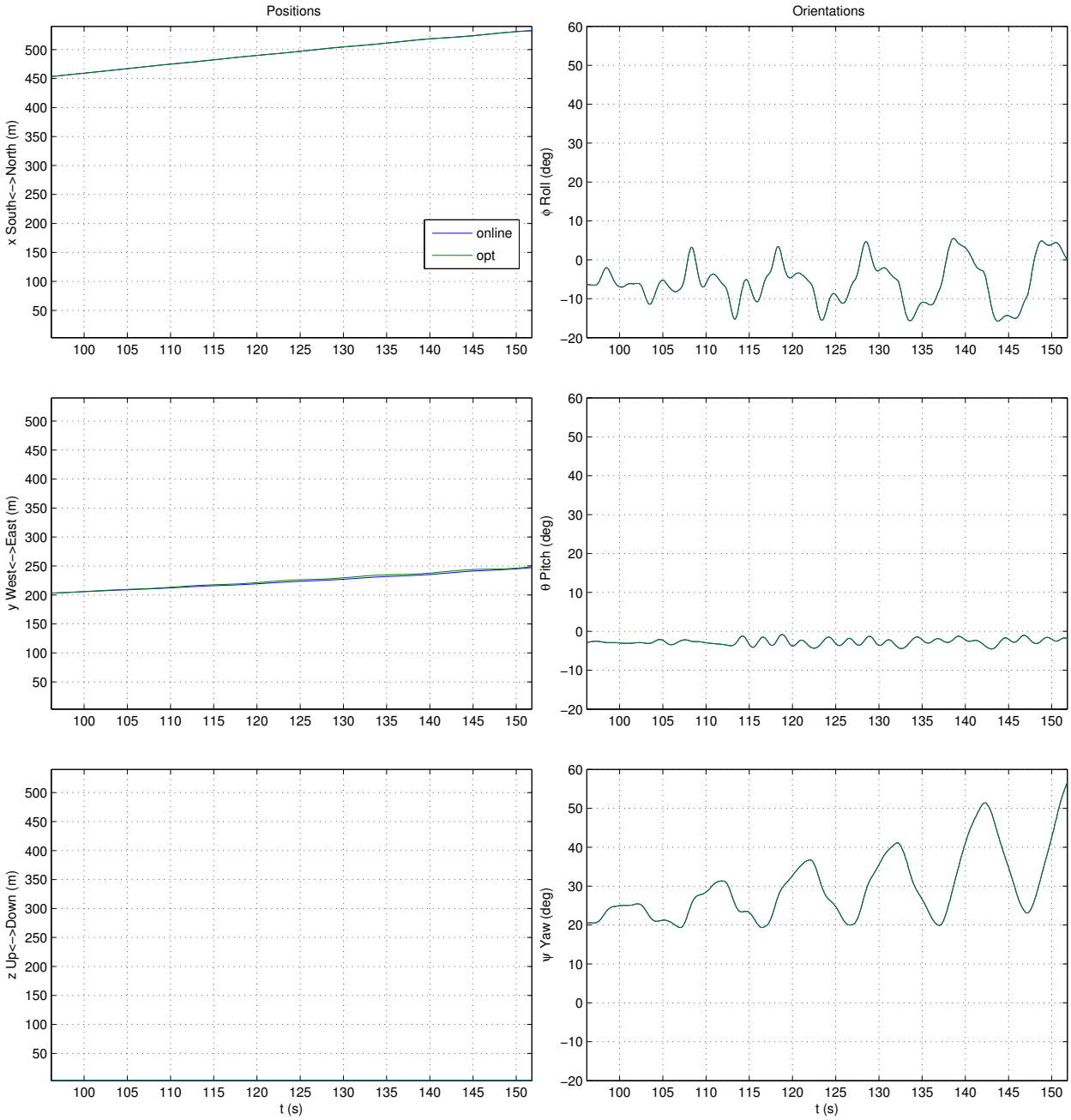

Figure 5.1: Vehicle pose $\boldsymbol{\eta}$ data set, yaw steps, 2133 rpm. Unfiltered data is presented as 'online', and post-processed data is presented as 'opt'.

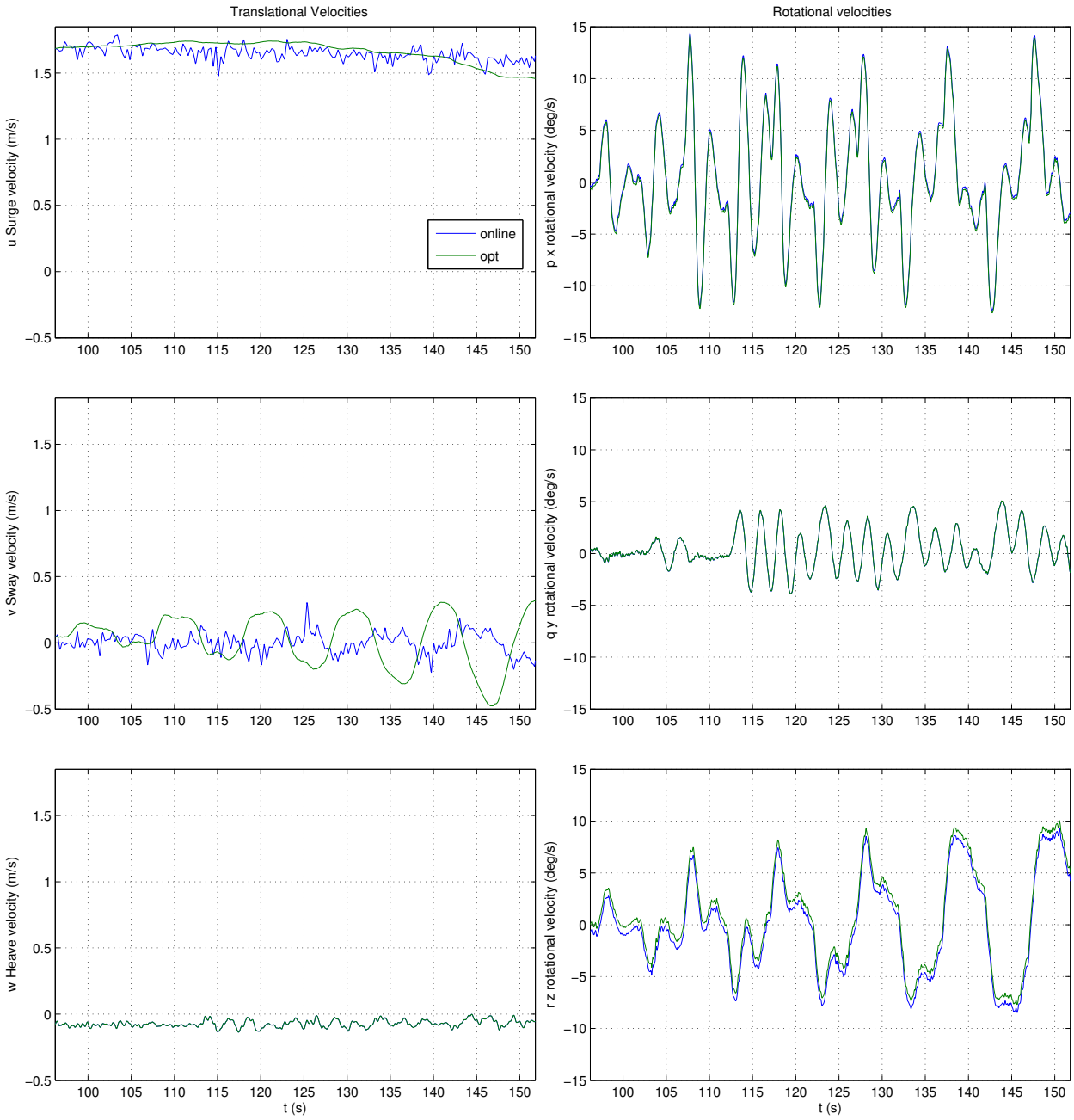

Figure 5.2: Vehicle velocity $\boldsymbol{\nu}$ data set, yaw steps, 2133 rpm. Unfiltered data is presented as 'online', and post-processed data is presented as 'opt'.

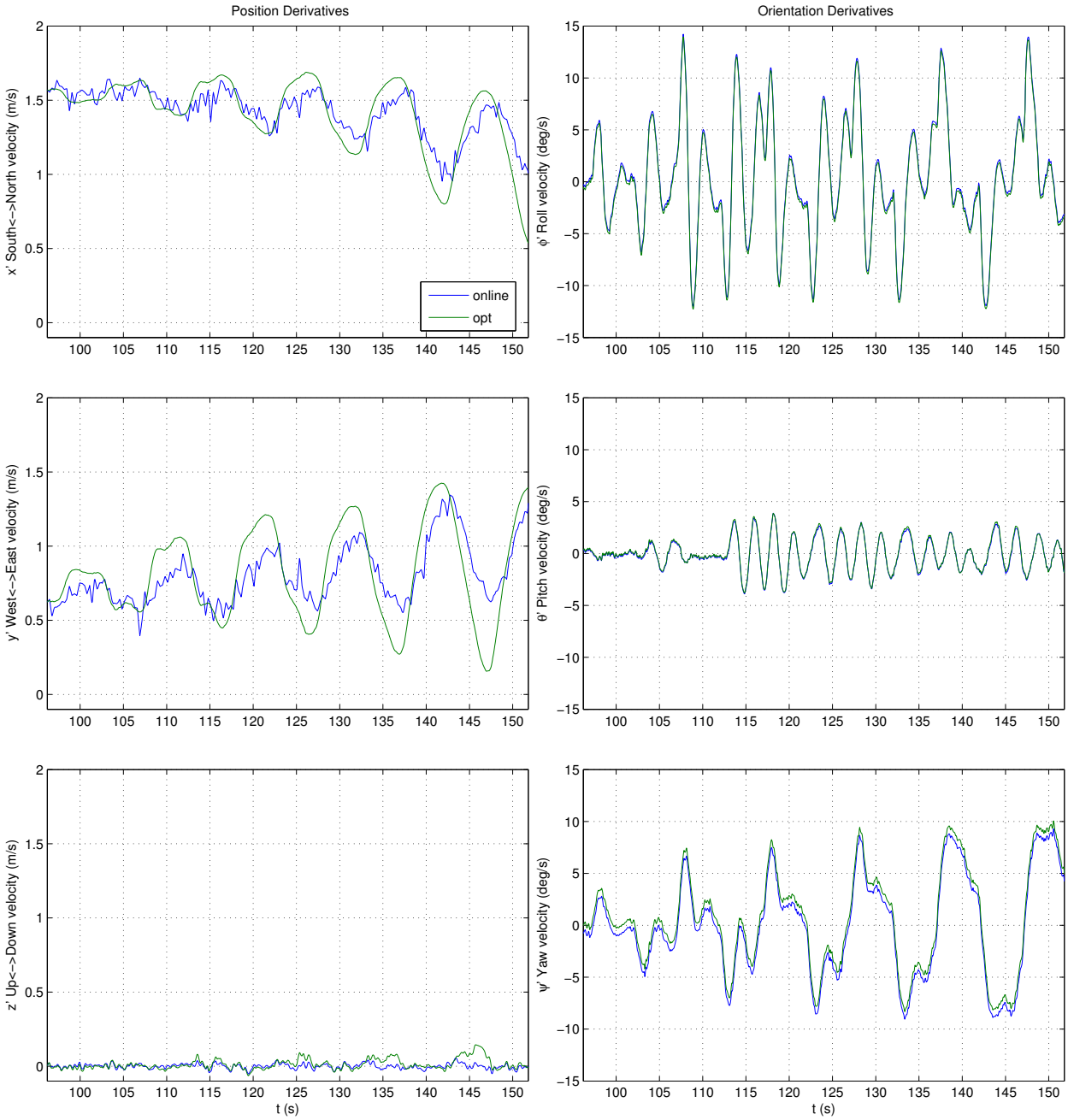

Figure 5.3: Vehicle pose derivative $\dot{\boldsymbol{\eta}}$ data set, yaw steps, 2133 rpm. Unfiltered data is presented as 'online', and post-processed data is presented as 'opt'.

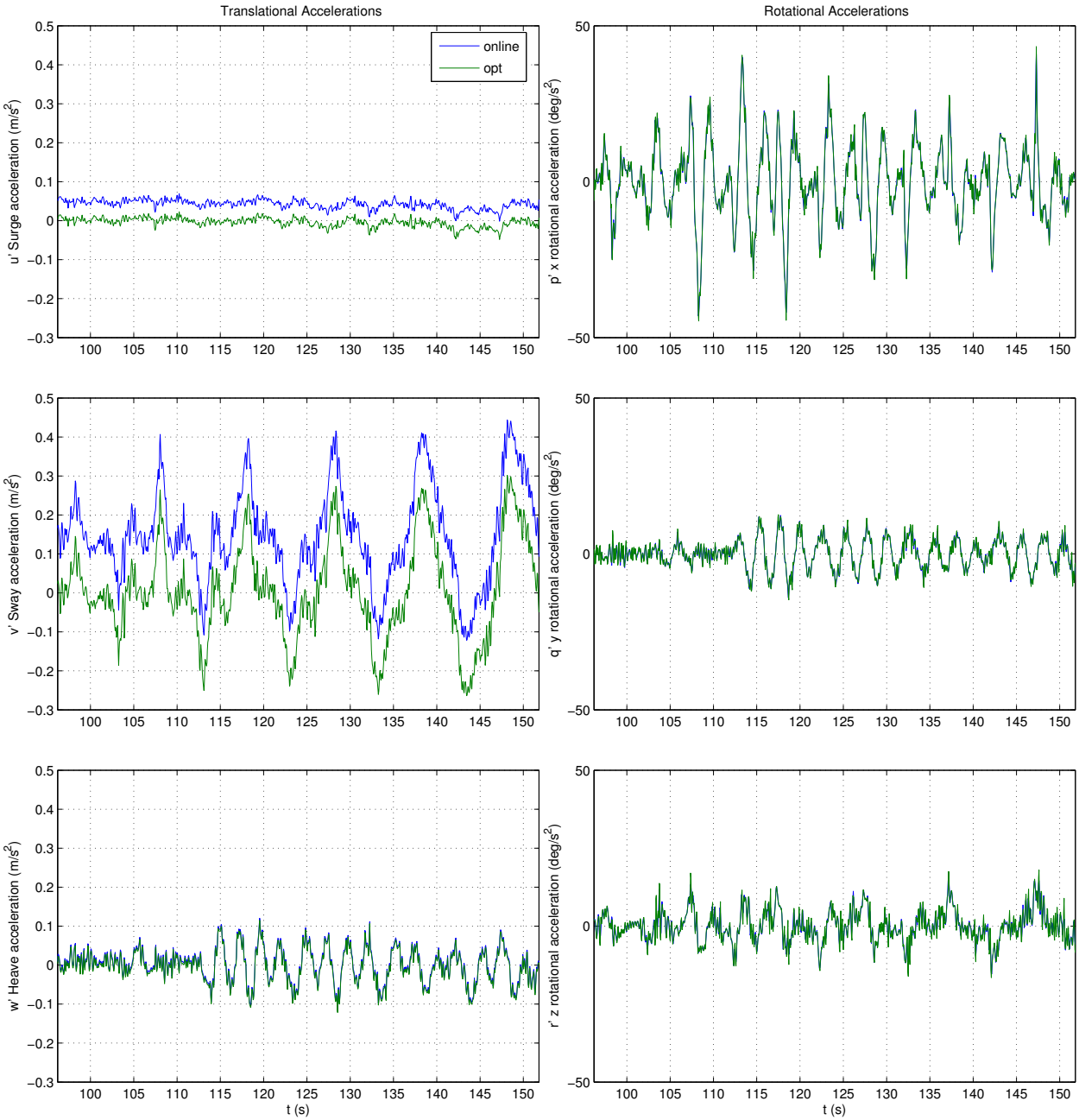

Figure 5.4: Vehicle velocity derivative $\dot{\boldsymbol{\nu}}$ data set, yaw steps, 2133 rpm. Unfiltered data is presented as 'online', and post-processed data is presented as 'opt'.

5.2 Model training

The force data $\bar{\boldsymbol{\tau}}(k)$ used to train the viscous hydrodynamic model is calculated by populating the right-hand side of (4.3) with quantities from the estimated state vector $\bar{\boldsymbol{x}}(k)$ and rate vector $\bar{\dot{\boldsymbol{x}}}(k)$ as calculated in Section 2.5, using the raw data which was collected as described in Section 5.1. The model synthesis algorithm in Chapter 4 is then used to populate each of the models in turn, which are described in Sections 3.2.1 - 3.2.8. Each model is trained against the same estimated viscous hydrodynamic force data set $\bar{\boldsymbol{\tau}}(k)$.

The velocity data used to train the unconstrained model is shown in Figure 5.5. The training force data is presented in Figure 5.6. The training set is the concatenation of four independent data sets. The first data set is composed of depth steps at a propeller speed of 2600 rpm, and the three remaining sets are composed of yaw steps at propeller speeds 1800, 2133, and 2600 rpm. Note that the concatenation produces an apparent discontinuity in the data at times 25, 84, and 142 seconds. This does not affect the training process because the model form is quasi-steady, and each sample is assumed to be independent with respect to time.

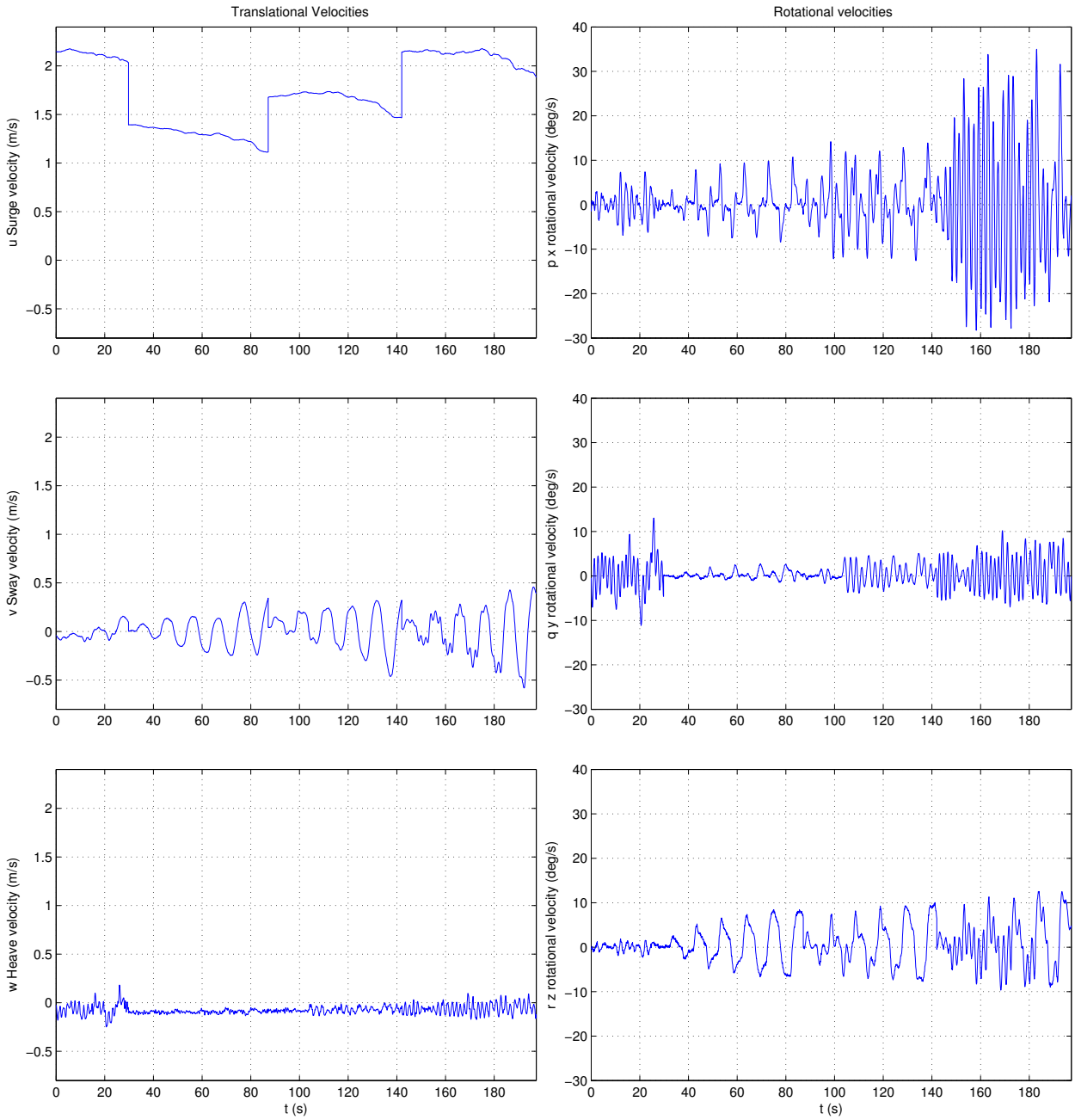

Figure 5.5: Training velocity data.

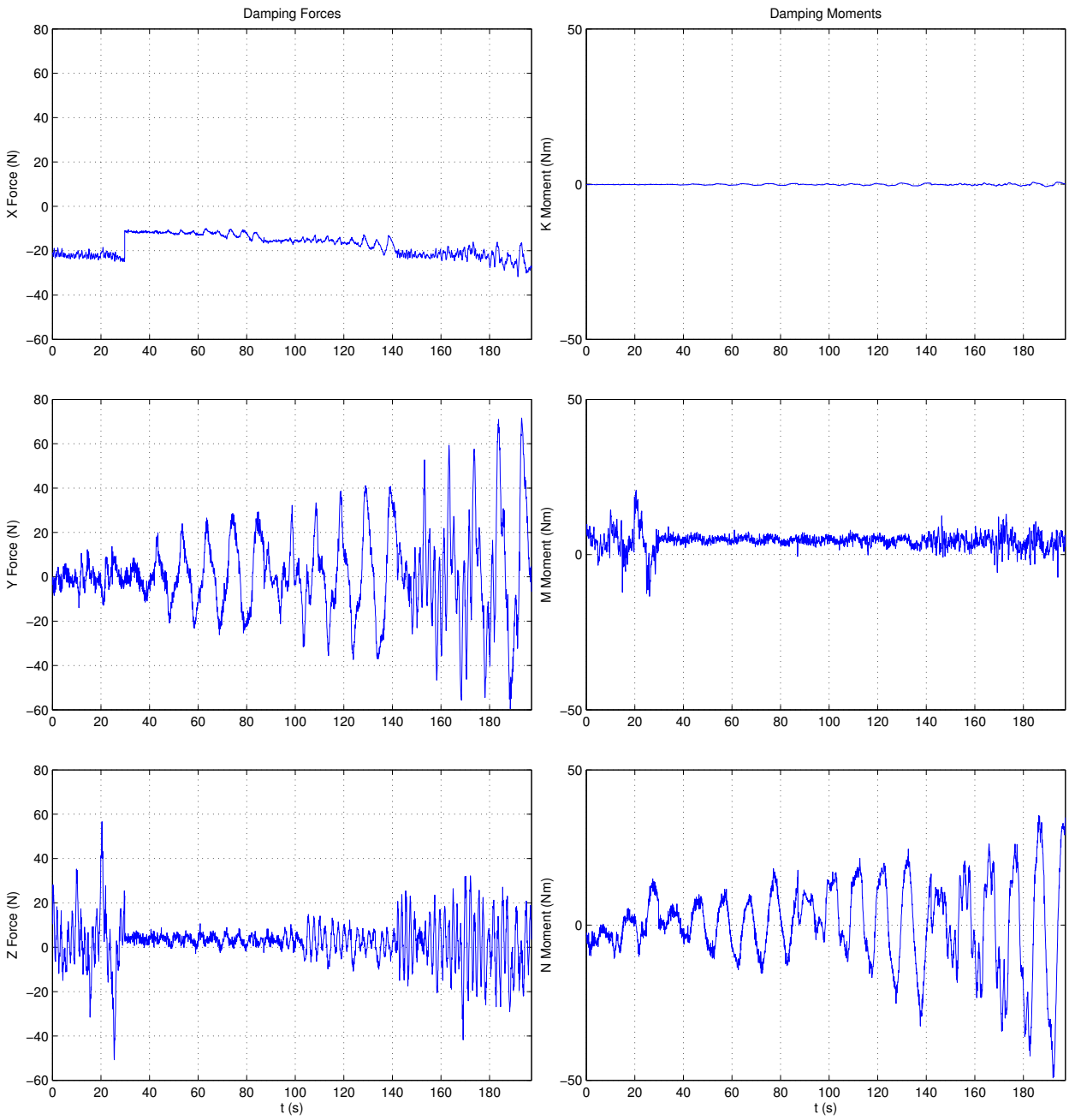

Figure 5.6: Training force data.

5.3 Model validation

The velocity data set which is used to validate the model is presented in Figure 5.7. It is composed of two legs. The first leg is a series of depth steps at propeller speed 2133 rpm. The second leg is a set of yaw steps at a propeller speed of 2350 rpm.

The validation force plots are presented in Figures 5.8 - 5.15, in order of decreasing model complexity. These plots show the force time series output of each model, plotted against the validation force time series. Equations for each model are presented in Appendix D, with coefficients in Appendix E. The validation force data set was generated in the same way as the training force data set was generated in Section 5.1, just with different raw data. Validation data was selected to represent maneuvers which were similar to those used to train the models, but at different forward speeds.

Both the training and validation force time series show large roll velocities p but very little hydrodynamic roll moment K. This is due to the small moment of inertia in the roll axis, which means that relatively a relatively small roll moment can cause a large change in roll velocity.

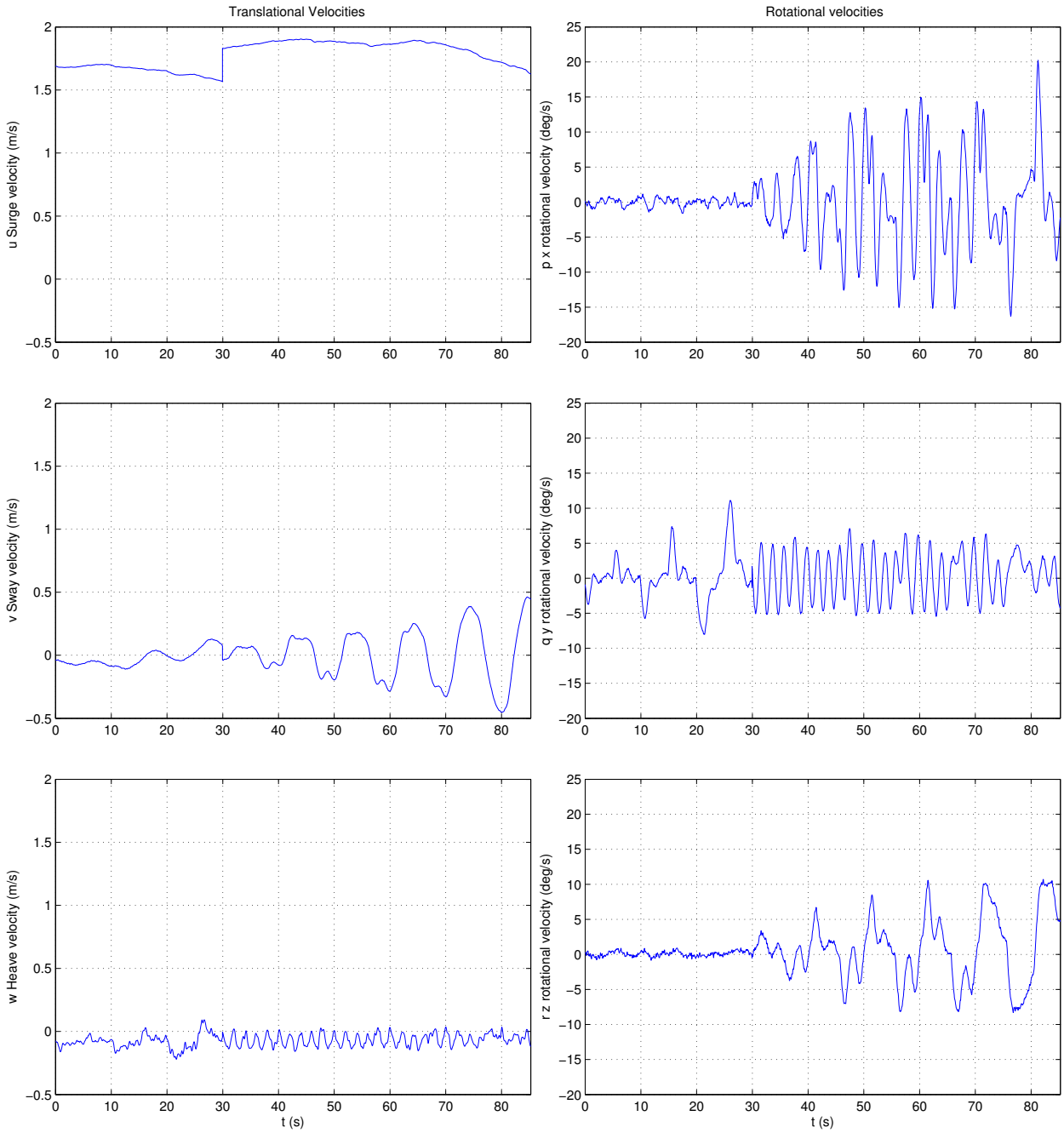

Figure 5.7: Validation velocity data

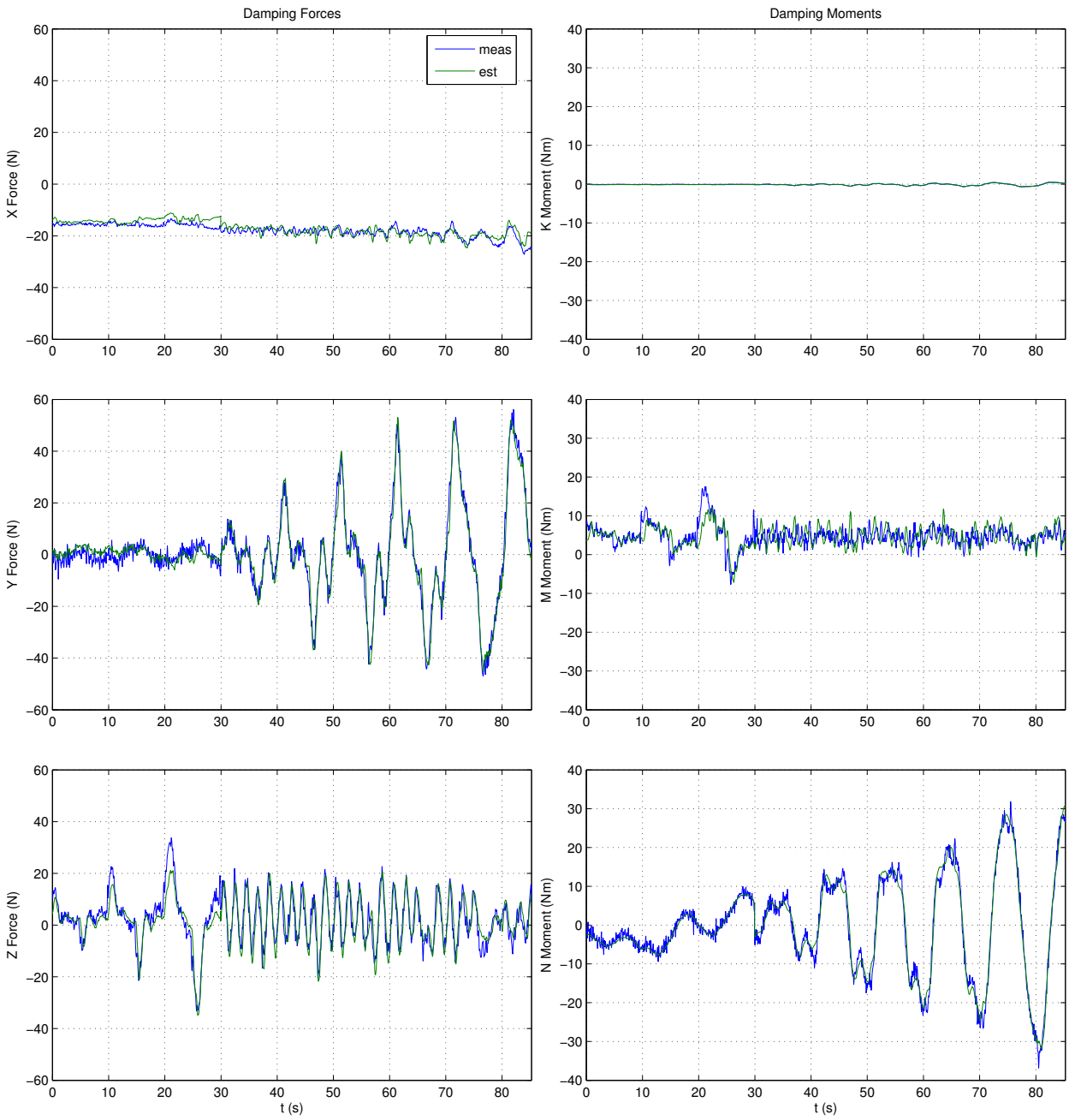

Figure 5.8: Validation force data, McFarland model, $\bar{n} = 216$

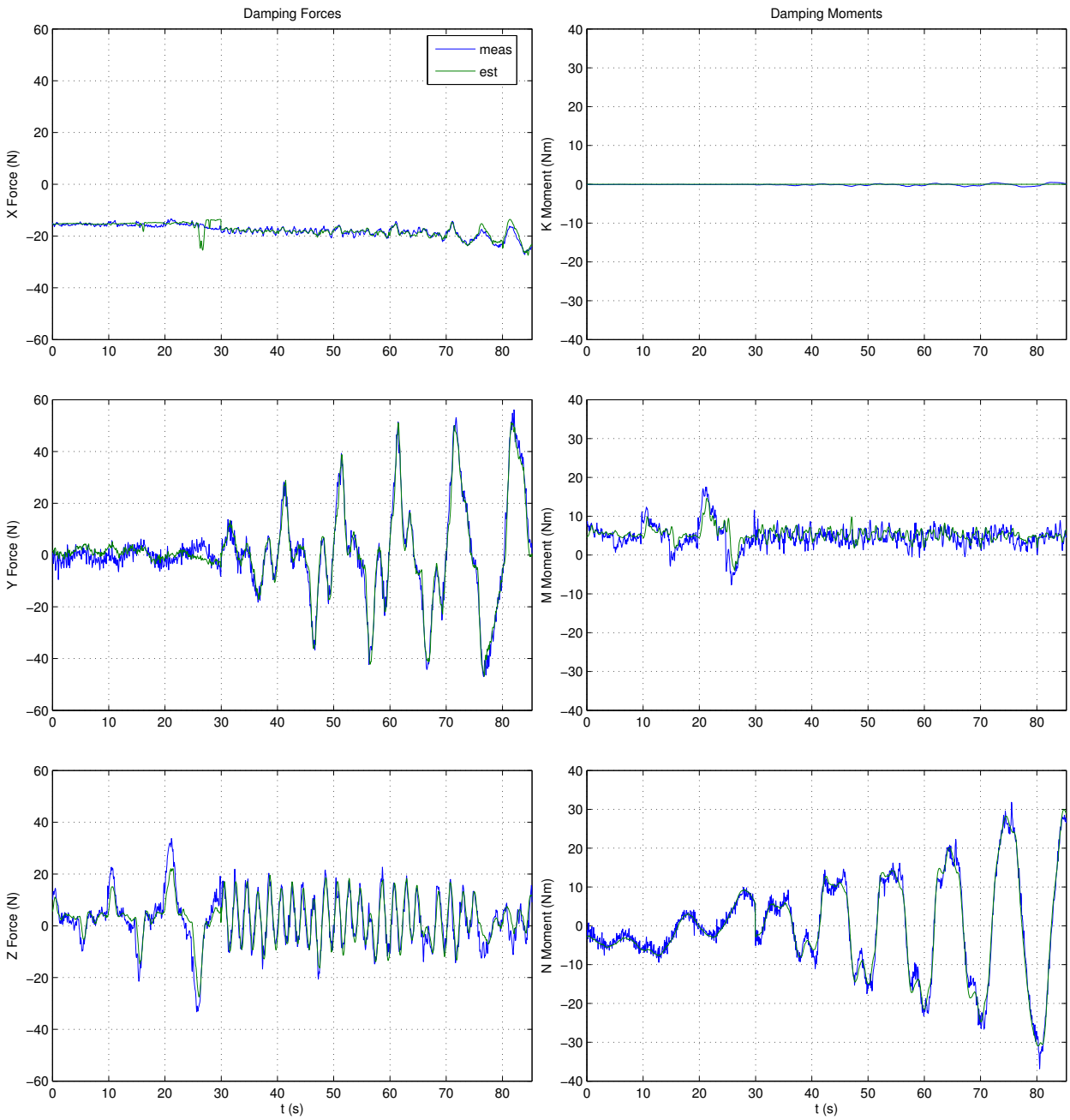

Figure 5.9: Validation force data, Pitch/Yaw model, $\bar{n} = 100$

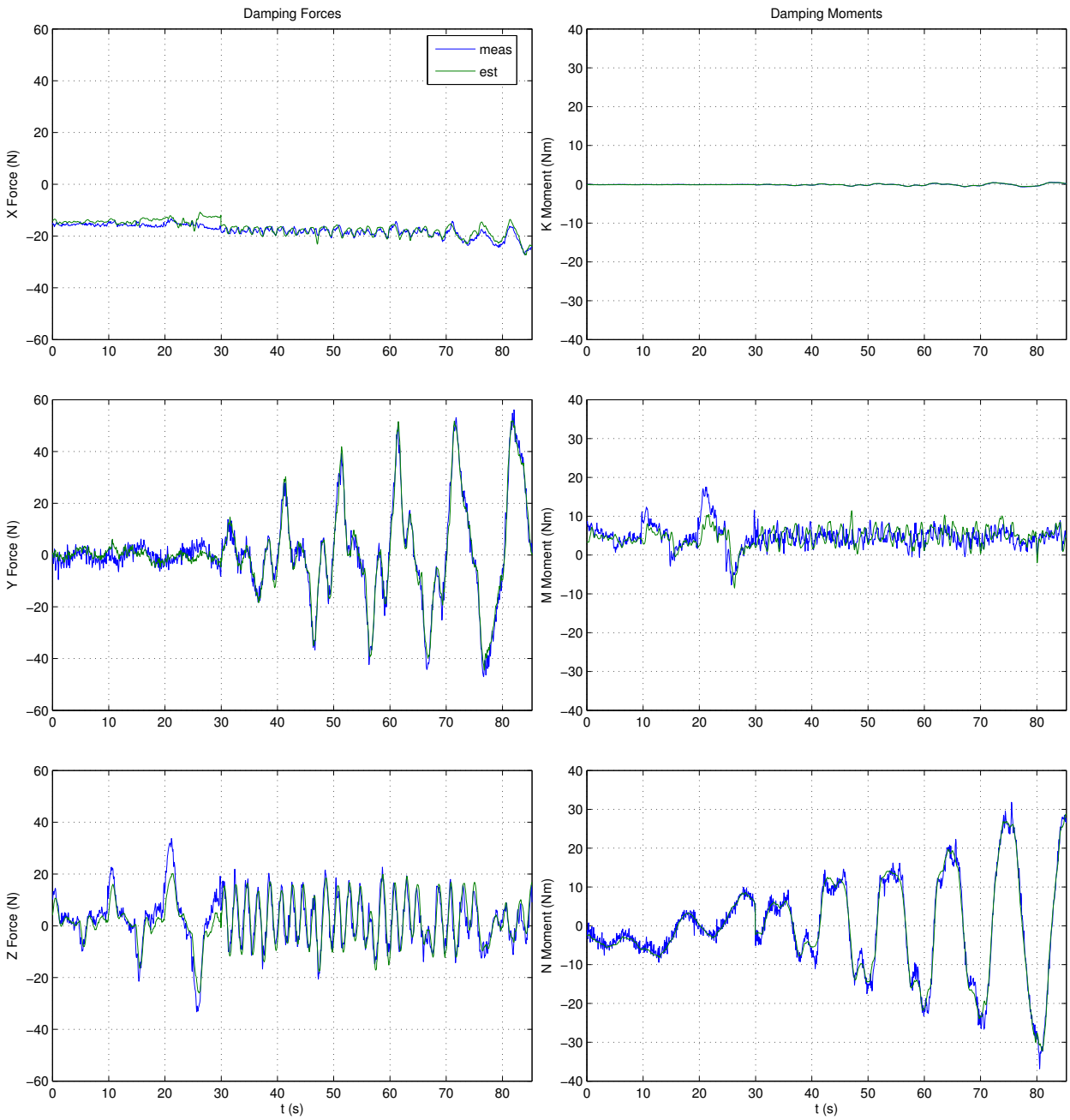

Figure 5.10: Validation force data, Gertler Hagen model, $\bar{n} = 88$

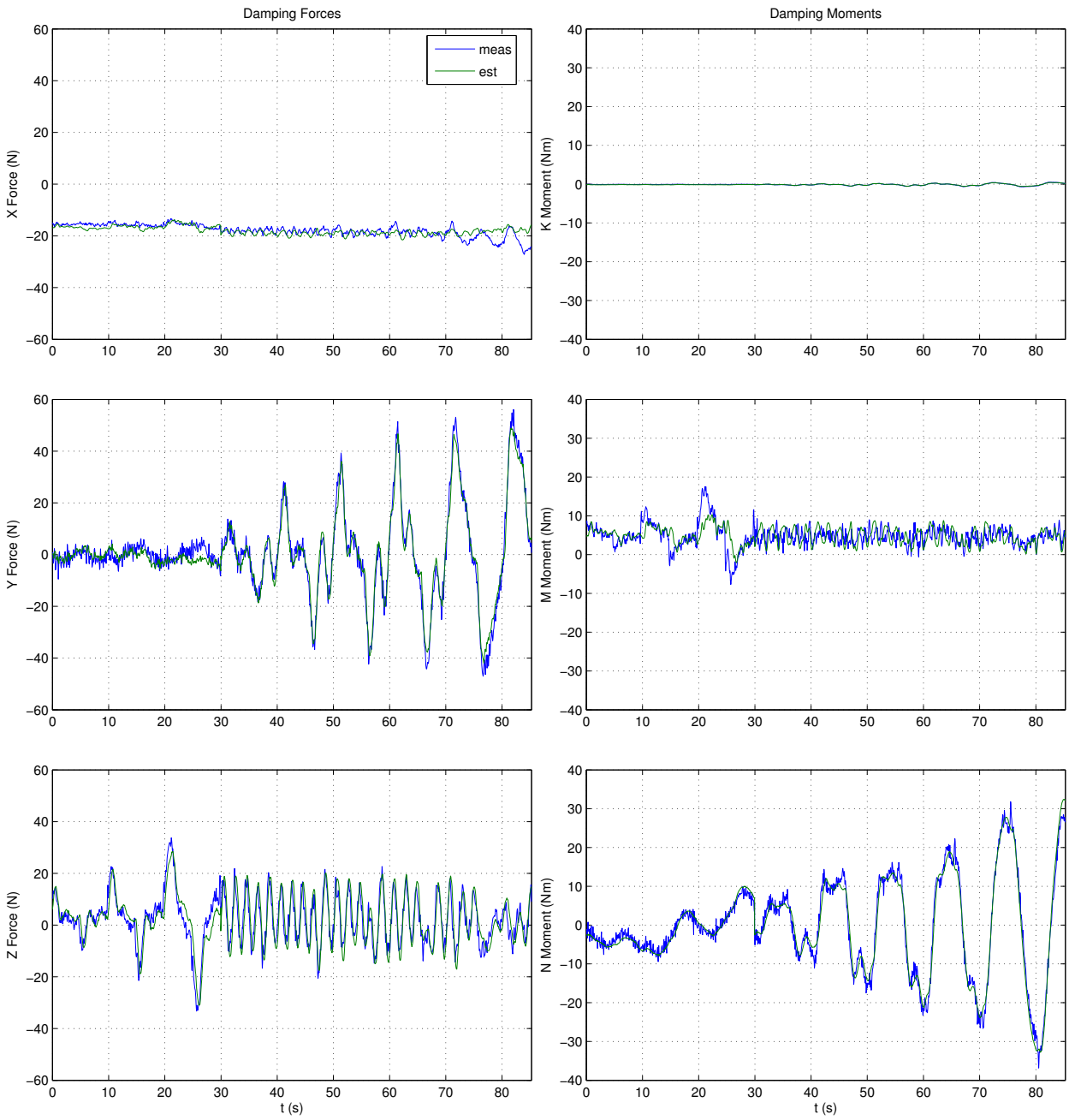

Figure 5.11: Validation force data, Linear model, $\bar{n} = 36$

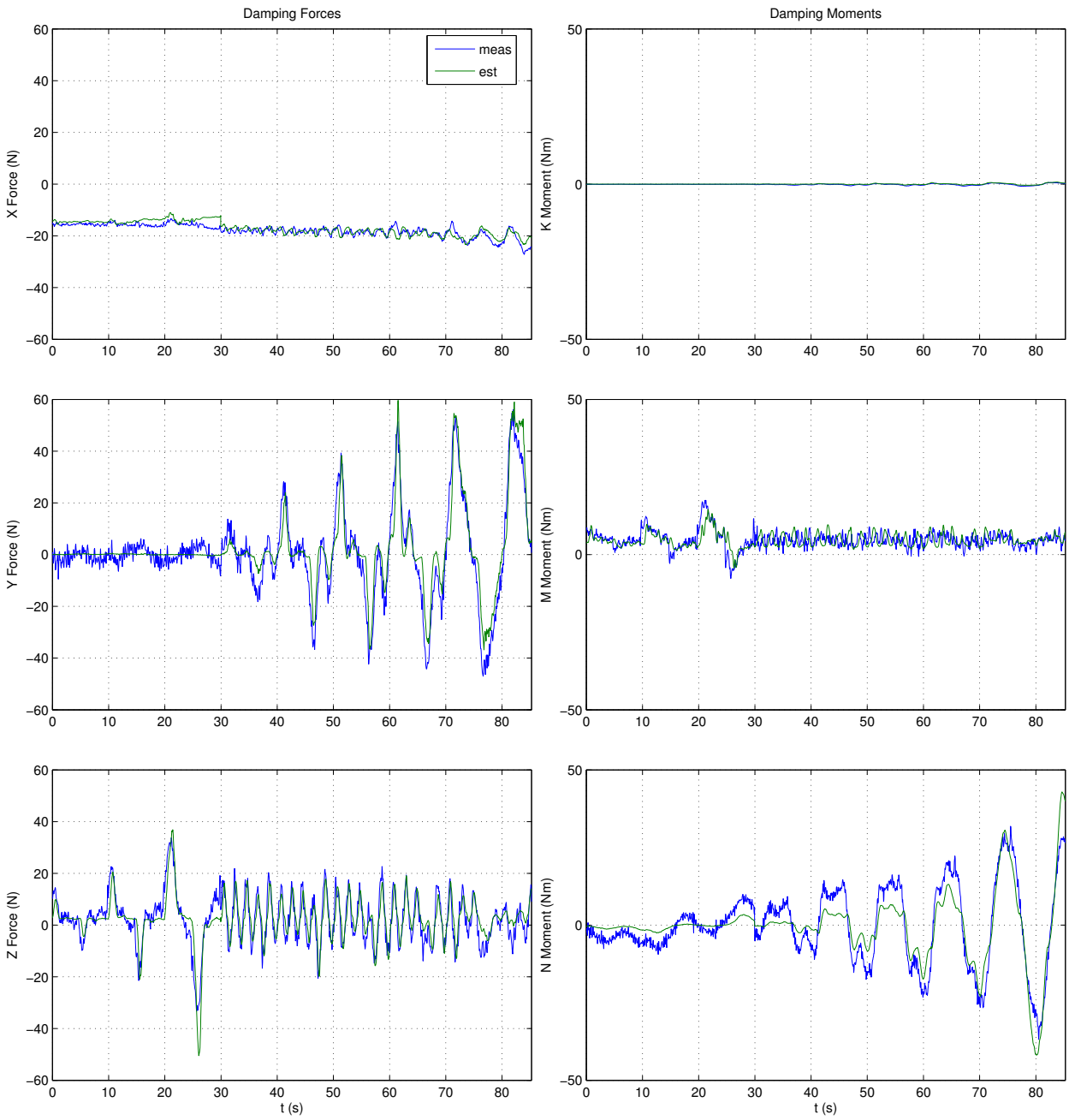

Figure 5.12: Validation force data, Coe model, $\bar{n} = 33$

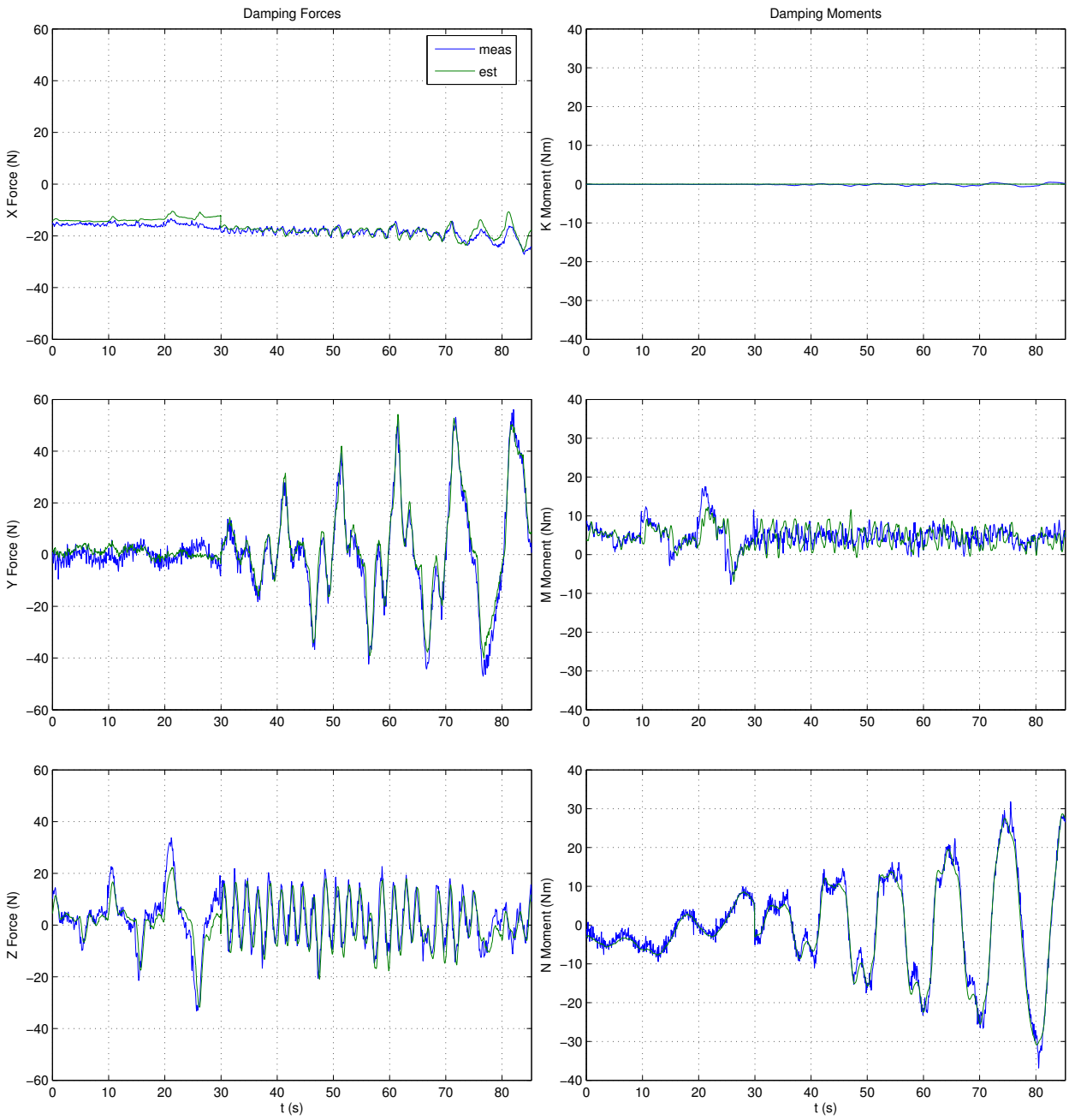

Figure 5.13: Validation force data, Prestero model, $\bar{n} = 30$

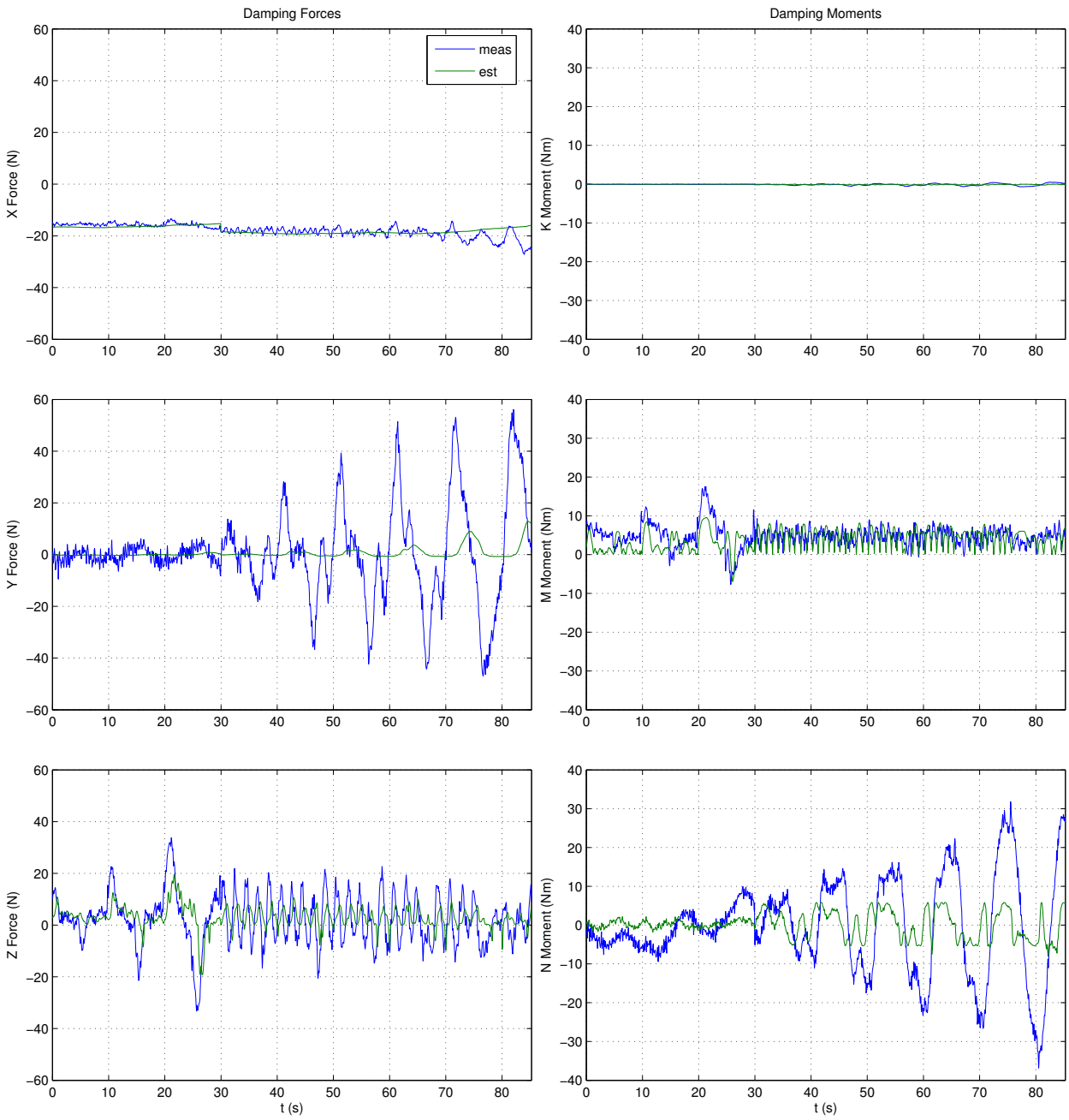

Figure 5.14: Validation force data, Uncoupled model, $\bar{n} = 22$

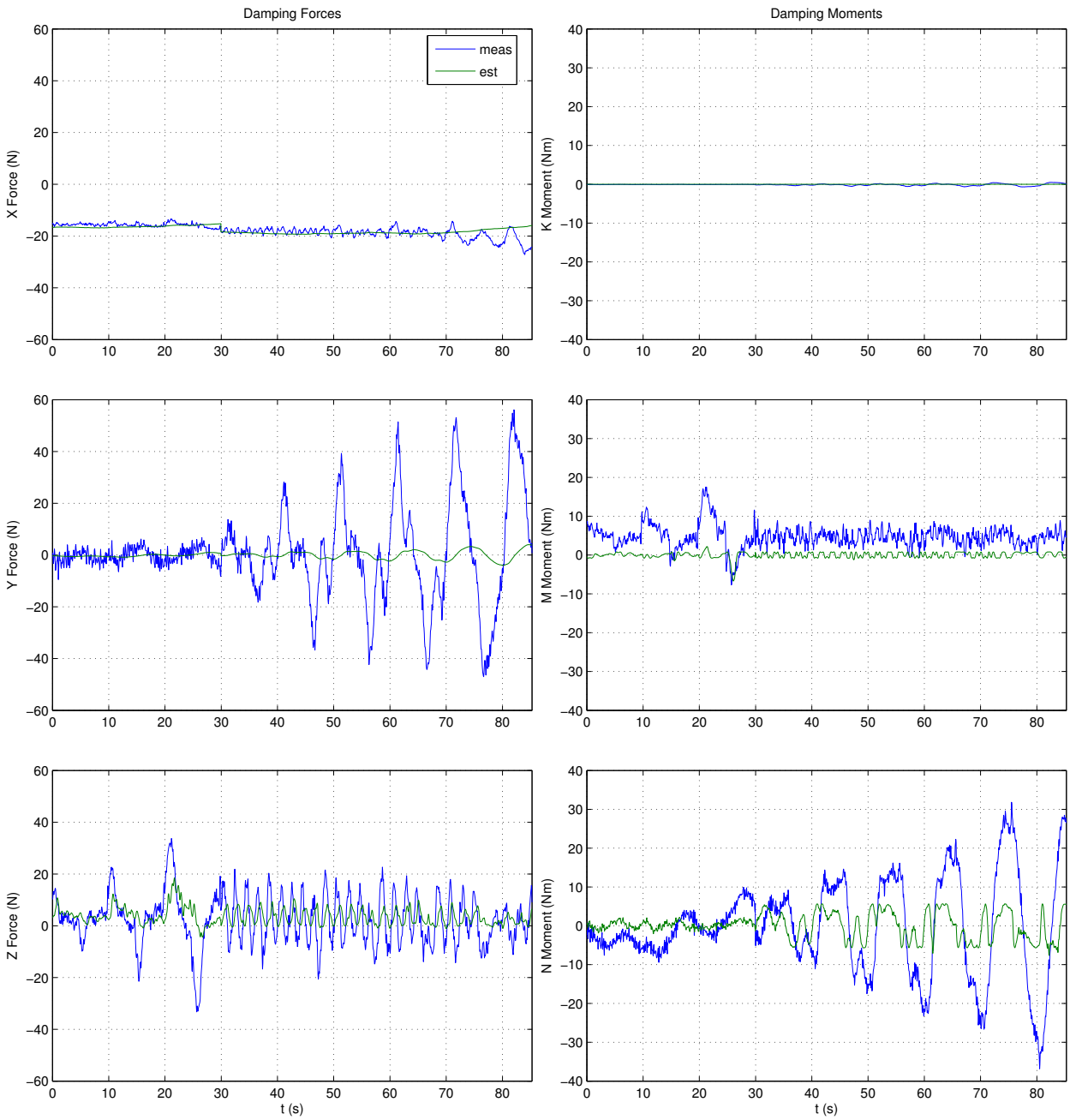

Figure 5.15: Validation force data, Fossen model, $\bar{n} = 12$

5.4 Model comparison

Model	$\bar{n}$	$J^V(K)$ $\left(J_0^V = 12.338\right)$	$J^V(K)/J_0^V$
McFarland	216	2.667	0.216
Pitch/Yaw	100	2.520	0.204
Gertler Hagen	88	2.650	0.215
Linear	36	2.849	0.231
Coe	33	4.237	0.343
Prestero	30	3.082	0.250
Uncoupled	24	9.408	0.763
Fossen	12	9.619	0.780

Table 5.1: Model validation error.

Model	$\bar{n}$	$J(K)$ $(J_0 = 13.047)$	$J(K)/J_0$
McFarland	216	2.505	0.192
Pitch/Yaw	100	2.504	0.192
Gertler Hagen	88	2.629	0.201
Linear	36	3.625	0.250
Coe	33	4.559	0.349
Prestero	30	3.214	0.246
Uncoupled	24	10.299	0.789
Fossen	12	10.471	0.802

Table 5.2: Model training error.

Let J_0 be the RMS value of the force time series from the training data set $\mathcal{T}$, and let J_0^V be the RMS value of the force time series from the validation data set $\mathcal{V}$.

The validation errors $J^V(K)$ for the model validation plots in Figures 5.8 - 5.15 are presented in Table 5.1, along with their values as normalized against J_0^V. The training errors $J(K)$ for the same set of models are presented in Table 5.2.

The Uncoupled and Fossen models are clearly inferior to the other models in representing the training and validation data sets. These models are *uncoupled*, in that they consider only the velocity in a particular dimension to contribute to the force in that dimension. The Fossen model assumes that each of the hydrodynamic forces X, Y, Z, K, M, N are a function

of only linear and sign-preserved quadratic functions of velocity in the same dimension as the force. For example, sway force Y is modeled as $Y(v) = v + v\,|v|$. As is evident in Figure 5.15, this assumption is not valid. The Uncoupled model includes absolute-value terms as well as sign-preserved terms, but does little better. However, these are also the models with the fewest coefficients, so part of their poor performance may be attributed to the optimizer having access to fewer degrees of freedom.

Of the remaining models, there is no one which is clearly superior to the rest. All are *coupled* models to some degree, in that they model a force in one dimension as a function of velocities in multiple dimensions. For example, each output of the Linear model is assumed to be a linear function of the entire velocity vector. The Pitch/Yaw model performs at least as well as any other model under consideration, despite having less than half the coefficients of the McFarland model, and being far simpler in its construction than the Gertler-Hagen model. The linear model stands out as a compromise between complexity and accuracy.

Chapter 6

Conclusions

6.1 Summary

This thesis has presented a comparison of viscous hydrodynamic models commonly used to calculate the forces and moments applied to an underwater vehicle as it moves through a viscous fluid. The Virginia Tech 690 AUV described in Chapter 1 was modeled as a rigid body in Chapter 2. The dynamical model incorporates hydrodynamic forces due to viscous damping, conservative viscous effects, and added mass, restoring forces due to gravity, and control forces due to actuation of control surfaces and a propeller. Several viscous hydrodynamic models were described in Chapter 3, with a synthesis algorithm used to determine the corresponding model coefficients developed in Chapter 4. Each model was then trained against a set of data collected in the field using the 690 AUV, with the relative performance compared in Chapter 5.

6.2 Conclusions

No single viscous hydrodynamic model of those described in Chapter 3 stands out as superior to the others, though some appear to perform worse than the others for modeling an underwater vehicle in six degrees of freedom. The Pitch/Yaw model performs at least as well as the other models, while being significantly smaller than the McFarland model, and being less complex in its construction than the Gertler-Hagen model. The Linear model is even smaller, and is only moderately less accurate than the Pitch/Yaw model. Either of these appear to be suitable for use with the dynamical model presented in Chapter 2.

The Uncoupled and Fossen models make the assumption that the force along a particular axis is due only to velocity along that axis. This assumption is clearly not valid for the training and validation data sets presented in Figures 5.5 and 5.7, and these models are unlikely to perform well for any but the most simple of maneuvers. The Coe model assumes that the fluid flow is symmetric about the port/starboard axis. This assumption also appears to be invalid for the studied data sets.

The training and validation data sets presented in Chapter 5 represent typical maneuvers made by a vehicle with an orthodox geometry. It is likely that the models would perform differently if they were trained against a different set of maneuvers, or if the vehicle geometry was in some way atypical. Both Gertler, Hagen, and Prestero developed their models to describe the viscous hydrodynamics as applied to 'torpedo' shaped underwater vehicles. The VT 690 is similar in size and proportion to the REMUS vehicle that Prestero referenced in his work, and also similar in proportion to the full-scale submarines that Gertler and Hagen were concerned with. It is unsurprising that the Gertler-Hagen and Prestero models are suitable to describe data collected with the 690. In contrast, a vehicle such as the Woods Hole Sentry described in [18] would likely require a viscous hydrodynamic model with a different

emphasis on which parameters were important, due to unconventional vehicle geometry.

The McFarland and Linear models make no assumptions about which coefficients are more or less important than others, though they do make assumptions about the character of the flow. McFarland assumes a quadratic relationship between force and velocity, where the Linear model assumes a linear relationship. The actual relationship is more complicated, and depends on Reynolds number, and also the dominance of skin friction over form drag, or vice versa.

Bibliography

[1] M. Gertler and G. R. Hagen, "Standard Equations of Motion for Submarine Simulation," Report 2510, Naval Ship Research and Development Center, June 1967.

[2] J. N. Newman, *Marine Hydrodynamics*. Cambridge, MA: MIT Press, 1977.

[3] J. Petrich and D. J. Stilwell, "Robust control for an autonomous underwater vehicle that suppresses pitch and yaw coupling," *Ocean Engineering*, vol. 38, no. 1, pp. 197 – 204, 2011.

[4] J. Petrich, W. Neu, and D. Stilwell, "Identification of a simplified auv pitch axis model for control design: Theory and experiments," in *OCEANS 2007*, pp. 1–7, Sept 2007.

[5] T. I. Fossen, *Guidance and Control of Ocean Vehicles*. Chichester, West Sussex, England: John Wiley & Sons, 1994.

[6] F. H. Imlay, "The Complete Expressions for "Added Mass" of a Rigid Body Moving in an Ideal Fluid," Report 1528, David Taylor Model Basin, July 1961.

[7] K. Wendel, "Hydrodynamic Masses and Hydrodynamic Moments of Inertia," Translation 260, David Taylor Model Basin, July 1956.

[8] J. P. Comstock, ed., *Principles of Naval Architecture*. 75 Trinity Place, New York, NY, 10006: The Society of Naval Architects and Marine Engineers, 1967.

[9] R. S. Duelley, "Autonomous Underwater Vehicle Propulsion Design," Master's thesis, Virginia Polytechnic Insitute and State University, Blacksburg, VA, August 2010.

[10] M. Caccia, G. Indiveri, and G. Veruggio, "Modeling and identification of open-frame variable configuration unmanned underwater vehicles," *Oceanic Engineering, IEEE Journal of*, vol. 25, pp. 227–240, April 2000.

[11] H. K. Khalil, *Nonlinear Systems.* Englewood Cliffs, NJ: Prentice Hall, 2002.

[12] T. Prestero, "Development of a six-degree of freedom simulation model for the remus autonomous underwater vehicle," in *OCEANS, 2001. MTS/IEEE Conference and Exhibition*, vol. 1, pp. 450–455 vol.1, 2001.

[13] C. McFarland and L. Whitcomb, "Comparative experimental evaluation of a new adaptive identifier for underwater vehicles," in *Robotics and Automation (ICRA), 2013 IEEE International Conference on*, pp. 4614–4620, May 2013.

[14] D. Smallwood and L. Whitcomb, "Adaptive identification of dynamically positioned underwater robotic vehicles," *Control Systems Technology, IEEE Transactions on*, vol. 11, pp. 505–515, July 2003.

[15] R. G. Coe, *Improved Underwater Vehicle Control and Maneuvering Analysis with Computational Fluid Dynamics Simulations.* PhD thesis, Virginia Tech, Blacksburg, VA, August 2013.

[16] J. A. Nelder and R. Mead, "A simplex method for function minimization," *The computer journal*, vol. 7, no. 4, pp. 308–313, 1965.

[17] J. C. Lagarias, J. A. Reeds, M. H. Wright, and P. E. Wright, "Convergence properties of the nelder–mead simplex method in low dimensions," *SIAM Journal on optimization*, vol. 9, no. 1, pp. 112–147, 1998.

[18] C. Kaiser, J. Kinsey, W. Pinner, D. Yoerger, C. German, and C. Van Dover, "Satellite based remote management and operation of a 6000m auv," in *Oceans, 2012*, pp. 1–7, Oct 2012.

[19] A. Graham, *Kronecker Products and Matrix Calculus with Applications*. Market Cross House, Cooper Street, Chichester, West Sussex, PO19 1EB, England: Ellix Horwood Limited, 1981.

[20] S. Sastry, *Nonlinear systems: analysis, stability, and control*. Springer, 1999.

Appendix A

Matrix mathematics

A.1 The vec operator

The notation herein is adopted from [19]. Let the columns of a matrix $\boldsymbol{A} \in \mathbb{R}^{m \times n}$ be denoted $\boldsymbol{A}_{\cdot j}$ and the rows $\boldsymbol{A}_{i\cdot}$, with $i \in [1, m]$ and $j \in [1, n]$. The matrix $\boldsymbol{A}$ may then be partitioned as either of

$$\boldsymbol{A} = \left[\ \boldsymbol{A}_{\cdot 1}, \ \boldsymbol{A}_{\cdot 2}, \ \cdots \ , \ \boldsymbol{A}_{\cdot n} \ \right] \tag{A.1}$$

or

$$\boldsymbol{A}^{\top} = \left[\ \boldsymbol{A}_{1\cdot}, \ \boldsymbol{A}_{2\cdot}, \ \cdots \ , \ \boldsymbol{A}_{m\cdot} \ \right] \tag{A.2}$$

Note that both $\boldsymbol{A}_{\cdot j}$ and $\boldsymbol{A}_{i\cdot}$ are defined to be column vectors.

The vec operator may be expressed

$$\mathrm{vec}(\boldsymbol{A}) \triangleq \begin{bmatrix} A_{\cdot 1} \\ A_{\cdot 2} \\ \vdots \\ A_{\cdot n} \end{bmatrix}, \tag{A.3}$$

with dimension $\mathrm{vec}(\boldsymbol{A}) \in \mathbb{R}^{mn}$.

For conformal matrices $\boldsymbol{A}$, $\boldsymbol{Y}$, and $\boldsymbol{B}$, it holds that

$$\mathrm{vec}(\boldsymbol{A}\boldsymbol{Y}\boldsymbol{B}) = \left(\boldsymbol{B}^{\top} \otimes \boldsymbol{A}\right) \mathrm{vec}(\boldsymbol{Y}) \tag{A.4}$$

The inverse vec operator is defined as follows. Let $\boldsymbol{b} \in \mathbb{R}^k$ be a column vector, where

$k = m \times n$ for some $m, n \in \mathbb{N}$. Then $\boldsymbol{b}$ can be expressed as

$$\boldsymbol{b} = \begin{bmatrix} \boldsymbol{B}_{\cdot 1} \\ \boldsymbol{B}_{\cdot 2} \\ \vdots \\ \boldsymbol{B}_{\cdot n} \end{bmatrix}, \tag{A.5}$$

where $\boldsymbol{B}_{\cdot j} \in \mathbb{R}^m$ with $j \in \{1, \ldots, n\}$. Let the inverse vec operator be denoted vec^{-1}, defined such that

$$\boldsymbol{B} = \begin{bmatrix} \boldsymbol{B}_{\cdot 1} & \boldsymbol{B}_{\cdot 2} & \cdots & \boldsymbol{B}_{\cdot n} \end{bmatrix} = \mathrm{vec}^{-1}(\boldsymbol{b}). \tag{A.6}$$

A.2 Skew-symmetric operator

For the vector $\lambda \in \mathbb{R}^3$ with $\lambda = [\lambda_1, \lambda_2, \lambda_3]^\top$, let

$$\boldsymbol{S}(\lambda) = \begin{bmatrix} 0 & -\lambda_3 & \lambda_2 \\ \lambda_3 & 0 & -\lambda_1 \\ -\lambda_2 & \lambda_1 & 0 \end{bmatrix} \tag{A.7}$$

be a map from $\mathbb{R}^3 \to \mathrm{so}(3)$, the set of skew-symmetric matrices [20]. This definition of $\boldsymbol{S}(\lambda)$ forms a matrix-representation of a cross product.

Appendix B

VT 690 parameters

Parameter	Description	Value	Unit
g	acceleration due to gravity	9.80665	m/s^2
ρ_f	fluid density (fresh water)	1000	kg/m^3
ρ_s	fluid density (salt water)	1015	kg/m^3

Table B.1: Physical constants

Parameter	Description	Value	Unit
d	diameter	0.1753	m
m	mass	41.458	kg
∇	displacement	41.702	kg
ℓ	length	2.057	m
d_p	propeller diameter	0.120	m
$r_B(x)$	center of buoyancy in x	0	m
$r_B(y)$	center of buoyancy in y	0	m
$r_B(z)$	center of buoyancy in z	0	m
$r_G(x)$	center of gravity in x	-0.0029	m
$r_G(y)$	center of gravity in y	-0.0002	m
$r_G(z)$	center of gravity in z	0.0084	m
w	wake fraction	0.3	

$$I_0 = \begin{bmatrix} 0.1707 & -0.0033 & 0.1407 \\ -0.0033 & 10.3659 & -0.0000 \\ 0.1407 & -0.0000 & 10.3508 \end{bmatrix}$$

Table B.2: Virginia Tech 690 parameters

$$M_A = \begin{bmatrix} -0.6673 & 0 & 0 & 0 & 0 & 0 \\ 0 & -40.1654 & 0 & 0 & 0 & 0 \\ 0 & 0 & -40.1654 & 0 & 0 & 0 \\ 0 & 0 & 0 & 0 & 0 & 0 \\ 0 & 0 & 0 & 0 & -8.0212 & 0 \\ 0 & 0 & 0 & 0 & 0 & -8.0212 \end{bmatrix}$$

Table B.3: Added mass model for a prolate spheroid with same volume and aspect ratios as the VT 690.

$$K'_\delta = \begin{bmatrix} -3.6686 \times 10^{-20} & 0 & 0 & 0 \\ 9.1716 \times 10^{-21} & 2.0463 \times 10^{-06} & 0.0019061 & -0.0020678 \\ -0.00208 & 0.0019506 & 0 & -4.5858 \times 10^{-21} \\ -2.9415 \times 10^{-05} & -2.7625 \times 10^{-05} & -2.6346 \times 10^{-05} & -2.7881 \times 10^{-05} \\ -0.001084 & 0.00082798 & 0 & 0 \\ -1.9695 \times 10^{-05} & 0 & -0.00088374 & 0.00097045 \end{bmatrix}$$

$$K'_{\delta^2} = \begin{bmatrix} -0.0012101 & -0.00094632 & -0.00091701 & -0.0010468 \\ 0.00031247 & -0.00015336 & -0.00016121 & -1.3609 \times 10^{-05} \\ -0.00018319 & -0.00015493 & 0.00025333 & -0.00029625 \\ 2.3553 \times 10^{-06} & 3.6638 \times 10^{-06} & -1.3085 \times 10^{-06} & 2.3553 \times 10^{-06} \\ 0.00014289 & 0.00013582 & 0.00011829 & -0.00013138 \\ -0.00015519 & 6.7519 \times 10^{-0}5 & 4.6321 \times 10^{-05} & 1.2038 \times 10^{-05} \end{bmatrix}$$

Table B.4: Control surface model coefficients

$$K_T(J) = -\,0.1378J^2 + 0.0483J + 0.0578$$
$$K_T(J) = -\,0.01174J^2 + 0.00575J + 0.00419$$

Table B.5: Propeller model equations

Appendix C

Damping model basis functions

$$\boldsymbol{\xi}_{\boldsymbol{\nu}}(\boldsymbol{\nu}) = \begin{bmatrix} u \\ v \\ w \\ p \\ q \\ r \end{bmatrix} \tag{C.1}$$

$$\boldsymbol{\xi}_{|\boldsymbol{\nu}|}(\boldsymbol{\nu}) = \begin{bmatrix} |u| \\ |v| \\ |w| \\ |p| \\ |q| \\ |r| \end{bmatrix} \tag{C.2}$$

$$\boldsymbol{\xi}_{\boldsymbol{\nu}\boldsymbol{\nu}}(\boldsymbol{\nu}) = \begin{bmatrix} u^2 \\ uv \\ uw \\ up \\ uq \\ ur \\ v^2 \\ vw \\ vp \\ vq \\ vr \\ w^2 \\ wp \\ wq \\ wr \\ p^2 \\ pq \\ pr \\ q^2 \\ qr \\ r^2 \end{bmatrix} \tag{C.3}$$

$$\boldsymbol{\xi}_{\boldsymbol{\nu}|\boldsymbol{\nu}|}(\boldsymbol{\nu}) = \begin{bmatrix} u\,|u| \\ u\,|v| \\ u\,|w| \\ u\,|p| \\ u\,|q| \\ u\,|r| \\ v\,|u| \\ v\,|v| \\ v\,|w| \\ v\,|p| \\ v\,|q| \\ v\,|r| \\ w\,|u| \\ w\,|v| \\ w\,|w| \\ w\,|p| \\ w\,|q| \\ w\,|r| \\ p\,|u| \\ p\,|v| \\ p\,|w| \\ p\,|p| \\ p\,|q| \\ p\,|r| \\ q\,|u| \\ q\,|v| \\ q\,|w| \\ q\,|p| \\ q\,|q| \\ q\,|r| \\ r\,|u| \\ r\,|v| \\ r\,|w| \\ r\,|p| \\ r\,|q| \\ r\,|r| \end{bmatrix} \tag{C.4}$$

$$\boldsymbol{\xi}_{\boldsymbol{\nu}V}(\boldsymbol{\nu}) = \begin{bmatrix} u\mathrm{V} \\ v\mathrm{V} \\ w\mathrm{V} \\ p\mathrm{V} \\ q\mathrm{V} \\ r\mathrm{V} \\ |u|\,\mathrm{V} \\ |v|\,\mathrm{V} \\ |w|\,\mathrm{V} \\ |p|\,\mathrm{V} \\ |q|\,\mathrm{V} \\ |r|\,\mathrm{V} \\ u\mathrm{V_v} \\ v\mathrm{V_v} \\ w\mathrm{V_v} \\ p\mathrm{V_v} \\ q\mathrm{V_v} \\ r\mathrm{V_v} \\ |u|\,\mathrm{V_v} \\ |v|\,\mathrm{V_v} \\ |w|\,\mathrm{V_v} \\ |p|\,\mathrm{V_v} \\ |q|\,\mathrm{V_v} \\ |r|\,\mathrm{V_v} \\ u\mathrm{V_w} \\ v\mathrm{V_w} \\ w\mathrm{V_w} \\ p\mathrm{V_w} \\ q\mathrm{V_w} \\ r\mathrm{V_w} \\ |u|\,\mathrm{V_w} \\ |v|\,\mathrm{V_w} \\ |w|\,\mathrm{V_w} \\ |p|\,\mathrm{V_w} \\ |q|\,\mathrm{V_w} \\ |r|\,\mathrm{V_w} \end{bmatrix} \tag{C.5}$$

$$\boldsymbol{\xi}_{\boldsymbol{\nu}\boldsymbol{\eta}}(\boldsymbol{\nu}) = \begin{bmatrix} u^2\,(\eta-1) \\ uv\,(\eta-1) \\ uw\,(\eta-1) \\ up\,(\eta-1) \\ uq\,(\eta-1) \\ ur\,(\eta-1) \\ v^2\,(\eta-1) \\ vw\,(\eta-1) \\ vp\,(\eta-1) \\ vq\,(\eta-1) \\ vr\,(\eta-1) \\ w^2\,(\eta-1) \\ wp\,(\eta-1) \\ wq\,(\eta-1) \\ wr\,(\eta-1) \\ p^2\,(\eta-1) \\ pq\,(\eta-1) \\ pr\,(\eta-1) \\ q^2\,(\eta-1) \\ qr\,(\eta-1) \\ r^2\,(\eta-1) \\ u\mathrm{V}\,(\eta-1) \\ v\mathrm{V}\,(\eta-1) \\ w\mathrm{V}\,(\eta-1) \\ p\mathrm{V}\,(\eta-1) \\ q\mathrm{V}\,(\eta-1) \\ r\mathrm{V}\,(\eta-1) \end{bmatrix} \tag{C.6}$$

The basis vector

$$\boldsymbol{\xi}(\boldsymbol{\nu}) = \begin{bmatrix} \boldsymbol{\xi}_{\boldsymbol{\nu}}(\boldsymbol{\nu}) \\ \boldsymbol{\xi}_{|\boldsymbol{\nu}|}(\boldsymbol{\nu}) \\ \boldsymbol{\xi}_{\boldsymbol{\nu}\boldsymbol{\nu}}(\boldsymbol{\nu}) \\ \boldsymbol{\xi}_{\boldsymbol{\nu}|\boldsymbol{\nu}|}(\boldsymbol{\nu}) \\ \boldsymbol{\xi}_{\boldsymbol{\nu}V}(\boldsymbol{\nu}) \\ \boldsymbol{\xi}_{\boldsymbol{\nu}\boldsymbol{\eta}}(\boldsymbol{\nu}) \end{bmatrix}, \tag{C.7}$$

is adequate to describe all models presented in Chapter 3. This basis vector has 132 terms. They are presented as nonlinear functions of the velocity vector ν, where

$$U = \sqrt{u^2 + v^2 + w^2} \tag{C.8}$$

$$V = \sqrt{v^2 + w^2} \tag{C.9}$$

$$V_v = V\text{sign}(v) \tag{C.10}$$

$$V_w = V\text{sign}(v) \tag{C.11}$$

$$\eta = \frac{u_c(n)}{U} \tag{C.12}$$

are functions of velocity used to make the model equations more concise. Note that $u_c(n)$ is the nominal forward velocity at level flight for the commanded propeller rate n, and should be treated as constant.

Appendix D

Damping model equations

The damping model equations $\tau_\nu^X(\boldsymbol{\nu}), \tau_\nu^Y(\boldsymbol{\nu}), \tau_\nu^Z(\boldsymbol{\nu}), \tau_\nu^K(\boldsymbol{\nu}), \tau_\nu^M(\boldsymbol{\nu}), \tau_\nu^N(\boldsymbol{\nu}) : \mathbb{R}^6 \to \mathbb{R}$ map from the velocity vector $\boldsymbol{\nu}$ to a force in the dimension represented by the superscript. The 6-DOF generalized damping force vector is

$$\tau_\nu(\boldsymbol{\nu}) = \begin{bmatrix} \tau_\nu^X(\boldsymbol{\nu}) \\ \tau_\nu^Y(\boldsymbol{\nu}) \\ \tau_\nu^Z(\boldsymbol{\nu}) \\ \tau_\nu^K(\boldsymbol{\nu}) \\ \tau_\nu^M(\boldsymbol{\nu}) \\ \tau_\nu^N(\boldsymbol{\nu}) \end{bmatrix}. \tag{D.1}$$

$$
\begin{aligned}
\tau_\nu^{\mathrm{X}}(\nu) =& \mathrm{X}_{\mathrm{p|w|}} p\,|w| + \mathrm{X}_{\mathrm{q|v|}} q\,|v| + \mathrm{X}_{\mathrm{r|u|}} r\,|u| + \mathrm{X}_{\mathrm{u|r|}} u\,|r| + \mathrm{X}_{\mathrm{v|q|}} v\,|q| \\
&+ \mathrm{X}_{\mathrm{w|p|}} w\,|p| + \mathrm{X}_{\mathrm{q|w|}} q\,|w| + \mathrm{X}_{\mathrm{r|v|}} r\,|v| + \mathrm{X}_{\mathrm{v|r|}} v\,|r| + \mathrm{X}_{\mathrm{w|q|}} w\,|q| + \mathrm{X}_{\mathrm{r|w|}} r\,|w| \\
&+ \mathrm{X}_{\mathrm{w|r|}} w\,|r| + \mathrm{X}_{\mathrm{u|u|}} u\,|u| + \mathrm{X}_{\mathrm{u|v|}} u\,|v| + \mathrm{X}_{\mathrm{v|u|}} v\,|u| + \mathrm{X}_{\mathrm{u|w|}} u\,|w| + \mathrm{X}_{\mathrm{v|v|}} v\,|v| \\
&+ \mathrm{X}_{\mathrm{w|u|}} w\,|u| + \mathrm{X}_{\mathrm{v|w|}} v\,|w| + \mathrm{X}_{\mathrm{w|v|}} w\,|v| + \mathrm{X}_{\mathrm{w|w|}} w\,|w| + \mathrm{X}_{\mathrm{p|p|}} p\,|p| + \mathrm{X}_{\mathrm{p|q|}} p\,|q| \\
&+ \mathrm{X}_{\mathrm{q|p|}} q\,|p| + \mathrm{X}_{\mathrm{p|r|}} p\,|r| + \mathrm{X}_{\mathrm{q|q|}} q\,|q| + \mathrm{X}_{\mathrm{r|p|}} r\,|p| + \mathrm{X}_{\mathrm{q|r|}} q\,|r| + \mathrm{X}_{\mathrm{r|q|}} r\,|q| \\
&+ \mathrm{X}_{\mathrm{r|r|}} r\,|r| + \mathrm{X}_{\mathrm{p|u|}} p\,|u| + \mathrm{X}_{\mathrm{u|p|}} u\,|p| + \mathrm{X}_{\mathrm{p|v|}} p\,|v| + \mathrm{X}_{\mathrm{q|u|}} q\,|u| + \mathrm{X}_{\mathrm{u|q|}} u\,|q| \\
&+ \mathrm{X}_{\mathrm{v|p|}} v\,|p| \\
\tau_\nu^{\mathrm{Y}}(\nu) =& \mathrm{Y}_{\mathrm{p|v|}} p\,|v| + \mathrm{Y}_{\mathrm{q|u|}} q\,|u| + \mathrm{Y}_{\mathrm{u|q|}} u\,|q| + \mathrm{Y}_{\mathrm{v|p|}} v\,|p| + \mathrm{Y}_{\mathrm{p|w|}} p\,|w| \\
&+ \mathrm{Y}_{\mathrm{q|v|}} q\,|v| + \mathrm{Y}_{\mathrm{r|u|}} r\,|u| + \mathrm{Y}_{\mathrm{u|r|}} u\,|r| + \mathrm{Y}_{\mathrm{v|q|}} v\,|q| + \mathrm{Y}_{\mathrm{w|p|}} w\,|p| + \mathrm{Y}_{\mathrm{q|w|}} q\,|w| \\
&+ \mathrm{Y}_{\mathrm{r|v|}} r\,|v| + \mathrm{Y}_{\mathrm{v|r|}} v\,|r| + \mathrm{Y}_{\mathrm{w|q|}} w\,|q| + \mathrm{Y}_{\mathrm{r|w|}} r\,|w| + \mathrm{Y}_{\mathrm{w|r|}} w\,|r| + \mathrm{Y}_{\mathrm{u|u|}} u\,|u| \\
&+ \mathrm{Y}_{\mathrm{u|v|}} u\,|v| + \mathrm{Y}_{\mathrm{v|u|}} v\,|u| + \mathrm{Y}_{\mathrm{u|w|}} u\,|w| + \mathrm{Y}_{\mathrm{v|v|}} v\,|v| + \mathrm{Y}_{\mathrm{w|u|}} w\,|u| + \mathrm{Y}_{\mathrm{v|w|}} v\,|w| \\
&+ \mathrm{Y}_{\mathrm{w|v|}} w\,|v| + \mathrm{Y}_{\mathrm{w|w|}} w\,|w| + \mathrm{Y}_{\mathrm{p|p|}} p\,|p| + \mathrm{Y}_{\mathrm{p|q|}} p\,|q| + \mathrm{Y}_{\mathrm{q|p|}} q\,|p| + \mathrm{Y}_{\mathrm{p|r|}} p\,|r| \\
&+ \mathrm{Y}_{\mathrm{q|q|}} q\,|q| + \mathrm{Y}_{\mathrm{r|p|}} r\,|p| + \mathrm{Y}_{\mathrm{q|r|}} q\,|r| + \mathrm{Y}_{\mathrm{r|q|}} r\,|q| + \mathrm{Y}_{\mathrm{r|r|}} r\,|r| + \mathrm{Y}_{\mathrm{p|u|}} p\,|u| \\
&+ \mathrm{Y}_{\mathrm{u|p|}} u\,|p| \\
\tau_\nu^{\mathrm{Z}}(\nu) =& \mathrm{Z}_{\mathrm{p|u|}} p\,|u| + \mathrm{Z}_{\mathrm{u|p|}} u\,|p| + \mathrm{Z}_{\mathrm{p|v|}} p\,|v| + \mathrm{Z}_{\mathrm{q|u|}} q\,|u| + \mathrm{Z}_{\mathrm{u|q|}} u\,|q| \\
&+ \mathrm{Z}_{\mathrm{v|p|}} v\,|p| + \mathrm{Z}_{\mathrm{p|w|}} p\,|w| + \mathrm{Z}_{\mathrm{q|v|}} q\,|v| + \mathrm{Z}_{\mathrm{r|u|}} r\,|u| + \mathrm{Z}_{\mathrm{u|r|}} u\,|r| + \mathrm{Z}_{\mathrm{v|q|}} v\,|q| \\
&+ \mathrm{Z}_{\mathrm{w|p|}} w\,|p| + \mathrm{Z}_{\mathrm{q|w|}} q\,|w| + \mathrm{Z}_{\mathrm{r|v|}} r\,|v| + \mathrm{Z}_{\mathrm{v|r|}} v\,|r| + \mathrm{Z}_{\mathrm{w|q|}} w\,|q| + \mathrm{Z}_{\mathrm{r|w|}} r\,|w| \\
&+ \mathrm{Z}_{\mathrm{w|r|}} w\,|r| + \mathrm{Z}_{\mathrm{u|u|}} u\,|u| + \mathrm{Z}_{\mathrm{u|v|}} u\,|v| + \mathrm{Z}_{\mathrm{v|u|}} v\,|u| + \mathrm{Z}_{\mathrm{u|w|}} u\,|w| + \mathrm{Z}_{\mathrm{v|v|}} v\,|v| \\
&+ \mathrm{Z}_{\mathrm{w|u|}} w\,|u| + \mathrm{Z}_{\mathrm{v|w|}} v\,|w| + \mathrm{Z}_{\mathrm{w|v|}} w\,|v| + \mathrm{Z}_{\mathrm{w|w|}} w\,|w| + \mathrm{Z}_{\mathrm{p|p|}} p\,|p| + \mathrm{Z}_{\mathrm{p|q|}} p\,|q| \\
&+ \mathrm{Z}_{\mathrm{q|p|}} q\,|p| + \mathrm{Z}_{\mathrm{p|r|}} p\,|r| + \mathrm{Z}_{\mathrm{q|q|}} q\,|q| + \mathrm{Z}_{\mathrm{r|p|}} r\,|p| + \mathrm{Z}_{\mathrm{q|r|}} q\,|r| + \mathrm{Z}_{\mathrm{r|q|}} r\,|q| \\
&+ \mathrm{Z}_{\mathrm{r|r|}} r\,|r|
\end{aligned}
$$

Table D.1: Equations of McFarland model (part one).

$$
\begin{aligned}
\tau_\nu^{\mathrm{K}}(\nu) =& \mathrm{K}_{\mathrm{p|p|}} p\,|p| + \mathrm{K}_{\mathrm{p|q|}} p\,|q| + \mathrm{K}_{\mathrm{q|p|}} q\,|p| + \mathrm{K}_{\mathrm{p|r|}} p\,|r| + \mathrm{K}_{\mathrm{q|q|}} q\,|q| \\
&+ \mathrm{K}_{\mathrm{r|p|}} r\,|p| + \mathrm{K}_{\mathrm{q|r|}} q\,|r| + \mathrm{K}_{\mathrm{r|q|}} r\,|q| + \mathrm{K}_{\mathrm{r|r|}} r\,|r| + \mathrm{K}_{\mathrm{p|u|}} p\,|u| + \mathrm{K}_{\mathrm{u|p|}} u\,|p| \\
&+ \mathrm{K}_{\mathrm{p|v|}} p\,|v| + \mathrm{K}_{\mathrm{q|u|}} q\,|u| + \mathrm{K}_{\mathrm{u|q|}} u\,|q| + \mathrm{K}_{\mathrm{v|p|}} v\,|p| + \mathrm{K}_{\mathrm{p|w|}} p\,|w| + \mathrm{K}_{\mathrm{q|v|}} q\,|v| \\
&+ \mathrm{K}_{\mathrm{r|u|}} r\,|u| + \mathrm{K}_{\mathrm{u|r|}} u\,|r| + \mathrm{K}_{\mathrm{v|q|}} v\,|q| + \mathrm{K}_{\mathrm{w|p|}} w\,|p| + \mathrm{K}_{\mathrm{q|w|}} q\,|w| + \mathrm{K}_{\mathrm{r|v|}} r\,|v| \\
&+ \mathrm{K}_{\mathrm{v|r|}} v\,|r| + \mathrm{K}_{\mathrm{w|q|}} w\,|q| + \mathrm{K}_{\mathrm{r|w|}} r\,|w| + \mathrm{K}_{\mathrm{w|r|}} w\,|r| + \mathrm{K}_{\mathrm{u|u|}} u\,|u| + \mathrm{K}_{\mathrm{u|v|}} u\,|v| \\
&+ \mathrm{K}_{\mathrm{v|u|}} v\,|u| + \mathrm{K}_{\mathrm{u|w|}} u\,|w| + \mathrm{K}_{\mathrm{v|v|}} v\,|v| + \mathrm{K}_{\mathrm{w|u|}} w\,|u| + \mathrm{K}_{\mathrm{v|w|}} v\,|w| + \mathrm{K}_{\mathrm{w|v|}} w\,|v| \\
&+ \mathrm{K}_{\mathrm{w|w|}} w\,|w| \\
\tau_\nu^{\mathrm{M}}(\nu) =& \mathrm{M}_{\mathrm{p|p|}} p\,|p| + \mathrm{M}_{\mathrm{p|q|}} p\,|q| + \mathrm{M}_{\mathrm{q|p|}} q\,|p| + \mathrm{M}_{\mathrm{p|r|}} p\,|r| + \mathrm{M}_{\mathrm{q|q|}} q\,|q| \\
&+ \mathrm{M}_{\mathrm{r|p|}} r\,|p| + \mathrm{M}_{\mathrm{q|r|}} q\,|r| + \mathrm{M}_{\mathrm{r|q|}} r\,|q| + \mathrm{M}_{\mathrm{r|r|}} r\,|r| + \mathrm{M}_{\mathrm{p|u|}} p\,|u| + \mathrm{M}_{\mathrm{u|p|}} u\,|p| \\
&+ \mathrm{M}_{\mathrm{p|v|}} p\,|v| + \mathrm{M}_{\mathrm{q|u|}} q\,|u| + \mathrm{M}_{\mathrm{u|q|}} u\,|q| + \mathrm{M}_{\mathrm{v|p|}} v\,|p| + \mathrm{M}_{\mathrm{p|w|}} p\,|w| + \mathrm{M}_{\mathrm{q|v|}} q\,|v| \\
&+ \mathrm{M}_{\mathrm{r|u|}} r\,|u| + \mathrm{M}_{\mathrm{u|r|}} u\,|r| + \mathrm{M}_{\mathrm{v|q|}} v\,|q| + \mathrm{M}_{\mathrm{w|p|}} w\,|p| + \mathrm{M}_{\mathrm{q|w|}} q\,|w| + \mathrm{M}_{\mathrm{r|v|}} r\,|v| \\
&+ \mathrm{M}_{\mathrm{v|r|}} v\,|r| + \mathrm{M}_{\mathrm{w|q|}} w\,|q| + \mathrm{M}_{\mathrm{r|w|}} r\,|w| + \mathrm{M}_{\mathrm{w|r|}} w\,|r| + \mathrm{M}_{\mathrm{u|u|}} u\,|u| + \mathrm{M}_{\mathrm{u|v|}} u\,|v| \\
&+ \mathrm{M}_{\mathrm{v|u|}} v\,|u| + \mathrm{M}_{\mathrm{u|w|}} u\,|w| + \mathrm{M}_{\mathrm{v|v|}} v\,|v| + \mathrm{M}_{\mathrm{w|u|}} w\,|u| + \mathrm{M}_{\mathrm{v|w|}} v\,|w| + \mathrm{M}_{\mathrm{w|v|}} w\,|v| \\
&+ \mathrm{M}_{\mathrm{w|w|}} w\,|w| \\
\tau_\nu^{\mathrm{N}}(\nu) =& \mathrm{N}_{\mathrm{p|p|}} p\,|p| + \mathrm{N}_{\mathrm{p|q|}} p\,|q| + \mathrm{N}_{\mathrm{q|p|}} q\,|p| + \mathrm{N}_{\mathrm{p|r|}} p\,|r| + \mathrm{N}_{\mathrm{q|q|}} q\,|q| \\
&+ \mathrm{N}_{\mathrm{r|p|}} r\,|p| + \mathrm{N}_{\mathrm{q|r|}} q\,|r| + \mathrm{N}_{\mathrm{r|q|}} r\,|q| + \mathrm{N}_{\mathrm{r|r|}} r\,|r| + \mathrm{N}_{\mathrm{p|u|}} p\,|u| + \mathrm{N}_{\mathrm{u|p|}} u\,|p| \\
&+ \mathrm{N}_{\mathrm{p|v|}} p\,|v| + \mathrm{N}_{\mathrm{q|u|}} q\,|u| + \mathrm{N}_{\mathrm{u|q|}} u\,|q| + \mathrm{N}_{\mathrm{v|p|}} v\,|p| + \mathrm{N}_{\mathrm{p|w|}} p\,|w| + \mathrm{N}_{\mathrm{q|v|}} q\,|v| \\
&+ \mathrm{N}_{\mathrm{r|u|}} r\,|u| + \mathrm{N}_{\mathrm{u|r|}} u\,|r| + \mathrm{N}_{\mathrm{v|q|}} v\,|q| + \mathrm{N}_{\mathrm{w|p|}} w\,|p| + \mathrm{N}_{\mathrm{q|w|}} q\,|w| + \mathrm{N}_{\mathrm{r|v|}} r\,|v| \\
&+ \mathrm{N}_{\mathrm{v|r|}} v\,|r| + \mathrm{N}_{\mathrm{w|q|}} w\,|q| + \mathrm{N}_{\mathrm{r|w|}} r\,|w| + \mathrm{N}_{\mathrm{w|r|}} w\,|r| + \mathrm{N}_{\mathrm{u|u|}} u\,|u| + \mathrm{N}_{\mathrm{u|v|}} u\,|v| \\
&+ \mathrm{N}_{\mathrm{v|u|}} v\,|u| + \mathrm{N}_{\mathrm{u|w|}} u\,|w| + \mathrm{N}_{\mathrm{v|v|}} v\,|v| + \mathrm{N}_{\mathrm{w|u|}} w\,|u| + \mathrm{N}_{\mathrm{v|w|}} v\,|w| + \mathrm{N}_{\mathrm{w|v|}} w\,|v| \\
&+ \mathrm{N}_{\mathrm{w|w|}} w\,|w|
\end{aligned}
$$

Table D.2: Equations of McFarland model (part two).

$$
\begin{aligned}
\tau_{\nu}^{\mathrm{X}}(\boldsymbol{\nu}) =& \mathrm{X_q} q + \mathrm{X_r} r + \mathrm{X_u} u + \mathrm{X_v} v + \mathrm{X_w} w + \mathrm{X_{qq}} q^2 + \mathrm{X_{rr}} r^2 + \mathrm{X_{|q|}} |q| \\
&+ \mathrm{X_{|r|}} |r| + \mathrm{X_{uu}} u^2 + \mathrm{X_{vv}} v^2 + \mathrm{X_{ww}} w^2 + \mathrm{X_{|v|}} |v| + \mathrm{X_{|w|}} |w| + \mathrm{X_{u|r|}} u |r| \\
&+ \mathrm{X_{q|w|}} q |w| + \mathrm{X_{r|v|}} r |v| + \mathrm{X_{v|r|}} v |r| + \mathrm{X_{w|q|}} w |q| + \mathrm{X_{u|v|}} u |v| + \mathrm{X_{u|w|}} u |w| \\
&+ \mathrm{X_{v|v|}} v |v| + \mathrm{X_{w|w|}} w |w| + \mathrm{X_{ur}} ur + \mathrm{X_{vr}} vr + \mathrm{X_{wq}} wq + \mathrm{X_{uv}} uv + \mathrm{X_{uw}} uw + \mathrm{X_{q|q|}} q |q| \\
&+ \mathrm{X_{r|r|}} r |r| + \mathrm{X_{q|u|}} q |u| + \mathrm{X_{u|q|}} u |q| \\
\tau_{\nu}^{\mathrm{Y}}(\boldsymbol{\nu}) =& \mathrm{Y_r} r + \mathrm{Y_v} v + \mathrm{Y_{rr}} r^2 + \mathrm{Y_{|r|}} |r| + \mathrm{Y_{uu}} u^2 + \mathrm{Y_{vv}} v^2 + \mathrm{Y_{|u|}} |u| \\
&+ \mathrm{Y_{|v|}} |v| + \mathrm{Y_{u|r|}} u |r| + \mathrm{Y_{r|v|}} r |v| + \mathrm{Y_{v|r|}} v |r| + \mathrm{Y_{u|v|}} u |v| + \mathrm{Y_{v|v|}} v |v| \\
&+ \mathrm{Y_{ur}} ur + \mathrm{Y_{vr}} vr + \mathrm{Y_{uv}} uv + \mathrm{Y_{r|r|}} r |r| \\
\tau_{\nu}^{\mathrm{Z}}(\boldsymbol{\nu}) =& \mathrm{Z_q} q + \mathrm{Z_w} w + \mathrm{Z_{qq}} q^2 + \mathrm{Z_{|q|}} |q| + \mathrm{Z_{uu}} u^2 + \mathrm{Z_{|u|}} |u| + \mathrm{Z_{ww}} w^2 \\
&+ \mathrm{Z_{|w|}} |w| + \mathrm{Z_{u|q|}} u |q| + \mathrm{Z_{q|w|}} q |w| + \mathrm{Z_{w|q|}} w |q| + \mathrm{Z_{u|w|}} u |w| + \mathrm{Z_{w|w|}} w |w| \\
&+ \mathrm{Z_{uq}} uq + \mathrm{Z_{wq}} wq + \mathrm{Z_{uw}} uw + \mathrm{Z_{q|q|}} q |q| \\
\tau_{\nu}^{\mathrm{K}}(\boldsymbol{\nu}) =& 0 \\
\tau_{\nu}^{\mathrm{M}}(\boldsymbol{\nu}) =& \mathrm{M_q} q + \mathrm{M_w} w + \mathrm{M_{qq}} q^2 + \mathrm{M_{|q|}} |q| + \mathrm{M_{uu}} u^2 + \mathrm{M_{|u|}} |u| + \mathrm{M_{ww}} w^2 \\
&+ \mathrm{M_{|w|}} |w| + \mathrm{M_{uq}} uq + \mathrm{M_{wq}} wq + \mathrm{M_{uw}} uw + \mathrm{M_{q|q|}} q |q| + \mathrm{M_{u|q|}} u |q| + \mathrm{M_{q|w|}} q |w| \\
&+ \mathrm{M_{w|q|}} w |q| + \mathrm{M_{u|w|}} u |w| + \mathrm{M_{w|w|}} w |w| \\
\tau_{\nu}^{\mathrm{N}}(\boldsymbol{\nu}) =& \mathrm{N_r} r + \mathrm{N_v} v + \mathrm{N_{rr}} r^2 + \mathrm{N_{|r|}} |r| + \mathrm{N_{uu}} u^2 + \mathrm{N_{vv}} v^2 + \mathrm{N_{|u|}} |u| \\
&+ \mathrm{N_{|v|}} |v| + \mathrm{N_{ur}} ur + \mathrm{N_{vr}} vr + \mathrm{N_{uv}} uv + \mathrm{N_{r|r|}} r |r| + \mathrm{N_{u|r|}} u |r| + \mathrm{N_{r|v|}} r |v| \\
&+ \mathrm{N_{v|r|}} v |r| + \mathrm{N_{u|v|}} u |v| + \mathrm{N_{v|v|}} v |v|
\end{aligned}
$$

Table D.3: Equations of Pitch/Yaw model.

$$
\begin{aligned}
\tau_{\nu}^{\mathrm{X}}(\nu) =& \mathrm{X_{qq}}q^2 + \mathrm{X_{rr}}r^2 + \mathrm{X_{uu}}u^2 + \mathrm{X_{vv}}v^2 + \mathrm{X_{ww}}w^2 + \mathrm{X_{vv\eta}}v^2\eta - 1 + \mathrm{X_{ww\eta}}w^2\eta - 1 \\
&+ \mathrm{X_{pr}}pr + \mathrm{X_{vr}}vr + \mathrm{X_{wq}}wq \\
\tau_{\nu}^{\mathrm{Y}}(\nu) =& \mathrm{Y_{uu}}u^2 + \mathrm{Y_{vV}}v\mathrm{V} + \mathrm{Y_{pq}}pq + \mathrm{Y_{qr}}qr + \mathrm{Y_{up}}up + \mathrm{Y_{ur}}ur + \mathrm{Y_{vq}}vq + \mathrm{Y_{wp}}wp \\
&+ \mathrm{Y_{wr}}wr + \mathrm{Y_{uv}}uv + \mathrm{Y_{vw}}vw + \mathrm{Y_{|r|V_v}}\,|r|\,\mathrm{V_v} + \mathrm{Y_{p|p|}}p\,|p| + \mathrm{Y_{vV\eta}}v\mathrm{V}\eta - 1 \\
&+ \mathrm{Y_{ur\eta}}ur\eta - 1 + \mathrm{Y_{uv\eta}}uv\eta - 1 \\
\tau_{\nu}^{\mathrm{Z}}(\nu) =& \mathrm{Z_{pp}}p^2 + \mathrm{Z_{rr}}r^2 + \mathrm{Z_{uu}}u^2 + \mathrm{Z_{vv}}v^2 + \mathrm{Z_{u|w|}}u\,|w| + \mathrm{Z_{wV}}w\mathrm{V} + \mathrm{Z_{pr}}pr \\
&+ \mathrm{Z_{uq}}uq + \mathrm{Z_{vp}}vp + \mathrm{Z_{vr}}vr + \mathrm{Z_{uw}}uw + \mathrm{Z_{|q|V_w}}\,|q|\,\mathrm{V_w} + \mathrm{Z_{|w|V}}\,|w|\,\mathrm{V} \\
&+ \mathrm{Z_{wV\eta}}w\mathrm{V}\eta - 1 + \mathrm{Z_{uq\eta}}uq\eta - 1 + \mathrm{Z_{uw\eta}}uw\eta - 1 \\
\tau_{\nu}^{\mathrm{K}}(\nu) =& \mathrm{K_{uu}}u^2 + \mathrm{K_{uu\eta}}u^2\eta - 1 + \mathrm{K_{vV}}v\mathrm{V} + \mathrm{K_{pq}}pq + \mathrm{K_{qr}}qr + \mathrm{K_{up}}up + \mathrm{K_{ur}}ur \\
&+ \mathrm{K_{vq}}vq + \mathrm{K_{wp}}wp + \mathrm{K_{wr}}wr + \mathrm{K_{uv}}uv + \mathrm{K_{vw}}vw + \mathrm{K_{p|p|}}p\,|p| \\
\tau_{\nu}^{\mathrm{M}}(\nu) =& \mathrm{M_{pp}}p^2 + \mathrm{M_{rr}}r^2 + \mathrm{M_{uu}}u^2 + \mathrm{M_{vv}}v^2 + \mathrm{M_{qV}}q\mathrm{V} + \mathrm{M_{wV}}w\mathrm{V} + \mathrm{M_{pr}}pr + \mathrm{M_{uq}}uq \\
&+ \mathrm{M_{vp}}vp + \mathrm{M_{vr}}vr + \mathrm{M_{uw}}uw + \mathrm{M_{|w|V}}\,|w|\,\mathrm{V} + \mathrm{M_{q|q|}}q\,|q| + \mathrm{M_{u|w|}}u\,|w| \\
&+ \mathrm{M_{wV\eta}}w\mathrm{V}\eta - 1 + \mathrm{M_{uq\eta}}uq\eta - 1 + \mathrm{M_{uw\eta}}uw\eta - 1 \\
\tau_{\nu}^{\mathrm{N}}(\nu) =& \mathrm{N_{uu}}u^2 + \mathrm{N_{rV}}r\mathrm{V} + \mathrm{N_{vV}}v\mathrm{V} + \mathrm{N_{pq}}pq + \mathrm{N_{qr}}qr + \mathrm{N_{up}}up + \mathrm{N_{ur}}ur + \mathrm{N_{vq}}vq \\
&+ \mathrm{N_{wp}}wp + \mathrm{N_{wr}}wr + \mathrm{N_{uv}}uv + \mathrm{N_{vw}}vw + \mathrm{N_{r|r|}}r\,|r| + \mathrm{N_{vV\eta}}v\mathrm{V}\eta - 1 + \mathrm{N_{ur\eta}}ur\eta - 1 \\
&+ \mathrm{N_{uv\eta}}uv\eta - 1
\end{aligned}
$$

Table D.4: Equations of Gertler Hagen model.

$$
\begin{aligned}
\tau_{\nu}^{\mathrm{X}}(\nu) =& \mathrm{X_p}p + \mathrm{X_q}q + \mathrm{X_r}r + \mathrm{X_u}u + \mathrm{X_v}v + \mathrm{X_w}w \\
\tau_{\nu}^{\mathrm{Y}}(\nu) =& \mathrm{Y_p}p + \mathrm{Y_q}q + \mathrm{Y_r}r + \mathrm{Y_u}u + \mathrm{Y_v}v + \mathrm{Y_w}w \\
\tau_{\nu}^{\mathrm{Z}}(\nu) =& \mathrm{Z_p}p + \mathrm{Z_q}q + \mathrm{Z_r}r + \mathrm{Z_u}u + \mathrm{Z_v}v + \mathrm{Z_w}w \\
\tau_{\nu}^{\mathrm{K}}(\nu) =& \mathrm{K_p}p + \mathrm{K_q}q + \mathrm{K_r}r + \mathrm{K_u}u + \mathrm{K_v}v + \mathrm{K_w}w \\
\tau_{\nu}^{\mathrm{M}}(\nu) =& \mathrm{M_p}p + \mathrm{M_q}q + \mathrm{M_r}r + \mathrm{M_u}u + \mathrm{M_v}v + \mathrm{M_w}w \\
\tau_{\nu}^{\mathrm{N}}(\nu) =& \mathrm{N_p}p + \mathrm{N_q}q + \mathrm{N_r}r + \mathrm{N_u}u + \mathrm{N_v}v + \mathrm{N_w}w
\end{aligned}
$$

Table D.5: Equations of Linear model.

$$
\begin{aligned}
\tau_{\nu}^{\mathrm{X}}(\nu) =& \mathrm{X_{pp}}p^2 + \mathrm{X_{qq}}q^2 + \mathrm{X_{rr}}r^2 + \mathrm{X_{uu}}u^2 + \mathrm{X_{vv}}v^2 + \mathrm{X_{ww}}w^2 + \mathrm{X_{w|w|}}w\,|w| \\
&+ \mathrm{X_{q|q|}}q\,|q| \\
\tau_{\nu}^{\mathrm{Y}}(\nu) =& \mathrm{Y_{v|v|}}v\,|v| + \mathrm{Y_{p|p|}}p\,|p| + \mathrm{Y_{r|r|}}r\,|r| \\
\tau_{\nu}^{\mathrm{Z}}(\nu) =& \mathrm{Z_{pp}}p^2 + \mathrm{Z_{qq}}q^2 + \mathrm{Z_{rr}}r^2 + \mathrm{Z_{uu}}u^2 + \mathrm{Z_{vv}}v^2 + \mathrm{Z_{ww}}w^2 + \mathrm{Z_{w|w|}}w\,|w| \\
&+ \mathrm{Z_{q|q|}}q\,|q| \\
\tau_{\nu}^{\mathrm{K}}(\nu) =& \mathrm{K_{p|p|}}p\,|p| + \mathrm{K_{r|r|}}r\,|r| + \mathrm{K_{v|v|}}v\,|v| \\
\tau_{\nu}^{\mathrm{M}}(\nu) =& \mathrm{M_{pp}}p^2 + \mathrm{M_{qq}}q^2 + \mathrm{M_{rr}}r^2 + \mathrm{M_{uu}}u^2 + \mathrm{M_{vv}}v^2 + \mathrm{M_{ww}}w^2 + \mathrm{M_{q|q|}}q\,|q| \\
&+ \mathrm{M_{w|w|}}w\,|w| \\
\tau_{\nu}^{\mathrm{N}}(\nu) =& \mathrm{N_{p|p|}}p\,|p| + \mathrm{N_{r|r|}}r\,|r| + \mathrm{N_{v|v|}}v\,|v|
\end{aligned}
$$

Table D.6: Equations of Coe model.

$$
\begin{aligned}
\tau_{\nu}^{\mathrm{X}}(\nu) =& \mathrm{X_{qq}}q^2 + \mathrm{X_{wq}}wq + \mathrm{X_{rr}}r^2 + \mathrm{X_{vr}}vr + \mathrm{X_{u|u|}}u\,|u| \\
\tau_{\nu}^{\mathrm{Y}}(\nu) =& \mathrm{Y_{v|v|}}v\,|v| + \mathrm{Y_{pq}}pq + \mathrm{Y_{ur}}ur + \mathrm{Y_{wp}}wp + \mathrm{Y_{uv}}uv + \mathrm{Y_{r|r|}}r\,|r| \\
\tau_{\nu}^{\mathrm{Z}}(\nu) =& \mathrm{Z_{w|w|}}w\,|w| + \mathrm{Z_{pr}}pr + \mathrm{Z_{uq}}uq + \mathrm{Z_{vp}}vp + \mathrm{Z_{uw}}uw + \mathrm{Z_{q|q|}}q\,|q| \\
\tau_{\nu}^{\mathrm{K}}(\nu) =& \mathrm{K_{p|p|}}p\,|p| \\
\tau_{\nu}^{\mathrm{M}}(\nu) =& \mathrm{M_{pr}}pr + \mathrm{M_{uq}}uq + \mathrm{M_{vp}}vp + \mathrm{M_{uw}}uw + \mathrm{M_{q|q|}}q\,|q| + \mathrm{M_{w|w|}}w\,|w| \\
\tau_{\nu}^{\mathrm{N}}(\nu) =& \mathrm{N_{pq}}pq + \mathrm{N_{ur}}ur + \mathrm{N_{wp}}wp + \mathrm{N_{uv}}uv + \mathrm{N_{r|r|}}r\,|r| + \mathrm{N_{v|v|}}v\,|v|
\end{aligned}
$$

Table D.7: Equations of Prestero model.

$$
\begin{aligned}
\tau_{\nu}^{\mathrm{X}}(\boldsymbol{\nu}) =& \mathrm{X_{u}}u + \mathrm{X_{uu}}u^2 + \mathrm{X_{|u|}}\,|u| + \mathrm{X_{u|u|}}u\,|u| \\
\tau_{\nu}^{\mathrm{Y}}(\boldsymbol{\nu}) =& \mathrm{Y_{v}}v + \mathrm{Y_{vv}}v^2 + \mathrm{Y_{|v|}}\,|v| + \mathrm{Y_{v|v|}}v\,|v| \\
\tau_{\nu}^{\mathrm{Z}}(\boldsymbol{\nu}) =& \mathrm{Z_{w}}w + \mathrm{Z_{ww}}w^2 + \mathrm{Z_{|w|}}\,|w| + \mathrm{Z_{w|w|}}w\,|w| \\
\tau_{\nu}^{\mathrm{K}}(\boldsymbol{\nu}) =& \mathrm{K_{p}}p + \mathrm{K_{pp}}p^2 + \mathrm{K_{|p|}}\,|p| + \mathrm{K_{p|p|}}p\,|p| \\
\tau_{\nu}^{\mathrm{M}}(\boldsymbol{\nu}) =& \mathrm{M_{q}}q + \mathrm{M_{qq}}q^2 + \mathrm{M_{|q|}}\,|q| + \mathrm{M_{q|q|}}q\,|q| \\
\tau_{\nu}^{\mathrm{N}}(\boldsymbol{\nu}) =& \mathrm{N_{r}}r + \mathrm{N_{rr}}r^2 + \mathrm{N_{|r|}}\,|r| + \mathrm{N_{r|r|}}r\,|r|
\end{aligned}
$$

Table D.8: Equations of Uncoupled model.

$$
\begin{aligned}
\tau_{\nu}^{\mathrm{X}}(\nu) =& \mathrm{X_u} u + \mathrm{X_{u|u|}} u \left|u\right| \\
\tau_{\nu}^{\mathrm{Y}}(\nu) =& \mathrm{Y_v} v + \mathrm{Y_{v|v|}} v \left|v\right| \\
\tau_{\nu}^{\mathrm{Z}}(\nu) =& \mathrm{Z_w} w + \mathrm{Z_{w|w|}} w \left|w\right| \\
\tau_{\nu}^{\mathrm{K}}(\nu) =& \mathrm{K_p} p + \mathrm{K_{p|p|}} p \left|p\right| \\
\tau_{\nu}^{\mathrm{M}}(\nu) =& \mathrm{M_q} q + \mathrm{M_{q|q|}} q \left|q\right| \\
\tau_{\nu}^{\mathrm{N}}(\nu) =& \mathrm{N_r} r + \mathrm{N_{r|r|}} r \left|r\right|
\end{aligned}
$$

Table D.9: Equations of Fossen model.

Appendix E

Damping model coefficients

$K_{p\|p\|} = 0.421$	$K_{p\|q\|} = 0.609$	$K_{p\|r\|} = -1.263$
$K_{p\|u\|} = -0.437$	$K_{p\|v\|} = -0.069$	$K_{p\|w\|} = -1.134$
$K_{q\|p\|} = 1.202$	$K_{q\|q\|} = 5.498$	$K_{q\|r\|} = -5.441$
$K_{q\|u\|} = -0.412$	$K_{q\|v\|} = 0.284$	$K_{q\|w\|} = 3.849$
$K_{r\|p\|} = -0.800$	$K_{r\|q\|} = -1.723$	$K_{r\|r\|} = 3.166$
$K_{r\|u\|} = 1.743$	$K_{r\|v\|} = 0.458$	$K_{r\|w\|} = 0.650$
$K_{u\|p\|} = -0.042$	$K_{u\|q\|} = -0.075$	$K_{u\|r\|} = -0.054$
$K_{u\|u\|} = -0.028$	$K_{u\|v\|} = -0.057$	$K_{u\|w\|} = 0.103$
$K_{v\|p\|} = -0.117$	$K_{v\|q\|} = -0.649$	$K_{v\|r\|} = -0.538$
$K_{v\|u\|} = -0.044$	$K_{v\|v\|} = 0.296$	$K_{v\|w\|} = 0.059$
$K_{w\|p\|} = -2.183$	$K_{w\|q\|} = -10.894$	$K_{w\|r\|} = 3.408$
$K_{w\|u\|} = 0.416$	$K_{w\|v\|} = 0.423$	$K_{w\|w\|} = 1.227$
$M_{p\|p\|} = 3.404$	$M_{p\|q\|} = -25.952$	$M_{p\|r\|} = 56.912$
$M_{p\|u\|} = -2.684$	$M_{p\|v\|} = 3.797$	$M_{p\|w\|} = 15.387$
$M_{q\|p\|} = -40.303$	$M_{q\|q\|} = -452.630$	$M_{q\|r\|} = 227.032$
$M_{q\|u\|} = 14.831$	$M_{q\|v\|} = 35.497$	$M_{q\|w\|} = 87.157$
$M_{r\|p\|} = -13.160$	$M_{r\|q\|} = -70.509$	$M_{r\|r\|} = -42.922$
$M_{r\|u\|} = 12.705$	$M_{r\|v\|} = 12.814$	$M_{r\|w\|} = -106.956$
$M_{u\|p\|} = 0.624$	$M_{u\|q\|} = 15.833$	$M_{u\|r\|} = -4.711$
$M_{u\|u\|} = 0.346$	$M_{u\|v\|} = 1.408$	$M_{u\|w\|} = -20.638$
$M_{v\|p\|} = 8.672$	$M_{v\|q\|} = -10.782$	$M_{v\|r\|} = 37.193$
$M_{v\|u\|} = -2.339$	$M_{v\|v\|} = 2.835$	$M_{v\|w\|} = -15.538$
$M_{w\|p\|} = 74.733$	$M_{w\|q\|} = 382.573$	$M_{w\|r\|} = -167.489$
$M_{w\|u\|} = -30.450$	$M_{w\|v\|} = -25.917$	$M_{w\|w\|} = -256.217$

Table E.1: Coefficients of McFarland model (part one).

$N_{p\|p\|} = 6.913$	$N_{p\|q\|} = 23.378$	$N_{p\|r\|} = -31.621$
$N_{p\|u\|} = 1.837$	$N_{p\|v\|} = 10.365$	$N_{p\|w\|} = -0.271$
$N_{q\|p\|} = -29.585$	$N_{q\|q\|} = 26.809$	$N_{q\|r\|} = -8.416$
$N_{q\|u\|} = -0.959$	$N_{q\|v\|} = -38.908$	$N_{q\|w\|} = 1.553$
$N_{r\|p\|} = 36.956$	$N_{r\|q\|} = -4.806$	$N_{r\|r\|} = -172.973$
$N_{r\|u\|} = -9.951$	$N_{r\|v\|} = -54.365$	$N_{r\|w\|} = -38.357$
$N_{u\|p\|} = 0.467$	$N_{u\|q\|} = 2.462$	$N_{u\|r\|} = 4.780$
$N_{u\|u\|} = -0.082$	$N_{u\|v\|} = 0.207$	$N_{u\|w\|} = 0.859$
$N_{v\|p\|} = 15.328$	$N_{v\|q\|} = -27.292$	$N_{v\|r\|} = 10.377$
$N_{v\|u\|} = 40.731$	$N_{v\|v\|} = 2.630$	$N_{v\|w\|} = 65.821$
$N_{w\|p\|} = 30.630$	$N_{w\|q\|} = 32.000$	$N_{w\|r\|} = -16.843$
$N_{w\|u\|} = -2.614$	$N_{w\|v\|} = 2.416$	$N_{w\|w\|} = 0.309$
$X_{p\|p\|} = 14.386$	$X_{p\|q\|} = -7.311$	$X_{p\|r\|} = 12.210$
$X_{p\|u\|} = -3.930$	$X_{p\|v\|} = 27.425$	$X_{p\|w\|} = -1.143$
$X_{q\|p\|} = 65.389$	$X_{q\|q\|} = 110.062$	$X_{q\|r\|} = -132.503$
$X_{q\|u\|} = -2.493$	$X_{q\|v\|} = -6.719$	$X_{q\|w\|} = -130.718$
$X_{r\|p\|} = -31.480$	$X_{r\|q\|} = 71.888$	$X_{r\|r\|} = -51.772$
$X_{r\|u\|} = 12.120$	$X_{r\|v\|} = -16.611$	$X_{r\|w\|} = -65.359$
$X_{u\|p\|} = 4.038$	$X_{u\|q\|} = -3.417$	$X_{u\|r\|} = -9.694$
$X_{u\|u\|} = -4.797$	$X_{u\|v\|} = -6.076$	$X_{u\|w\|} = 5.298$
$X_{v\|p\|} = 4.020$	$X_{v\|q\|} = -51.364$	$X_{v\|r\|} = -47.324$
$X_{v\|u\|} = -1.016$	$X_{v\|v\|} = 15.379$	$X_{v\|w\|} = 12.878$
$X_{w\|p\|} = -72.197$	$X_{w\|q\|} = -158.110$	$X_{w\|r\|} = 101.042$
$X_{w\|u\|} = -3.131$	$X_{w\|v\|} = 41.099$	$X_{w\|w\|} = 166.415$

Table E.2: Coefficients of McFarland model (part two).

$Y_{p\|p\|} = -18.832$	$Y_{p\|q\|} = -97.226$	$Y_{p\|r\|} = 13.242$
$Y_{p\|u\|} = -1.010$	$Y_{p\|v\|} = 5.678$	$Y_{p\|w\|} = 60.986$
$Y_{q\|p\|} = -44.506$	$Y_{q\|q\|} = 94.616$	$Y_{q\|r\|} = 18.679$
$Y_{q\|u\|} = 4.399$	$Y_{q\|v\|} = 64.111$	$Y_{q\|w\|} = -146.467$
$Y_{r\|p\|} = 6.206$	$Y_{r\|q\|} = 70.418$	$Y_{r\|r\|} = 292.750$
$Y_{r\|u\|} = 127.465$	$Y_{r\|v\|} = 37.412$	$Y_{r\|w\|} = 82.615$
$Y_{u\|p\|} = -1.237$	$Y_{u\|q\|} = -8.137$	$Y_{u\|r\|} = -15.759$
$Y_{u\|u\|} = 0.061$	$Y_{u\|v\|} = -5.583$	$Y_{u\|w\|} = 12.070$
$Y_{v\|p\|} = -15.297$	$Y_{v\|q\|} = 56.665$	$Y_{v\|r\|} = -29.545$
$Y_{v\|u\|} = -7.707$	$Y_{v\|v\|} = -17.556$	$Y_{v\|w\|} = -172.677$
$Y_{w\|p\|} = -47.373$	$Y_{w\|q\|} = -23.042$	$Y_{w\|r\|} = -83.367$
$Y_{w\|u\|} = 0.446$	$Y_{w\|v\|} = -48.022$	$Y_{w\|w\|} = 219.663$
$Z_{p\|p\|} = -27.700$	$Z_{p\|q\|} = -130.647$	$Z_{p\|r\|} = 72.983$
$Z_{p\|u\|} = 10.177$	$Z_{p\|v\|} = -55.280$	$Z_{p\|w\|} = -4.591$
$Z_{q\|p\|} = -85.098$	$Z_{q\|q\|} = -739.176$	$Z_{q\|r\|} = 148.626$
$Z_{q\|u\|} = -69.017$	$Z_{q\|v\|} = 85.807$	$Z_{q\|w\|} = -7.284$
$Z_{r\|p\|} = -17.462$	$Z_{r\|q\|} = 1.944$	$Z_{r\|r\|} = -62.976$
$Z_{r\|u\|} = 3.701$	$Z_{r\|v\|} = -54.306$	$Z_{r\|w\|} = -107.167$
$Z_{u\|p\|} = -6.032$	$Z_{u\|q\|} = 23.018$	$Z_{u\|r\|} = 0.161$
$Z_{u\|u\|} = 1.606$	$Z_{u\|v\|} = -4.307$	$Z_{u\|w\|} = -20.993$
$Z_{v\|p\|} = -44.648$	$Z_{v\|q\|} = -22.020$	$Z_{v\|r\|} = 101.527$
$Z_{v\|u\|} = 2.822$	$Z_{v\|v\|} = -17.424$	$Z_{v\|w\|} = -40.746$
$Z_{w\|p\|} = 62.075$	$Z_{w\|q\|} = 683.620$	$Z_{w\|r\|} = -331.695$
$Z_{w\|u\|} = 7.333$	$Z_{w\|v\|} = -168.431$	$Z_{w\|w\|} = -214.787$

Table E.3: Coefficients of McFarland model (part three).

$M_{\|q\|} = -42.982$	$M_{\|u\|} = 7.211$	$M_{\|w\|} = 9.980$
$M_q = -32.864$	$M_{q\|q\|} = -399.594$	$M_{q\|w\|} = 357.056$
$M_{qq} = 177.677$	$M_{u\|q\|} = 22.226$	$M_{u\|w\|} = -31.717$
$M_{uq} = 26.883$	$M_{uu} = -2.688$	$M_{uw} = -30.366$
$M_w = 15.934$	$M_{w\|q\|} = -24.792$	$M_{w\|w\|} = -247.212$
$M_{wq} = 119.546$	$M_{ww} = -31.641$	$N_{\|r\|} = 24.570$
$N_{\|u\|} = -0.457$	$N_{\|v\|} = 5.262$	$N_r = -69.444$
$N_{r\|r\|} = -230.128$	$N_{r\|v\|} = -41.975$	$N_{rr} = 38.016$
$N_{u\|r\|} = -13.758$	$N_{u\|v\|} = -1.584$	$N_{ur} = 36.961$
$N_{uu} = 0.296$	$N_{uv} = 26.619$	$N_v = 29.537$
$N_{v\|r\|} = 13.671$	$N_{v\|v\|} = -3.383$	$N_{vr} = -16.937$
$N_{vv} = -1.785$	$X_{\|q\|} = -8.865$	$X_{\|r\|} = -20.647$

Table E.4: Coefficients of Pitch/Yaw model (part one).

$X_{\|v\|} = -5.822$	$X_{\|w\|} = -289.657$	$X_q = 38.588$
$X_{q\|q\|} = 10.405$	$X_{q\|u\|} = -12.530$	$X_{q\|w\|} = -0.160$
$X_{qq} = -121.700$	$X_r = -2.735$	$X_{r\|r\|} = -1.063$
$X_{r\|v\|} = -6.930$	$X_{rr} = -179.315$	$X_u = -4.049$
$X_{u\|q\|} = 4.947$	$X_{u\|r\|} = 22.226$	$X_{u\|v\|} = 7.091$
$X_{u\|w\|} = 140.551$	$X_{ur} = 5.048$	$X_{uu} = -3.205$
$X_{uv} = -6.477$	$X_{uw} = 127.326$	$X_v = 12.077$
$X_{v\|r\|} = 11.937$	$X_{v\|v\|} = -9.962$	$X_{vr} = -90.356$
$X_{vv} = -34.251$	$X_w = -281.395$	$X_{w\|q\|} = -2.070$
$X_{w\|w\|} = 10.704$	$X_{wq} = 222.169$	$X_{ww} = -85.123$
$Y_{\|r\|} = -25.614$	$Y_{\|u\|} = 0.570$	$Y_{\|v\|} = 9.042$
$Y_r = 89.191$	$Y_{r\|r\|} = 343.718$	$Y_{r\|v\|} = 68.086$
$Y_{rr} = -67.064$	$Y_{u\|r\|} = 8.033$	$Y_{u\|v\|} = -9.606$
$Y_{ur} = 76.294$	$Y_{uu} = -0.283$	$Y_{uv} = 19.888$
$Y_v = -61.323$	$Y_{v\|r\|} = -70.951$	$Y_{v\|v\|} = -10.251$
$Y_{vr} = 40.002$	$Y_{vv} = -12.196$	$Z_{\|q\|} = -102.057$
$Z_{\|u\|} = 9.773$	$Z_{\|w\|} = 23.624$	$Z_q = 92.536$
$Z_{q\|q\|} = -546.335$	$Z_{q\|w\|} = 134.567$	$Z_{qq} = 254.350$
$Z_{u\|q\|} = 52.373$	$Z_{u\|w\|} = -42.509$	$Z_{uq} = -119.005$
$Z_{uu} = -3.645$	$Z_{uw} = -21.081$	$Z_w = 16.235$
$Z_{w\|q\|} = 129.997$	$Z_{w\|w\|} = 113.691$	$Z_{wq} = -2.749$
$Z_{ww} = 149.076$		

Table E.5: Coefficients of Pitch/Yaw model (part two).

$K_{p\|p\|} = -0.237$	$K_{pq} = -0.583$	$K_{qr} = -0.310$
$K_{up} = -0.340$	$K_{ur} = 1.907$	$K_{uu} = -0.045$
$K_{uu\eta} = 0.036$	$K_{uv} = -0.062$	$K_{vV} = 0.443$
$K_{vq} = -0.078$	$K_{vw} = 0.776$	$K_{wp} = 1.901$
$K_{wr} = 1.453$	$M_{\|w\|V} = -32.799$	$M_{pp} = -5.640$
$M_{pr} = -31.501$	$M_{q\|q\|} = -251.463$	$M_{qV} = 79.596$
$M_{rr} = 97.339$	$M_{u\|w\|} = -5.177$	$M_{uq} = 12.387$
$M_{uq\eta} = -71.786$	$M_{uu} = 0.433$	$M_{uw} = -18.369$
$M_{uw\eta} = 23.355$	$M_{vp} = -32.185$	$M_{vr} = 22.863$
$M_{vv} = -13.677$	$M_{wV} = -158.955$	$M_{wV\eta} = 447.471$
$N_{pq} = 26.010$	$N_{qr} = -142.285$	$N_{r\|r\|} = -86.843$
$N_{rV} = -71.725$	$N_{up} = 2.258$	$N_{ur} = -7.536$
$N_{ur\eta} = -19.382$	$N_{uu} = 0.174$	$N_{uv} = 40.385$
$N_{uv\eta} = -53.380$	$N_{vV} = 2.137$	$N_{vV\eta} = 233.038$
$N_{vq} = 92.873$	$N_{vw} = -104.915$	$N_{wp} = -32.363$
$N_{wr} = 77.046$	$X_{pr} = 46.808$	$X_{qq} = -20.656$
$X_{rr} = -101.413$	$X_{uu} = -4.741$	$X_{vr} = -73.945$
$X_{vv} = -5.450$	$X_{vv\eta} = -277.541$	$X_{wq} = 211.457$
$X_{ww} = -125.554$	$X_{ww\eta} = -535.179$	$Y_{\|r\|V_v} = -34.748$
$Y_{p\|p\|} = -11.052$	$Y_{pq} = -2.672$	$Y_{qr} = 222.970$
$Y_{up} = -0.349$	$Y_{ur} = 136.984$	$Y_{ur\eta} = 120.628$
$Y_{uu} = -0.512$	$Y_{uv} = -7.132$	$Y_{uv\eta} = 38.785$
$Y_{vV} = -14.757$	$Y_{vV\eta} = -146.281$	$Y_{vq} = -3.192$
$Y_{vw} = 184.238$	$Y_{wp} = -36.544$	$Y_{wr} = -229.309$
$Z_{\|q\|V_w} = 36.223$	$Z_{\|w\|V} = 23.353$	$Z_{pp} = -10.934$
$Z_{pr} = -26.595$	$Z_{rr} = 115.580$	$Z_{u\|w\|} = -13.669$
$Z_{uq} = -86.918$	$Z_{uq\eta} = -156.538$	$Z_{uu} = 1.321$
$Z_{uw} = 7.711$	$Z_{uw\eta} = 138.100$	$Z_{vp} = 61.987$
$Z_{vr} = 16.340$	$Z_{vv} = 9.955$	$Z_{wV} = -112.528$
$Z_{wV\eta} = 161.153$		

Table E.6: Coefficients of Gertler Hagen model.

$K_p = -0.797$	$K_q = -0.422$	$K_r = 3.068$
$K_u = -0.069$	$K_v = -0.014$	$K_w = 0.416$
$M_p = -0.901$	$M_q = 12.278$	$M_r = 9.002$
$M_u = 0.744$	$M_v = -1.812$	$M_w = -47.521$
$N_p = 8.161$	$N_q = -4.966$	$N_r = -51.246$
$N_u = 0.265$	$N_v = 80.359$	$N_w = -1.345$
$X_p = 5.060$	$X_q = 0.857$	$X_r = -4.045$
$X_u = -10.789$	$X_v = 0.601$	$X_w = -17.526$
$Y_p = 2.077$	$Y_q = -1.232$	$Y_r = 258.895$
$Y_u = -0.901$	$Y_v = -29.859$	$Y_w = 5.839$
$Z_p = 0.745$	$Z_q = -168.088$	$Z_r = -7.026$
$Z_u = 1.438$	$Z_v = -2.057$	$Z_w = -12.369$

Table E.7: Coefficients of Linear model.

$K_{p\|p\|} = -1.226$	$K_{r\|r\|} = 16.675$	$K_{v\|v\|} = 1.035$
$M_{pp} = -8.884$	$M_{q\|q\|} = 40.718$	$M_{qq} = -60.815$
$M_{rr} = 77.192$	$M_{uu} = 0.723$	$M_{vv} = 6.540$
$M_{w\|w\|} = -482.956$	$M_{ww} = -193.793$	$N_{p\|p\|} = -9.737$
$N_{r\|r\|} = -201.880$	$N_{v\|v\|} = 208.945$	$X_{pp} = 29.738$
$X_{q\|q\|} = -125.804$	$X_{qq} = 101.079$	$X_{rr} = -149.377$
$X_{uu} = -4.850$	$X_{vv} = -33.916$	$X_{w\|w\|} = 38.693$
$X_{ww} = -43.192$	$Y_{p\|p\|} = 44.996$	$Y_{r\|r\|} = 1683.953$
$Y_{v\|v\|} = -32.547$	$Z_{pp} = -32.444$	$Z_{q\|q\|} = -1534.722$
$Z_{qq} = 149.675$	$Z_{rr} = 61.460$	$Z_{uu} = 0.750$
$Z_{vv} = 8.833$	$Z_{w\|w\|} = -67.430$	$Z_{ww} = -23.706$

Table E.8: Coefficients of Coe model.

$K_{p\|p\|} = -0.353$	$M_{pr} = -22.459$	$M_{q\|q\|} = -250.074$
$M_{uq} = 22.623$	$M_{uw} = -32.422$	$M_{vp} = -22.251$
$M_{w\|w\|} = -31.920$	$N_{pq} = 6.767$	$N_{r\|r\|} = -195.270$
$N_{ur} = -6.708$	$N_{uv} = 43.028$	$N_{v\|v\|} = -6.034$
$N_{wp} = -32.300$	$X_{qq} = 23.848$	$X_{rr} = -111.927$
$X_{u\|u\|} = -4.977$	$X_{vr} = -124.570$	$X_{wq} = 76.491$
$Y_{pq} = 27.265$	$Y_{r\|r\|} = 269.198$	$Y_{ur} = 123.271$
$Y_{uv} = -14.739$	$Y_{v\|v\|} = 4.678$	$Y_{wp} = -94.628$
$Z_{pr} = -12.869$	$Z_{q\|q\|} = -276.530$	$Z_{uq} = -62.194$
$Z_{uw} = -29.314$	$Z_{vp} = 37.568$	$Z_{w\|w\|} = 170.698$

Table E.9: Coefficients of Prestero model.

$K_{\|p\|} = -1.498$	$K_p = -0.075$	$K_{p\|p\|} = -0.240$
$K_{pp} = 2.859$	$M_{\|q\|} = 139.575$	$M_q = 13.778$
$M_{q\|q\|} = -279.981$	$M_{qq} = -692.804$	$N_{\|r\|} = 11.007$
$N_r = 147.626$	$N_{r\|r\|} = -976.678$	$N_{rr} = -101.831$
$X_{\|u\|} = -7.690$	$X_{uu} = -1.288$	$Y_{\|v\|} = -2.547$
$Y_v = 1.244$	$Y_{v\|v\|} = 29.208$	$Y_{vv} = 34.022$
$Z_{\|w\|} = -152.441$	$Z_w = -162.758$	$Z_{w\|w\|} = 402.700$
$Z_{ww} = 759.005$		

Table E.10: Coefficients of Uncoupled model.

$K_p = -0.073$	$K_{p\|p\|} = -0.166$	$M_q = 33.480$
$M_{q\|q\|} = -350.243$	$N_r = 153.211$	$N_{r\|r\|} = -1037.336$
$X_u = -7.690$	$X_{u\|u\|} = -1.288$	$Y_v = 7.607$
$Y_{v\|v\|} = 2.322$	$Z_w = -20.704$	$Z_{w\|w\|} = -287.599$

Table E.11: Coefficients of Fossen model.